RESERVOIR LENGTH EFFECTS ON THE SEISMIC RESPONSE OF CONCRETE GRAVITY DAMS

By

TERRENCE A. BAUMBER

A Thesis

Submitted to the School of Graduate Studies

in Partial Fulfilment of the Requirements

for the Degree

Doctor of Philosophy

McMaster University

December 1992

RESERVOIR LENGTH EFFECTS ON THE SEISMIC RESPONSE OF CONCRETE GRAVITY DAMS

DOCTOR OF PHILOSOPHY (1992) McMASTER UNIVERSITY
(Civil Engineering and Engineering Mechanics) Hamilton, Ontario

TITLE: Reservoir Length Effects on the Seismic Response of Concrete Gravity Dams

AUTHOR: Terrence A. Baumber, B.Sc. (University of Alberta)
M.Eng. (McMaster University)

SUPERVISOR: Professor A. Ghobarah

NUMBER OF PAGES: xx, 199

ABSTRACT

The behaviour of a concrete gravity dam-reservoir-foundation system is a very complex system to analyze. Currently, the length of the reservoir is assumed infinite during the seismic analysis and design of dam structures. Since many of the natural reservoir systems are finite, this assumption may significantly miscalculate the response of the dam monolith to earthquake ground motion. The objective of this research is to investigate the effect of a finite length upstream reservoir on the monolith's seismic response, including consideration of the reservoir's characteristics.

This study is comprised of three main components. First, a closed form solution of the dam-reservoir problem is developed. The ground motion is assumed to only excite the dam monolith. Second, a detailed analysis procedure is used to investigate the response of the monolith when both the monolith and the reservoir's far boundary is excited. Lastly, a stress analysis is conducted to examine the effect of a finite length reservoir on the dynamic tensile stresses that are developed in the monolith.

The finite length of the upstream reservoir was found to be a very important parameter in defining the response of the dam monolith to seismic input. The response of the dam-reservoir-foundation system was found to be significantly different when the reservoir's length was assumed to be finite than when it was

assumed infinite. The ratio of the reservoir length to dam height (L/H), the reservoir-foundation interface, the monolith's elastic modulus, the phase of the ground motion between the monolith and the reservoir's far boundary, and the reservoir's far boundary have all been determined to be important aspects in defining the monolith's dynamic and seismic response.

ACKNOWLEDGEMENT

I wish to express my gratitude to my supervisor, Dr. A. Ghobarah, for his interest, guidance, patience, and friendship throughout the course of this research, the preparation of this thesis, and my time at McMaster University. I am especially grateful for his efforts in reviewing the working drafts of this thesis.

The friendship and help offered by all the people involved in the Department of Civil Engineering at McMaster University is gratefully acknowledged.

I would like to especially thank Susan F. Liver for her understanding, encouragement, love, and friendship during the course of this research.

Finally, I would like to thank Elizabeth and Ralph Rea, and Lawrence Baumber for their constant support, understanding, and encouragement throughout the course of my graduate work. This thesis is dedicated to the memory of my father, Anthony Baumber.

TABLE OF CONTENTS

Table of Contents (cont'd)

Table of Contents (cont'd)

Table of Contents (cont'd)

List of Tables

List of Tables (cont'd)

List of Figures

List of Figures (cont'd)

List of Figures (cont'd)

List of Figures (cont'd)

List of Figures (cont'd)

LIST OF NOTATION

a	half of load length
$\ddot{a}_g(t)$	the ground acceleration
C_j	modal damping of mode j
C^2	E_w / ρ_o = square of speed of sound in water
[C]	the damping matrix for the monolith
E_w	bulk modulus of water
F_y	distributed load
G	shear modulus
H	height of dam which is taken the same as the height of reservoir
i	square root of -1
j	integer from 1 to n indicating the mode number of the dam monolith
k	integer indicating soil column
K_j	modal stiffness of mode j
[K]	the stiffness matrix for the monolith
L	length of reservoir
L′	fitted parameter
m	integer ranging from 1 to infinity indicating vertical mode number of reservoir

List of Notation (cont'd)

M_j	modal mass of mode j
[M]	the mass matrix for the monolith
n	integer ranging from 0 to infinity which represents the horizontal mode number of the reservoir
$P(x,y,t)$	pressure, in excess of hydrostatic
$P(x,y,\omega)$	amplitude of pressure at frequency ω
$P_j(x,y,\omega)$	pressure due to vibration of dam in its' j^{th} mode of vibration
$P_o(x,y,\omega)$	pressure due to vibration of dam in its rigid body mode
P_{oj}	pressure acting on centre soil column
P_{+1j}	pressure acting on soil column to the left of centre column
P_{-1j}	pressure acting on soil column to the right of centre column
q	damping caused by the reservoir-foundation interface
$R_{res}(\omega)$	amplitude of the additional hydrodynamic forces at frequency ω
$\{R_{res}\}$	the additional hydrodynamic forces acting on the dam face due to the reservoir
t	time
$u_f(x,y,t)$	horizontal velocity of fluid
$\{u(x,y,t)\}$	the displacement of the monolith
$v_f(x,y,t)$	vertical velocity of fluid
$v(x_s,0)$	vertical displacement of soil
x	horizontal lateral coordinate direction

List of Notation (cont'd)

x_s	horizontal coordinate direction
y	vertical coordinate direction
$Y_j(t)$	modal displacement of j^{th} mode
$Y_j(\omega)$	amplitude of modal displacement at frequency ω
$Y_{tot}(x,y,\omega)$	overall response of the monolith
α	wave reflection coefficient
β_m	vertical separation constant of the m^{th} vertical mode of the reservoir
Γ_1	Participation factor for the first mode of the monolith
Γ_2	Participation factor for the second mode of the monolith
Δx_s	width of soil column (= 2a)
ζ_k	pressure parameter
η_s	equivalent hysteretic damping
Θ	slope of the reservoir bottom
Θ_k	displacement parameter
κ	horizontal separation constant
ν	poisson's ratio
ρ_o	average density of water
$\rho(t)$	density of water
$\phi_j(x,y)$	mode shape of j^{th} mode
$\phi_j^*(0,y)$	mode shape at dam face

List of Notation (cont'd)

ω	frequency of excitation
ω_j	natural circular frequency of mode j
ω_m^r	circular frequency of the m^{th} mode of the reservoir

CHAPTER 1

INTRODUCTION

1.1 BACKGROUND

The evaluation of the ability of a dam to survive earthquakes is an important subject. Dams are constructed in order to impound water for power generation, irrigation, navigation, and flood control. Failure of a dam can result in substantial economic loss and, more importantly, considerable loss of life. The principal types of dams are earth and rock, arch, and concrete gravity dams. The three types of dams behave quite differently during earthquake ground motion because of their different structural systems. The dynamic response and the failure mechanisms also vary with the material used in the construction of the dam. Concrete gravity dams are complex structures to analyze due to the importance of the interaction between the dam monolith, the upstream reservoir, and the foundations.

To simplify the analysis, the majority of available research assumed the reservoir to be infinite in length and completely straight. However, this assumption does not satisfactorily represent the natural reservoir systems. In the case of many dams, the created reservoir is a finite lake while the river becomes an insignificant feature of the system. An example of this type of dam-reservoir-foundation system

is the Pacioma Dam located in California (National Academy Press, 1990). In other cases, the crest of the dam structure may be placed parallel to the river's course. The far bank of the river and the dam structure will thus create a finite length upstream reservoir. Also, rivers tend to meander through the countryside and therefore are never completely straight. A bend in the river's course upstream of the dam in fact creates a finite length reservoir. An example of this type of dam-reservoir-foundation system is the Lower Crystal Springs Dam in California (National Academy Press, 1990).

The primary consideration for siting a dam structure in a particular location is the geological conditions of the surrounding area and especially directly underneath the dam monoliths. The length or geometry of the upstream reservoir that is eventually created has not been considered as a factor that may influence the structural design of the dam. Many dams have been constructed such that this upstream reservoir is finite in length. Examples of a few of the well known dam structures which impound finite length upstream reservoirs are listed in table 1.1. In this research program, an analytical study is conducted to investigate the effect of a finite length reservoir on the response of a concrete gravity dam monolith. The effect of several important reservoir characteristics is investigated.

1.2 INFINITE LENGTH RESERVOIR

Westergaard (1933) was the first to examine the problem of the dynamic forces in a dam-reservoir system. The dam monolith was assumed to be triangular in cross section and the upstream reservoir to be infinite in length. A theoretical pressure distribution assuming that the monolith behaved rigidly was developed. From this pressure distribution, shearing forces and bending moments along the dam height can be determined. The author suggested that these forces be treated as additional static forces to be considered along with the hydrostatic forces that are developed. An approximate pressure distribution which can be used for design purposes was proposed. The author also suggested that the effect of the upstream reservoir could be considered by assuming that it contributes additional mass that moves with the dam monolith.

The earthquake event of December 11, 1967 caused significant damage to the Koyna Dam (Chopra and Chakrabarti, 1972). This is an 85.3 m (280 ft) high concrete gravity dam located in southern India. Significant cracking of the concrete was observed near the change in slope of the monolith's cross section on both the upstream and downstream sides. The experience at the Koyna Dam during the 1967 earthquake event prompted researchers to begin to examine the problem of concrete gravity dams subjected to dynamic loads.

Chopra (1967) analyzed the system assuming that the monolith behaves rigidly. Explicit expressions for the pressures generated in the reservoir were

developed. The reservoir was assumed to be infinite in length. The author realized that the hydrodynamic pressures were dependent on the frequency of excitation of the assumed ground motion. In his study, the ground motion was assumed to be a series of unit harmonics of varying frequencies.

The analysis technique developed by Chopra was expanded several times to incorporate additional components of the system. The behaviour of the dam monolith was assumed to be elastic. The effect of the fundamental mode of vibration of the dam monolith was first considered (Chopra, 1968). It was determined to be very important in the monolith's response. The higher modes of vibration were then incorporated into the analysis by Chakrabarti and Chopra (1973a and b). A more complicated analytical procedure was developed involving the use of a substructuring technique in which the monolith and the reservoir were analyzed separately. The interaction between these two substructures was incorporated through the use of a boundary condition at the reservoir-monolith interface. These studies were also the first to determine the importance of the vertical component of the earthquake ground motion.

The flexibility of the monolith's foundation was considered by Chopra, Chakrabarti, and Gupta (1980). It was found that increasing flexibility of this foundation reduced the magnitude of the monolith's response and the frequency at which the fundamental response peak occurred.

The analytical work conducted thus far by Chopra and his coresearchers solved the equations of motion of the reservoir in a closed form manner. Saini, Bettes, and Zienkiewicz (1978) developed an analysis technique in which the reservoir was modelled using both finite and infinite elements. The reservoir was again assumed to be infinite in length. The results of this study compare well with those obtained by Chopra and his colleagues. Roughly at the same time, Hall and Chopra (1980) also developed a finite element analysis technique for the reservoir substructure. The reservoir was again assumed to be infinite in length. A one-dimensional boundary condition to account for the reservoir-foundation interaction was developed by these authors. The flexibility of the reservoir's foundation was found to reduce the magnitude of the monolith's response (Hall and Chopra, 1980; and Fenves and Chopra, 1984).

A simplified analysis technique was developed by Fenves and Chopra (1985a and b) in which both hydrodynamic and foundation flexibility effects were considered. Methods involving the use of the fundamental mode of vibration alone (Fenves and Chopra, 1985a) and the use of higher modes of vibration (Fenves and Chopra, 1985b) were developed. These techniques enable the designer to perform an analysis of the dam-reservoir-foundation assuming an infinite length reservoir for the initial design of the dam structure.

Several attempts have been made to employ the boundary element technique to the problem of the dam-reservoir-foundation system (Wepf, Wolf, and Bachmann,

1988; and Jablonski and Humar, 1990). The main advantage of this technique is that it permits the analysis of large problems that involve a large number of elements. The boundary element technique only uses the nodes on the boundary of the body to determine the response of the entire system.

Attempts were made to model the behaviour of the monolith after the concrete first experienced cracking (Pal, 1976; El-Aidi and Hall, 1989a and b). Cracking of the concrete was predicted in these studies to occur on both the upstream and downstream sides of the monolith, just below the change in slope of the cross section. This is the same location for cracking as experienced by the Koyna Dam (Chakrabarti and Chopra, 1972). The elastic model developed by Chopra and his colleagues is not capable of predicting the post-cracking behaviour once the tensile capacity of the concrete has been reached.

Leger and Katsouli (1989) examined the problem of stability of the dam monolith during seismic excitation. This study determined that stability considerations are most critical during strong shaking. The authors determined that the static stability safety factors were inadequate to prevent sliding or overturning from occurring during earthquake ground motion. Larger safety factors were therefore suggested in order to ensure stability during major earthquake events.

The linear analysis of the dam-reservoir-foundation system was further developed to incorporate the effects of a sediment layer on the bottom of the upstream reservoir (Cheng, 1986; Medina, Dominquez, and Tassoulas, 1990; and

Bougacha and Tassoulas, 1991a and b). Sediments were considered to increase bottom absorption of the input energy and increase the damping in the system. The layer of sediment was found to primarily affect the magnitude of the frequency at which the fundamental mode of the overall system occurred. The layer of sediment was assumed to be completely saturated. The depth of the layer of sediment also influenced the magnitude of the system's response. The response decreased as the layer increased in thickness. Several of these studies found that assuming that the sediments were partially saturated was more critical than assuming that the sediments were completely saturated.

An experimental study on the behaviour of a dam monolith was conducted (Donlon and Hall, 1989). A scale model of the Pine Flat Dam (California) was developed and tested on a horizontal shake table. The model experienced cracking of the concrete on the upstream and downstream sides just below the change in slope of the monolith's cross section. This result agrees well with both the elastic and inelastic analyses that have been performed in the past on this structure. The elastic analysis (Fenves and Chopra, 1984) and the inelastic analysis (El-Aidi and Hall, 1989b) both determined that the stress experienced by the monolith will cause cracking of the concrete at the same location. It should be noted that the scale model itself was not analyzed numerically using either of the two above mentioned techniques to confirm the results of the shake table experimental study.

Two excellent review papers are available in the literature on the seismic behaviour of dams by Chopra (1987) and Hall (1988). Hall's review article presents a much more detailed review of the subject concentrating on the major experimental work that has been conducted.

1.3 FINITE LENGTH RESERVOIR

Limited work to date has focused on the problem of assuming a finite length upstream reservoir. Hall and Chopra (1980) were the first to examine this problem. They investigated the response of a dam monolith that impounds a finite reservoir of a triangular cross section. The analytical procedure used is similar to that developed by Chopra and his colleagues for the infinite length reservoir problem. The ground motion was assumed to excite both the monolith and the reservoir bottom. The water in the reservoir was assumed inviscid, irrotational, and compressible. The reservoir-foundation interface was modelled using a one-dimensional boundary condition which neglects shear effects. It was discovered that additional response peaks occurred in the Fourier representation of the monolith's response when the finite length assumption was made. These response peaks occurred at excitation frequencies greater than that of the fundamental frequency of the overall system. The finite length reservoir problem was however not explored any further.

Liu (1986) examined the same problem except that the water in the upstream reservoir was assumed to be incompressible. The assumption of the water in the upstream reservoir being incompressible removes the frequency dependency of the reservoir's response. Pressure waves travel principally through changes of the density of the water with time. Including the effects of the compressible nature of water, or its frequency dependent nature, allows the propagation of the pressure waves in the reservoir to be considered. Experimental studies (Duron, 1987) have shown that compressibility effects are very important in the response of concrete dams to dynamic loads. In Liu's study, it was found that the slope of the reservoir's bottom, therefore the length of the reservoir, affected the pressures generated at the dam face. As the length of the reservoir increased, the pressures at the dam face decreased in magnitude.

Antes and Von Estorff (1987) studied the dam-reservoir-foundation problem using the boundary element technique. The reservoir's foundation was modelled assuming that it behaved as a two-dimensional elastic solid. The response of this foundation was therefore modelled by solving the two dimensional wave equation for an elastic solid. The dam monolith itself was assumed to be rigid and the water in the reservoir was assumed to be compressible. The work done by the authors primarily concentrated on the development of the analytical technique utilizing the new model for the reservoir's foundation. The time histories of the hydrodynamic force appear to be comprised of many frequency components. The results of the

finite length reservoir case was not compared to those when the reservoir was assumed infinite in length. The authors examined the effect of varying the value of the elastic modulus of the reservoir's foundation. It was found that as the elastic modulus decreased, the hydrodynamic force also decreased. The case of the far boundary being flexible and the reservoir bottom being rigid was compared to the case when both boundaries were considered rigid. It was determined that the increased flexibility of the far boundary reduced the magnitude of the hydrodynamic force that the monolith experienced.

Aviles and Sanchez-Sesma (1989) showed that the reservoir's length affects the magnitude of the pressures generated at the dam face. The authors showed that the phase of the ground motion between the far boundary and the monolith greatly affects the pressures in a short reservoir. Phase effects were no longer important for a reservoir length to height ratio of three. The water in the reservoir was assumed to be incompressible. The reservoir's equations of motion were solved using a least squares approach.

1.4 RESERVOIR-FOUNDATION INTERACTION

Insufficient research has been conducted into the subject of the interaction between the reservoir and its foundation. This reservoir-foundation interface is a major source of energy dissipation for the dam-reservoir-foundation system. Two main approaches have been used. First, a one dimensional boundary condition was

developed by Hall and Chopra (1980). It was developed based on equilibrium of pressures in the reservoir and the resulting stresses in the foundation. Only vertical equilibrium was considered. This boundary condition had been used to examine the effect of the flexibility of the reservoir's foundation on the monolith's response (Fenves and Chopra, 1984). The boundary condition assumes that the foundation is comprised of a series of independent one-dimensional soil columns. The advantage of this formulation is that it can be incorporated into the reservoir's equations of motion quite easily. The main disadvantage of the formulation is that it neglects the effects of shear stresses that are developed in the foundation. A source of energy dissipation is therefore neglected in the analysis of the reservoir substructure.

The other approach that is used in the analysis of dam-reservoir-foundation systems is to assume that the reservoir's foundation acts as a two-dimensional elastic solid (Cheng, 1986; Antes and Von Estorff, 1987; Medina, Dominquez, and Tassoulas, 1990; and Bougacha and Tassoulas, 1991a and b). The motion of this foundation was therefore governed by the two-dimensional wave equation. The main advantage of this technique is that shear stress effects are considered in the analysis. The effects of a finite layer of sediments on the bottom of the upstream reservoir can be considered as well using this foundation model.

The reservoir-foundation interface is an important source of energy dissipation in the dam-reservoir-foundation system. In order to obtain an accurate estimate of the system's response to earthquake ground motion, this interface must be treated

correctly. The two dimensional approach that has been proposed requires a large number of elements be used to model the foundation. A simplified two dimensional boundary condition is required for design purposes in order that the effect of the shear stresses in the foundation be considered yet still allow the analysis to be performed efficiently.

1.5 OBJECTIVES AND SCOPE

The objective of this research study is to examine the effect of a finite length upstream reservoir on the response of a concrete gravity dam monolith to earthquake ground motion. The parameters of interest are the ratio of the reservoir length to dam height, the model used for the reservoir-foundation interface, the monolith's modulus of elasticity, the cross sectional geometry of the reservoir, and the nature of the ground motion.

To achieve the objective of this research, an analytical study was conducted. There are three components to this investigation. First, a closed form solution of the dam-reservoir-foundation system was developed assuming a finite length upstream reservoir. The effect of the ratio of the reservoir length to the dam height, the value of the wave reflection coefficient, and the value of the monolith's modulus of elasticity were investigated. The ground motion is assumed to excite the dam monolith only and takes the form of a series of unit harmonics of varying frequencies. Second, a detailed analytical procedure for the dam-finite reservoir-

foundation system was established using the finite element technique. A two-dimensional model for the reservoir-foundation interface was developed. This detailed analytical procedure is utilized to investigate the effect of the ratio of the reservoir length to dam height, the model for the reservoir-foundation interface, and the cross sectional geometry of the upstream reservoir on the response of the monolith. The ground motion is assumed to affect both the far end boundary of the finite length reservoir and the dam monolith. Lastly, a stress analysis using four actual earthquake ground motion records was performed. The effect of the finite reservoir assumption on the dynamic tensile stresses developed in the monolith was investigated.

In this thesis, the closed form solution technique for the dam-finite reservoir-foundation system is described in Chapter 2. The results of a parametric study assuming that the ground motion only excites the monolith are presented. A simplified analytical technique is also developed in this chapter. Chapter 3 presents the formulation of the detailed analysis technique. The verification of this analytical technique is also presented. Chapter 4 presents the results of a numerical study conducted using the detailed analytical technique assuming that the ground motion excites both the far boundary of the finite length upstream reservoir and the dam monolith. The results of the stress analysis are presented in Chapter 5. The conclusions of the study are summarized in Chapter 6.

Table 1.1 - Examples of the finite reservoir configurations

Dam	Location	Length[1],(L) (m)	Height,(H) (m)	L/H	Type[2]
Xiang Hong Dian[3]	China	400	87.5	4.6	A
Quan Shui[4]	China	200	80	2.5	A
Monticello[5]	USA	1750	93	18.8	A
Techi[6]	Taiwan	1600	180	8.9	A
Crystal[7]	USA	1750	181	9.7	G
Gray Canyon[7]	USA	1000	175	5.7	G
Koyna[8]	India	2000	103	19.4	G
Pine Flat[9]	USA	1340	122	11.0	G
St. Francis[10]	USA	305	56.4	5.4	A
Manuel M. Dieguez[11]	Mexico	100	114	0.9	A
La Soledad[11]	Mexico	300	91.5	3.3	A

[1] Reservoir lengths were determined from maps of the particular area, approximate
[2] Type: A = Arch Dam; G = Gravity Dam
[3] Clough, et. al., 1984a
[4] Clough, et. al., 1984b
[5] Clough, et. al., 1987
[6] Clough, et. al., 1982
[7] Mandzhavidze and Mamradze, 1966
[8] Chopra and Chakrabarti, 1972
[9] Fenves and Chopra, 1984
[10] Outland, 1977
[11] Secretaria de Recursos Hidraulicos, 1976

CHAPTER 2

DAM - FINITE RESERVOIR SYSTEM

2.1 INTRODUCTION

In this chapter, a simplified procedure for the analysis of dam-finite reservoir systems is presented. The reservoir's system of equations are solved in a closed form to yield explicit expressions for the pressures on the dam monolith. These pressures are then introduced into the overall analysis technique for the dam-reservoir-foundation system. The procedures for the analysis of each separate substructure are first discussed in detail. This is followed by discussion of the overall solution approach. The results obtained from the presented analytical procedure are then compared to available solutions of special cases existing in the literature. This is done in order to verify the proposed analytical technique. In particular, the proposed procedure is compared to the work of Fenves and Chopra (1984b) in which the upstream reservoir is considered to be infinite in length.

The next section of this chapter deals with the response of the dam-finite reservoir system obtained using the present analytical technique. First, the effect of the finite length assumption on the pressures in the reservoir is discussed. Next, the effect of the reservoir length to dam height ratio on the overall system's response is

examined. The effect of the wave reflection coefficient on the system's response is also studied. Finally, the effect of the dam's stiffness on the response of the dam-reservoir system is evaluated. The last section of this chapter presents a simplified analysis procedure intended for use during initial design stages.

2.2 ANALYTICAL PROCEDURE

The analytical procedure used in this study utilizes a frequency domain substructuring technique. The dam-reservoir-foundation system is divided into three separate subsystems. These are the dam monolith, the dam's foundation, and the upstream reservoir. The dam substructure is considered to be a two-dimensional elastic solid. The monolith is assumed to be under plane stress conditions. The construction joints between monoliths are assumed smooth and frictionless. Neighbouring monoliths are considered not to interact with one another. The foundation underneath the dam monolith is considered to be a visco-elastic half space. The reservoir substructure is analyzed assuming a finite reservoir length. The reservoir is idealized as a rectangular tank of length L, and height H. The height of the dam and of the reservoir are assumed to be equal. A schematic representation of the physical system is shown in figure 2.1. The far boundary is assumed to be unaffected by the earthquake ground motion. This boundary is assumed to be rigid except for its absorptive capacity. The bottom of the reservoir and the far boundary are assumed to have the same absorptive capacity. This absorptive capacity is

modelled using the boundary condition developed by Hall and Chopra (1980). Analytical expressions for the pressures in the finite length reservoir are derived and used to determine the response of the dam monolith. The ground acceleration is assumed to be a unit harmonic of varying frequency. It is also assumed to act only in the horizontal direction. The vertical component of the ground motion has been shown to cause considerable motion of the monolith (Fenves and Chopra, 1984b; and Hall and Chopra, 1980). The response of the dam-finite reservoir-foundation system to the vertical component of the earthquake ground motion is left for future research. Addition of the vertical component requires only a few simple modifications to the analytical procedure. Only the first two modes of vibration are considered in this analysis.

2.2.1 The Monolith Substructure

The dynamic response of a concrete gravity dam is governed by the standard equations of motion for a structure subjected to earthquake ground motion (Clough and Penzien, 1975), as given by:

$$[M]\ \{\ddot{u}(x,y,t)\} + [C]\ \{\dot{u}(x,y,t)\} + [K]\ \{u(x,y,t)\} = -[M]\ \ddot{a}_g(t) + \{R_{res}(t)\} \quad (2.1)$$

where:

[M]	= the mass matrix for the monolith
[C]	= the damping matrix for the monolith
[K]	= the stiffness matrix for the monolith
{u(x,y,t)}	= the displacement of the monolith
$\ddot{a}_g(t)$	= the ground acceleration
$\{R_{res}(t)\}$	= the additional hydrodynamic forces acting on the dam face due to the reservoir
x	= horizontal lateral coordinate direction
y	= vertical coordinate direction
t	= time

The contribution of the upstream reservoir is represented by a new term on the right hand side of equation (2.1). This term represents the additional loading on the dam face due to the pressures generated in the reservoir.

Equation (2.1) can be simplified by expressing the displacements in terms of the modes of vibration of the dam monolith.

$$\{u(x,y,t)\} = \sum_{j=1}^{n} Y_j(t)\ \{\phi_j(x,y)\} \quad (2.2)$$

where :

$Y_j(t)$	= modal displacement of j^{th} mode
$\phi_j(x,y)$	= mode shape of j^{th} mode
j	= integer from 1 to n indicating the mode number of the dam monolith

Substitution of equation (2.2) into equation (2.1) and premultiplying by the transpose of the mode shape vector yields a reduced system of equations:

$$M_j \ddot{Y}_j(t) + C_j \dot{Y}_j(t) + K_j Y_j(t) = -\{\phi_j(x,y)\}^T [M] \ddot{a}_g(t) + \{\phi_j(x,y)\}^T \{R_{res}(t)\} \quad (2.3)$$

where M_j = modal mass of mode j
C_j = modal damping of mode j
K_j = modal stiffness of mode j

The modal displacements, $Y_j(t)$, and the added forces due to the reservoir, $R_{res}(t)$, are assumed to have a harmonic time dependency. This is expressed in equations (2.4) and (2.5).

$$Y_j(t) = Y_j(\omega) e^{i\omega t} \quad (2.4)$$

where: ω = frequency of excitation
$Y_j(\omega)$ = amplitude of modal displacement at frequency ω
i = square root of -1

$$R_{res}(t) = R_{res}(\omega)\, e^{i\omega t} \tag{2.5}$$

where: $R_{res}(\omega)$ = amplitude of the additional hydrodynamic forces at frequency ω

The ground acceleration is assumed to be a unit harmonic impulse.

$$\ddot{a}_g(t) = e^{i\omega t} \tag{2.6}$$

Substitution of equations (2.4), (2.5), and (2.6) into equation (2.3) yields the reduced equations of motion of the dam monolith in the frequency domain.

$$[-\omega^2 M_j + i\,\omega\, C_j + K_j]\, Y_j(\omega) = -\{\phi_j(x,y)\}^T [M] + \{\phi_j(x,y)\}^T \{R_{res}(\omega)\} \tag{2.7}$$

Converting the modal damping and stiffness to their equivalent modal mass terms and assuming constant hysteretic damping, the dam's equation of motion takes the form:

$$[-\omega^2 + (1+i\eta_s)\ \omega_j^2]\ M_j\ Y_j(\omega) = -\{\phi_j(x,y)\}^T\ [M] + \{\phi_j(x,y)\}^T\ \{R_{res}(\omega)\} \tag{2.8}$$

where: ω_j = natural circular frequency of mode j
η_s = equivalent hysteretic damping

All quantities are known in equation (2.8) except for that of the additional hydrodynamic forces, $R_{res}(\omega)$. This term can be evaluated by examining the reservoir substructure.

2.2.2 The Reservoir Substructure

The motion of the water in the reservoir is assumed to be inviscid, non-convective, and irrotational. The equations that describe the motion of the fluid are therefore the simplified Navier-Stokes equations.

$$\rho(t)\ \frac{\partial u_f(x,y,t)}{\partial t} = -\frac{\partial P(x,y,t)}{\partial x}$$

$$\rho(t)\,\frac{\partial \dot{v}_f(x,y,t)}{\partial t} = -\frac{\partial P(x,y,t)}{\partial y} \qquad (2.10)$$

where:

$\rho(t)$	= density of water
$\dot{u}_f(x,y,t)$	= horizontal velocity of fluid
$\dot{v}_f(x,y,t)$	= vertical velocity of fluid
$P(x,y,t)$	= pressure, in excess of hydrostatic

The continuity equation for a compressible fluid can be written as:

$$\frac{\partial \rho(t)}{\partial t} + \frac{\partial(\rho(t)\dot{u}_f(x,y,t))}{\partial x} + \frac{\partial(\rho(t)\dot{v}_f(x,y,t))}{\partial y} = 0 \qquad (2.11)$$

In fluid mechanics, water is usually considered as an incompressible fluid since its density does not fluctuate significantly with time. Pressure waves are, however, transmitted by changes in the fluid's density. Fluctuations in density must therefore be allowed so that the pressures can propagate in the reservoir. To allow these density fluctuations but yet still maintain the assumption of a constant density, Lamb's (1945) relationship between the pressure in the water and its density is used:

$$\rho(t) = \rho_o + \frac{\rho_o P(x,y,t)}{E_w} \tag{2.12}$$

where: ρ_o = average density of water
E_w = bulk modulus of water

As the density of the water is only changing slightly, it is assumed to vary with time but not space. The spatial derivatives of the density are therefore equal to zero. Only the derivative of the density with respect to time has a non-zero value. Equation (2.12) can now be substituted into equation (2.11) to yield:

$$\frac{1}{E_w}\frac{\partial P(x,y,t)}{\partial t} + \frac{\partial \tilde{u}_f(x,y,t)}{\partial x} + \frac{\partial \tilde{v}_f(x,y,t)}{\partial y} = 0 \tag{2.13}$$

Equation (2.13) represents the continuity equation for an incompressible fluid that still accounts for the time-dependent nature of the pressure in the reservoir.

Combining equations (2.9), (2.10), and (2.13) and eliminating the x and y component of the fluid particle velocity yields an equation which describes the spatial and temporal variation of pressure in the reservoir:

$$\frac{\rho_o}{E_w}\frac{\partial^2 P(x,y,t)}{\partial t^2} - \frac{\partial^2 P(x,y,t)}{\partial x^2} + \frac{\partial^2 P(x,y,t)}{\partial y^2} \tag{2.14}$$

If the pressure is assumed to have an harmonic time variation as well, it can be expressed as:

$$P(x,y,t) = P(x,y,\omega)\, e^{i\omega t} \tag{2.15}$$

where: $P(x,y,\omega)$ = amplitude of pressure at frequency ω

Introducing equation (2.15) into equation (2.14) yields:

$$\nabla^2 P(x,y,\omega) + \frac{\omega^2}{C^2} P(x,y,\omega) = 0 \tag{2.16}$$

where: $C^2 = E_w / \rho_o$ = square of speed of sound in water

This equation, along with the appropriate boundary conditions, describe the distribution of pressure in the reservoir. The boundary conditions of the finite reservoir system are presented in equations (2.17) to (2.20).

$$\frac{\partial P}{\partial x}(0,y,\omega) = -\rho_o + \omega^2 \rho_o \sum_{j=1}^{n} \{\phi_j^x(0,y)\} Y_j(\omega) \qquad (2.17)$$

where: $\phi_j^x(0,y)$ = mode shape at dam face

$$\frac{\partial P}{\partial x}(-L,y,\omega) = +i\ \omega\ q\ P(-L,y,\omega) \qquad (2.18)$$

where: q = damping caused by the reservoir-foundation interface
L = length of reservoir

$$\frac{\partial P}{\partial y}(x,0,\omega) = +i\ \omega\ q\ P(x,0,\omega) \qquad (2.19)$$

$$P(x,H,\omega) = 0 \qquad (2.20)$$

where: H = height of dam which is taken the same as the height of reservoir

The boundary condition given in equation (2.17) represents the acceleration of the dam face. The first term on the right hand side represents the absolute acceleration of the dam in its rigid body mode. This acceleration is proportional to the density of the fluid. The second term represents the relative acceleration of the

dam in its individual modes of vibration. Equations (2.18) and (2.19) represent the pressure gradients due to the absorptive capacity of the far boundary and the bottom of the reservoir, respectively. The absorption capacity of the reservoir's foundation is modelled according to the one-dimensional boundary condition developed by Hall and Chopra (1980). In this formulation, the stress generated in the reservoir's foundation is assumed to propagate away from the reservoir in a direction normal to the reservoir-foundation interface. Equation (2.20) states that the pressure at the free surface of the reservoir is zero. Previous work (Chopra, 1967) has shown that the surface waves have a negligible effect on the pressures in the reservoir and can therefore be neglected.

The pressures in the reservoir, at a specific frequency of excitation, can now be determined by solving equation (2.16) subject to the boundary conditions of equations (2.17) to (2.20). Equation (2.16) is solved by using the separation of variables technique. The principle of superposition is used on equation (2.17) so that the pressures due to the rigid body mode and the individual modes of vibration of the dam monolith are determined separately.

$$P_o(x,y,\omega) = +2\rho_o \sum_{m=1}^{\infty} \frac{\beta_m^2 \, I_{om}(\omega) \, [\, e^{\kappa x} \, (\frac{\kappa + i\omega q}{\kappa - i\omega q}) + e^{-2\kappa L} \, e^{-\kappa x} \,] \, \tilde{Y}(y,\omega)}{\kappa \, [\, (\frac{\kappa + i\omega q}{\kappa - i\omega q} - e^{-2\kappa L} \,] \, [\, H \, (\beta_m^2 - (\omega q)^2) + i\omega q \,]} \quad (2.21)$$

where: $P_o(x,y,\omega)$ = pressure due to vibration of dam in its rigid body mode

β_m = vertical separation constant of the m^{th} vertical mode of the reservoir

m = integer ranging from 1 to infinity indicating vertical mode number of reservoir

κ = horizontal separation constant

$$P_j(x,y,\omega) = -2\omega^2\rho_o \sum_{m=1}^{\infty} \frac{\beta_m^2 \, I_{jm}(\omega) \, [\, e^{\kappa x} \, (\frac{\kappa + i\omega q}{\kappa - i\omega q}) + e^{-2\kappa L} \, e^{-\kappa x} \,] \, \tilde{Y}(y,\omega) \, Y_j(\omega)}{\kappa \, [\, (\frac{\kappa + i\omega q}{\kappa - i\omega q}) - e^{-2\kappa L} \,] \, [\, H \, (\beta_m^2 - (\omega q)^2) + i\omega q \,]} \quad (2.22)$$

where: $P_j(x,y,\omega)$ = pressure due to vibration of dam in its' j^{th} mode of vibration

$$\tilde{Y}(y,\omega) = \frac{1}{2\beta_m} \, [\, (\beta_m + \omega q) \, e^{i\beta_m y} + (\beta_m - \omega q) \, e^{-i\beta_m y} \,] \quad (2.23)$$

$$I_{om}(\omega) = \int_0^H \tilde{Y}_m(y,\omega)\, dy \tag{2.24}$$

$$I_{jm} = \int_0^H \tilde{Y}_m(y,\omega)\, \phi_j(0,y)\, dy \tag{2.25}$$

$$\kappa = \sqrt{\beta_m^2 - \left(\frac{\omega}{C}\right)^2} \tag{2.26}$$

The solution to these boundary value problems are given in equations (2.21) and (2.22). Equation (2.21) is the closed form solution representing the pressures in the reservoir due to the vibration of the dam monolith in its rigid body mode. Equation (2.22) is the closed form solution representing the pressures in the reservoir due to the vibration of the monolith in its j^{th} mode of vibration.

2.2.3 Solution Procedure

The equations of motion are solved numerically. The mass and stiffness matrices for the dam monolith are generated using the finite element technique. The additional stiffness resulting from the foundation underneath the dam monolith is

calculated assuming that it behaves as a visco-elastic half-space. Mode shapes and frequencies of vibration of the monolith are first calculated assuming an empty reservoir.

To calculate the added modal force terms, the additional hydrodynamic forces, resulting from the effects of the reservoir, equations (2.21) and (2.22) were multiplied by the individual mode shapes and this product integrated over the height of the dam, H. To perform these integrations in a closed form, a parabola was fitted to the first two modes of vibration.

The earthquake ground motion used in this study was assumed as a unit harmonic that has an acceleration magnitude of 0.305 m/s^2 (1 ft/s^2). The response determined from the analysis is therefore the Fourier representation of the response. This means that the response of the structure is determined for discrete values of the frequency of excitation over a specific range. The response of the structure to the ground motion is determined for each mode individually. The Fourier representations of the individual modes' responses are combined using a straight sum of the product of the monolith's modal response and the appropriate mode shapes. This combination rule is given in equation (2.27).

$$Y_{tot}(x,y,\omega) = \sum_{j=1}^{n} Y_j(\omega)\ \phi_j(x,y) \qquad (2.27)$$

where: $Y_{tot}(x,y,\omega)$ = overall response of the monolith

The response of the monolith is non-dimensionalized by dividing by the magnitude of the unit harmonic. The frequency of excitation is normalized to the dam's fundamental frequency excluding reservoir interaction effects.

2.3 VERIFICATION OF ANALYTICAL PROCEDURE

In deriving the expressions for the pressure components given by equations (2.21) and (2.22), a finite length reservoir upstream of the dam is assumed. As the length of the reservoir increases, the pressure components are expected to approach those derived by Fenves and Chopra (1984b) for an infinite length reservoir. At the limit as the length of the reservoir approaches infinity in equations (2.21) and (2.22), the pressure at the dam face (x = 0) is given by the following two equations:

$$P_o(0,y,\omega) = -2\rho_o \sum_{m=1}^{\infty} \frac{\beta_m^2\ I_{om}(\omega)\ \bar{Y}(y,\omega)}{\kappa_m\ [\ H\ (\beta_m^2 - (\omega q)^2\ ) + i\omega q\ ]} \qquad (2.28)$$

$$P_j(0,y,\omega) = +2\omega^2\rho_o \sum_{m=1}^{\infty} \frac{\beta_m^2 \, I_{jm}(\omega) \, \bar{Y}_m(y,\omega) \, Y_j(\omega)}{\kappa_m \, [\, H \, (\beta_m^2 - (\omega q)^2) + i\omega q \,]} \qquad (2.29)$$

These two equations are identical to the expressions derived by Fenves and Chopra (1984b). The same coordinate system was used in deriving their expressions as was used in this study.

A second verification of the analytical procedure dealt with the response of the dam monolith. This is intended to verify both the analytical method and the computer program developed to perform this analysis. As the ratio of the reservoir's length to the dam's height (L/H) increases to infinity, the results obtained should approach those determined when an infinite length reservoir is assumed. A 91.44 m (300 ft.) dam, idealized as having a triangular cross section, was analyzed. The downstream face has a slope of 0.8:1 as illustrated in figure 2.1. The elastic modulus of the concrete was taken to be 18 600 MPa (2.7 million psi). This modulus is low for most of the concrete typically used in practice. This value was selected so as to be able to directly compare the approach and solutions in this study to those of Fenves and Chopra (1984b). The dam's foundation was assumed to be rigid. The water level in the reservoir was taken to be equal to the dam's height. The reservoir's foundation was considered absorptive and the wave reflection coefficient was taken to be 0.9. Two modes of vibration were considered in this analysis. Only

the monolith's fundamental mode of vibration was considered in the analysis performed by Fenves and Chopra (1984b).

Four curves representing the response of the dam monolith for L/H ratios of 5, 10, 20, and 40, are shown in figure 2.2. When the finite length boundary condition is imposed on the system, many additional peaks are created in the response. When the L/H ratio is equal to 5 (heavy solid line), several distinct peaks are evident in the response. These occur at normalized frequencies greater than one. These peaks are referred to as supplementary response peaks. As the L/H ratio increases to 10, the number of these supplementary response peaks increase. The magnitude of these peaks decreases. This is presented in figure 2.2 by the thin dotted line. Eventually, for very long reservoirs (L/H = 40), the response of the monolith with a finite length reservoir is practically identical to that of a monolith with an infinite length reservoir. The response of a monolith with a reservoir that has an L/H ratio of 40 is presented by the thin solid line in figure 2.2. The heavy dotted line in figure 2.2 represents the response when the reservoir is assumed infinite in length. This curve is the same as that determined by the analytical procedure of Fenves and Chopra (1984b). As evident from these two curves, the response of the system approaches that of the system when the reservoir is considered to be infinite in length as the L/H ratio increases.

2.4 RESPONSE OF DAM

The cross section of a dam monolith is essentially triangular with a rectangular area situated at the top of the section. This additional area is needed to support a roadway and to provide for other services for the dam. In this study, however, the cross section is idealized as having a triangular shape as shown in figure 2.1. This triangular section is sometimes referred to as the structural section. Neglecting the mass and stiffness of the rectangular shaped top section will affect the computed frequencies and mode shapes. This in turn will affect the dynamic stresses that are caused by the earthquake ground motion. Chopra and Chakrabarti (1972) illustrated this point using the Pine Flat Dam cross section subjected to the Koyna earthquake of December 11, 1967. Inclusion of the top rectangular section lead to a lengthening of the fundamental period (excluding reservoir effects) by approximately 14%. It was also found that the maximum principal dynamic stresses varied significantly between the two cases. This idealization is made, however, as it is of interest to compare the overall response of a dam monolith to earthquake ground motion assuming finite and infinite length reservoirs and to be able to compare with available solutions. Although it may not be possible to obtain the monolith's true response to the ground motion using the structural section, a qualitative comparison of the monolith's relative response can still be made. Incorporating the additional mass at the top of the monolith can be accomplished relatively simply once the analytical procedure has been established.

The dam monolith selected for analysis in this study is 91.44 m high with a downstream slope of 0.8:1. The foundation under the dam monolith was considered to be rigid. Two values of elastic moduli for the dam's concrete were used. These values were 18 600 MPa and 42 000 MPa. These are considered to be the extremes of the range of typical concrete properties. These values for the concrete modulus allow direct comparison with the work of Fenves and Chopra (1984b).

In addition to the monolith stiffness, two other parameters were varied to determine their effect on the monolith's overall response. First, five values were used in this study for the ratio of the reservoir's length to the dam's height (L/H). The values used were 10, 7.5, 5, 2.5, and 1. Reservoirs of a length that is smaller than the height of the dam were deemed unrealistic. When the ratio of the reservoir length to dam height is greater than 10, the monolith response was found to approach the response of the infinite reservoir case. Cases of L/H ratios greater than 10 were found not to provide any more information about the behaviour than a reservoir with an L/H value of 10.

The second parameter to be evaluated was the wave reflection coefficient. This parameter was varied from 1.0 to 0.0 in intervals of 0.1. A value of 1.0 implies that the reservoir's foundation is completely reflective. A value of 0.0 implies maximum absorption of the pressure waves.

2.4.1 Pressures In Reservoir

When the reservoir is considered to be infinite in length, the pressures are only allowed to propagate in the upstream direction. These pressure waves are assumed to decay exponentially as they travel away from the dam face. Therefore, these waves carry energy away from the dam face. The only pressures that significantly affect the monolith are those that are travelling in the vertical direction. If the reservoir's foundation is considered to be completely reflective, the pressure waves oscillate vertically with frequencies given by (Fenves and Chopra, 1984b):

$$\omega_m^r = \frac{(2m - 1)\,\pi\, C}{2\, H} \tag{2.30}$$

where ω_m^r = circular frequency of the m^{th} mode of the reservoir

The magnitudes of the pressures on the dam face, and therefore the response of the monolith, are infinite at these frequencies if the reservoir-foundation interface is considered to be completely reflective. This can be seen by examining equations (2.28) and (2.29). The denominator of these equations must be zero in order that the magnitude of the pressure becomes infinite. As the second term does not vanish, the horizontal separation constant of the system therefore must be equal to zero. Using equations (2.26) and (2.30), the horizontal separation constant is given by the following expression.

$$\kappa = \sqrt{\left[\frac{(2m-1)\,\pi}{2H}\right]^2 - \frac{\omega^2}{C^2}} \qquad (2.31)$$

When the frequency of excitation is such that κ in equation (2.31) is zero, the magnitude of the pressure becomes infinite. This is resonance of the pressures in the reservoir. Resonance only occurs at frequencies equal to those of the vertical separation constants because of the assumed behaviour of the horizontal component of the pressure.

When the finite reservoir length condition is imposed, the horizontal component of the pressure waves are allowed to travel both upstream and downstream in the reservoir. In this case, the pressures given by equations (2.21) and (2.22) will have infinite magnitudes when the reservoir's bottom is assumed completely reflective. As for the infinite length case, the denominator of these expressions must be zero. In this case, there are two conditions that will cause the magnitudes of the pressures to be infinite. The first condition is that the horizontal separation constant is zero. This implies a vertical pressure wave that decays exponentially upstream. This is identical to the infinite length reservoir case.

The second condition for an infinite pressure magnitude is when the second term in the denominator of equations (2.21) and (2.22) becomes zero. This condition is expressed by the formula:

$$\left(\frac{\kappa + i\,\omega\,q}{\kappa - i\,\omega\,q}\right) - e^{-2\kappa L} = 0 \qquad (2.32)$$

When the reservoir's foundation is considered to be completely reflective, this equation has imaginary valued roots, κ, and are found to be equal to integer multiples of π/L. This can be thought of as resonance of the reservoir in the horizontal direction.

The vertical and horizontal separation constants, β_m and κ_n, can be substituted into equation (2.26) which can be rearranged to yield the natural circular frequencies of the reservoir in the form:

$$\omega = C\sqrt{\left[\frac{(2m - 1)\,\pi}{2\,H}\right]^2 + \left[\frac{n\,\pi}{L}\right]^2} \qquad (2.33)$$

where n = integer ranging from 0 to infinity which represents the horizontal mode number of the reservoir

When n is equal to zero in equation (2.33), the calculated frequency is for resonance in the vertical direction. The frequency of excitation for the condition of horizontal resonance ($n \neq 0$) is a combination of both the vertical and horizontal separation constants of the reservoir. This implies that there is coupling of these two components.

When the reservoir's foundation is considered to be absorptive, the vertical and horizontal separation constants are no longer solely real and imaginary valued,

respectively. The separation constants are shifted in magnitude and each have both real and imaginary components.

2.4.2 Effect of Length to Height (L/H) Ratio

The pressure spikes that occur at the resonant frequencies of the reservoir will in turn affect the response of the dam monolith. For an infinite length reservoir, peak responses will occur in two instances. First, response peaks are expected at frequencies which correspond to the natural frequencies of the dam monolith. The response peak occurring at a normalized frequency of 2.08 in figure 2.2 (heavy dotted line) is an example of this type of peak. For these types of peaks, a portion of the water in the reservoir can be thought of as vibrating with the dam monolith. This has the affect of adding mass and additional damping to the monolith. The additional mass will tend to reduce the resonant frequencies of the monolith from the values when the reservoir is assumed empty. This results, for example, in the fundamental frequency of the monolith to be less than a normalized frequency of one. The additional damping will tend to reduce the magnitude of the monolith's response.

The second cause of response peaks is the additional hydrodynamic forces that are the result of resonance of the reservoir. The fundamental response peak shown in figure 2.2 (heavy dotted line) is an example of this type of peak. For reservoirs having an infinite length, this resonance causes significant pressures to occur at the

frequencies associated with the vertical separation constants of the reservoir. The pressures generated in the reservoir act on the dam face and induce a hydrodynamic force onto the monolith. The pressures, and therefore the additional hydrodynamic forces, have peak values at these frequencies. The additional hydrodynamic forces will then in turn cause the dam monolith to vibrate. This mechanism results in the creation of the response peak at the frequencies associated with the vertical resonance of the reservoir.

Similar effects occur when the constraint of a finite length reservoir is added to the system. The presence of the far end boundary of the reservoir causes additional eigen frequencies to occur in the reservoir. As mentioned earlier, these frequencies are associated with the horizontal resonance of the pressures in the reservoir. Additional hydrodynamic forces are created at these frequencies as well. The additional frequency components of these forces cause additional response peaks to occur in the same manner as described in the infinite case. These additional peaks are shown in figure 2.3. This figure represents the response of a monolith with a reservoir having an L/H ratio of 5. The modulus of elasticity of the dam's concrete material is 18 600 MPa. The first peak at a frequency of approximately 0.8 in this figure is due to the vibration of the dam monolith in its fundamental mode. This peak is also affected by the force created by the resonance of the reservoir in its fundamental vertical eigen mode. The peaks to the right of this fundamental peak are due to the effects of the additional hydrodynamic forces. The small peak directly

to the right of the fundamental response peak is due to the resonance of the pressures in the reservoir in its eigen mode corresponding to its fundamental vertical and horizontal separation constants. This peak has a very small magnitude and is located at a normalized frequency of approximately 1.0. The next several response peaks (normalized frequencies of 1.23 and 1.49) are due to the resonance of the pressures in its eigen modes corresponding to the coupled fundamental vertical and the second and third horizontal separation constants, respectively.

As the frequency of excitation increases towards the second mode of the dam monolith, the monolith's modes no longer solely dominate the response. The effects of the additional hydrodynamic forces caused by the coupled horizontal and vertical resonances of the pressures amplify the motion caused by the resonance of the monolith's second mode. This is contrary to the infinite length case where the resonance of this mode dominates over the effects of the hydrodynamic forces. In this case, the resonant frequencies of the monolith and the reservoir do not coincide.

As the L/H ratio increases from one to ten, the number additional frequency components present in the response increases. This can be seen by comparing figures 2.4, 2.5, and 2.6. These figures represent the overall response of a dam having a modulus of 18 600 MPa and L/H ratios of 1, 5, and 10, respectively. The wave reflection coefficient is equal to 0.9. This phenomena is explained by examination of equation (2.33). This equation is applicable for the case where the bottom of the reservoir is completely reflective (wave reflection coefficient equal to

one). The separation constants of the horizontal components of the pressures are inversely proportional to the length of the reservoir. The spacing between the separation constants therefore decreases as the reservoir length increases. This in turn causes an increase in the number of frequencies at which additional hydrodynamic forces occur. An increase in the number of response peaks therefore also occurs. Similar effects are seen for other values of the wave reflection coefficient. The length of the reservoir affects the monolith's response in a similar manner for other values of the wave reflection coefficient.

2.4.3 Effect of Wave Reflection Coefficient

The wave reflection coefficient is an indicator of the absorptive capacity of the reservoir's foundation. This coefficient ranges from a value of 1.0 to 0.0. When the coefficient has a value of 1.0, the pressure wave coming into contact with the reservoir-foundation interface is completely reflected back into the reservoir. The reservoir-foundation interface provides no additional damping to the reservoir substructure. The maximum amount of energy from the pressure wave is absorbed into the foundation when the wave reflection coefficient has a value of 0.0. The interface provides the greatest amount of additional damping at this coefficient value. The additional damping (equation (2.19)) is a result of the increased flexibility of the reservoir's foundation as the value of the wave reflection coefficient decreases. The

relationship between the wave reflection coefficient, α, and the additional damping, q, provided at the interface is presented in equation (2.34).

$$q = \frac{1}{C}\left(\frac{1 - \alpha}{1 + \alpha}\right) \tag{2.34}$$

The response of a monolith impounding a reservoir having an L/H ratio of 5 is presented in figure 2.7. The wave reflection coefficient has values of 0.9, 0.7, and 0.5. The magnitude of the fundamental response peak decreases as the wave reflection coefficient decreases as can be seen in figure 2.7.

The response at frequencies greater than that of the fundamental mode is significantly affected by the value of the wave reflection coefficient. The supplementary response peaks that are created by the coupled vertical and horizontal resonance of the pressure waves are infinite in magnitude when the wave reflection coefficient is equal to 1.0. This represents the case of a completely reflective reservoir bottom. The magnitudes of the supplementary response peaks become finite and decrease as the value of this coefficient decreases. Eventually for small values of the coefficient, the response of the monolith approaches the response when the reservoir is considered to be infinite in length. In this case, the pressures resonating horizontally in the reservoir are damped out leaving only the vertically resonating components of pressure acting on the dam face.

Figure 2.8 presents the relationship between the L/H ratio and the wave reflection coefficient at which the finite reservoir response is no longer significantly different than that of the infinite reservoir response. The responses were considered to be significantly different if the difference in magnitude between the two cases at any frequency of excitation is greater than one percent. For example, the finite reservoir effects are no longer present at a wave reflection coefficient value of 0.5 when the L/H ratio is equal to 5 (figure 2.7). The response of the dam monolith when finite reservoir effects are considered approaches that of the infinite case for larger wave reflection coefficient values when the L/H ratio is large. When the reservoir is considered to be long, an increased length of reservoir bottom is available to dissipate energy from this sub-structure.

The added mass for the fundamental mode of a monolith impounding a reservoir having L/H ratios of one and infinity (wave reflection coefficient equal to 0.9) are presented in figure 2.9. The added mass is calculated using the formula presented by Fenves and Chopra (1984b) and equation (2.22). The modal mass, M_1, has a value of 1.0. It can be seen from the figure that the added mass that is created by a finite length reservoir is greater than that created by an infinite reservoir for frequencies less than that of the fundamental frequency of the monolith. This increased added mass causes a decrease in the frequency of the monolith's fundamental mode. This can be seen in figure 2.10 which represents the response of the monolith investigated in figure 2.9. This shift is approximately two percent

and can be explained by the change in magnitude of the pressures created in a short finite length reservoir. This frequency shift is a direct result of the increased pressures that occur in the reservoir.

As the wave reflection coefficient decreases, the amount of the frequency shift is reduced. The change in the frequency shift can be seen by comparing figures 2.10, 2.11, and 2.12. These figures represent the response of a monolith impounding a reservoir having an L/H ratio equal to one (heavy solid line) and infinity (light solid line). The wave reflection coefficient has values of 0.9, 0.7, and 0.5 for figures 2.10, 2.11, and 2.12, respectively. As the amount of bottom absorption increases, the change in the added mass relative to the infinite length case decreases. This decreasing relative change in magnitude of the added mass therefore results in the frequency shift between the two cases to decrease as well.

The decrease in the magnitude of the fundamental response peak can also be seen by comparing figures 2.10, 2.11, and 2.12. This effect can be explained by examining the value of the added damping at this peak's frequency. The added damping is calculated using the formula presented by Fenves and Chopra (1984b) and equation (2.22). The absolute magnitude of the added damping is larger when the reservoir is finite in length than when the reservoir is infinite in length. For a wave reflection coefficient of 0.9, the added modal damping values are 0.076 and 0.025 for the finite and infinite length cases, respectively. This is comparable to twice the damping ratio multiplied by the modal mass of the monolith. This product

has a value of 0.1. As the value of the coefficient decreases, the added damping becomes larger. For a wave reflection coefficient value of 0.7, the modal damping values increase to 0.182 and 0.076, for the finite and infinite length cases, respectively. The large increase in the added damping value for the finite length case causes the response peak's magnitude to be significantly reduced.

The added modal damping values further increase to 0.185 and 0.110 when the wave reflection coefficient value is reduced to 0.5. The peak for the infinite length reservoir case continues to reduce in magnitude whereas the peak for the finite length case does not decrease as significantly as seen in figure 2.12. This is due to the small increase in the added damping that occurs for the finite length reservoir between the cases where the wave reflection coefficient is 0.7 and 0.5. The increase in the added damping values therefore is responsible for the decrease in magnitude of the fundamental peak.

2.4.4 Effect of Dam's Stiffness

The dashed line in figure 2.13 presents the response of a monolith impounding an infinite length reservoir. The monolith has an elastic modulus of 42 000 MPa and the reservoir has a wave reflection coefficient of 0.9. Supplementary response peaks are again created when the upstream reservoir is assumed to be finite in length. The finite reservoir assumption allows the reservoir to resonate in the horizontal as well as in the vertical direction. The effect of the finite reservoir length assumption can

be seen in the solid line presented in figure 2.13. This curve represents the response of the monolith when a reservoir having an L/H ratio of 5 is impounded. The supplementary response peaks have significant magnitudes near the resonant frequencies of the monolith substructure. This is similar to the case of a more flexible (E_s = 18 600 MPa) monolith.

The response below a normalized frequency of one must be noted. The principal effect caused by an increase in the dam monolith's elastic modulus is to change the shape of the fourier representation of its response. The most significant change occurs at normalized frequencies below one. Two distinct response peaks are present when the reservoir is considered to be infinite in length and the dam's elastic modulus is increased to 42 000 MPa. These two peaks are well defined when the elastic modulus is large because there is sufficient separation between the fundamental vertical eigen frequency of the reservoir and the frequency of the fundamental mode of the dam monolith. For more flexible dams (18 600 MPa), these two peaks are fused into a single peak. There is not sufficient separation between the reservoir's eigen frequency and the fundamental frequency of the monolith. This result for the finite length reservoir case confirms earlier conclusions by Fenves and Chopra (1984b) for the infinite length reservoir case.

The peak at a normalized frequency of 0.62 is a result of the response of the dam monolith to the added force created by the resonance of the reservoir in its fundamental pure vertical eigen mode. The next two supplementary response peaks

are created by the response of the monolith to the added forces created by the resonance of the reservoir in its eigen modes corresponding to its first vertical and its first and second horizontal separation constants, respectively. The second supplementary response peak is also influenced by the resonance of the monolith itself in its fundamental mode of vibration. This can be seen in this peak's increased magnitude relative to that of the first supplementary response peak.

The frequency shift and magnitude reduction that occur at the fundamental response peak when the reservoir is considered to be short is also present for stiff dams. This is presented in figure 2.14. The solid line presents the response of a dam monolith impounding a reservoir having an L/H ratio of 1.0. The wave reflection coefficient is taken equal to 0.9. The dashed line in this figure is the response of the system when the reservoir is considered to be infinite in length. The L/H ratio at which this occurs is however increased as the dam's stiffness increases. This magnitude reduction and frequency shift first occurs at an L/H ratio of 2.5 when the dam's elastic modulus is 42 000 MPa. This is contrary to a flexible dam monolith, where this effect first occurs at an L/H ratio of 1.0. The finite length assumption also increases the magnitude of the system's response at the higher frequencies as in the case of a more flexible dam monolith.

The increasing value of the modulus of elasticity of the monolith results in the monolith's modes of vibration interacting with the reservoir's modes at different frequencies. This can be seen in comparing figures 2.3 and 2.13. The increasing

stiffness of the dam monolith results in its frequencies of vibration to increase in value. This in turn results in the monolith's modes exciting different reservoir modes. The response of the monolith therefore will be significantly different for the various values of the monolith's modulus of elasticity.

2.5 SIMPLIFIED ANALYSIS PROCEDURE

The closed form solution technique can be simplified to produce an analysis that is intended for initial design procedures. The effects of the finite length reservoir on the response of the dam monolith are considered. In the derivation of this analysis, it is assumed that two modes of vibration are important in the overall response of the dam. The reservoir is idealized as being rectangular in geometry. The dam's foundation is assumed to be completely rigid. Under these assumptions, equation (2.8) can be simplified to the following set of equations:

$$Y_2(\omega) = \frac{\left[F2 - \frac{(F1)\,(Z21)}{Z11} \right]}{\left[Z22 - \frac{(Z12)\,(Z21)}{Z11} \right]} \tag{2.35}$$

$$Y_1(\omega) = \frac{[\ F1 - (Z12)\ Y_2(\omega)\ ]}{Z11} \tag{2.36}$$

where:

$$Z11 = (\ -\omega^2 + 2i\omega\omega_1\varepsilon_1 + \omega_1^2)\ M_j + \omega^2\ M^*_{11} \tag{2.37}$$

$$Z12 = \omega^2\ M^*_{12} \tag{2.38}$$

$$Z21 = \omega^2\ M^*_{21} \tag{2.39}$$

$$Z22 = (-\omega^2 + 2i\omega\omega_2\varepsilon_2 + \omega_2^2\ )\ M_2 + \omega^2\ M^*_{22} \tag{2.40}$$

$$F1 = -\Gamma_1 + \int_0^H \phi_1(0,y)\ P_o(0,y,\omega)\ dy \tag{2.41}$$

$$F2 = -\Gamma_2 + \int_0^H \phi_2(0,y)\ P_o(0,y,\omega)\ dy \tag{2.42}$$

$$M^{\star}_{11} = \int_0^H \phi_1(0,y)\ P_1(0,y,\omega)\ dy \tag{2.43}$$

$$M^{\star}_{22} = \int_0^H \phi_2(0,y)\ P_2(0,y,\omega)\ dy \tag{2.44}$$

$$M^{\star}_{21} = \int_0^H \phi_2(0,y)\ P_1(0,y,\omega)\ dy \tag{2.45}$$

$$M^{\star}_{12} = \int_0^H \phi_1(0,y)\ P_2(0,y,\omega)\ dy \tag{2.46}$$

Γ_1 and Γ_2 are participation factors for the first and second modes of the monolith, respectively.

In order to conduct the simplified analysis procedure, a separate dynamic analysis is first performed on the dam monolith to determine its dynamic characteristics. These include the frequencies of free vibration ω_1 and ω_2 and the mode shapes. These characteristics are then used to evaluate equations (2.37), (2.40), (2.41), and (2.42). The closed form solution for the pressures in a finite length rectangular reservoir given by equations (2.21) and (2.22), and the parabolic approximation for the monolith's mode shape, are used to evaluate the remaining terms. The modal responses are once again combined using equation (2.27).

In order to evaluate the accuracy of the proposed simplified procedure, a numerical example is analyzed and the response obtained from the simplified procedure is compared with the closed form solution. Consider the case of a monolith impounding a reservoir having an L/H ratio of 5.0 and a triangular cross

section. The monolith height was assumed to be 91.44 m with a downstream slope of 0.8:1. The modulus of elasticity of the concrete used was assumed to be 18 600 MPa. The response obtained using both the closed form solution technique and the simplified procedure are plotted in figure 2.15. The simplified approach underestimates the response by 7.6%. The closed form solution technique predicts this response to be 31.4 and the simplified method predicts it to be 29.0.

The supplementary response peaks are also predicted quite accurately. The response peak at an excitation frequency of 8.74 Hz has its magnitude overestimated by 10.5% as compared to the closed form solution. The response peaks that occur at higher frequencies are predicted with less accuracy as the excitation frequency increases. The accuracy of both techniques begins to diminish as the frequency of excitation becomes greater than that of the second mode of vibration of the monolith. This occurs since only two modes of vibration are considered in both of the analyses.

This simplified analysis technique is effective in determining the response of the system to earthquake ground motion when it is assumed to only excite the monolith. The ground motion must only have significant energy at frequencies less than that of the monolith's second mode of vibration. Typically, this frequency range is similar to that at which both intermediate and high a/v ground motion events have significant energy. In this example, the frequency range that is applicable is from 0 to 15 Hz. The analysis procedure can not accurately predict the response of the

system at higher frequencies. More modes of vibration must be included in the dynamic analysis in order to obtain an accurate estimate of the response at these frequencies.

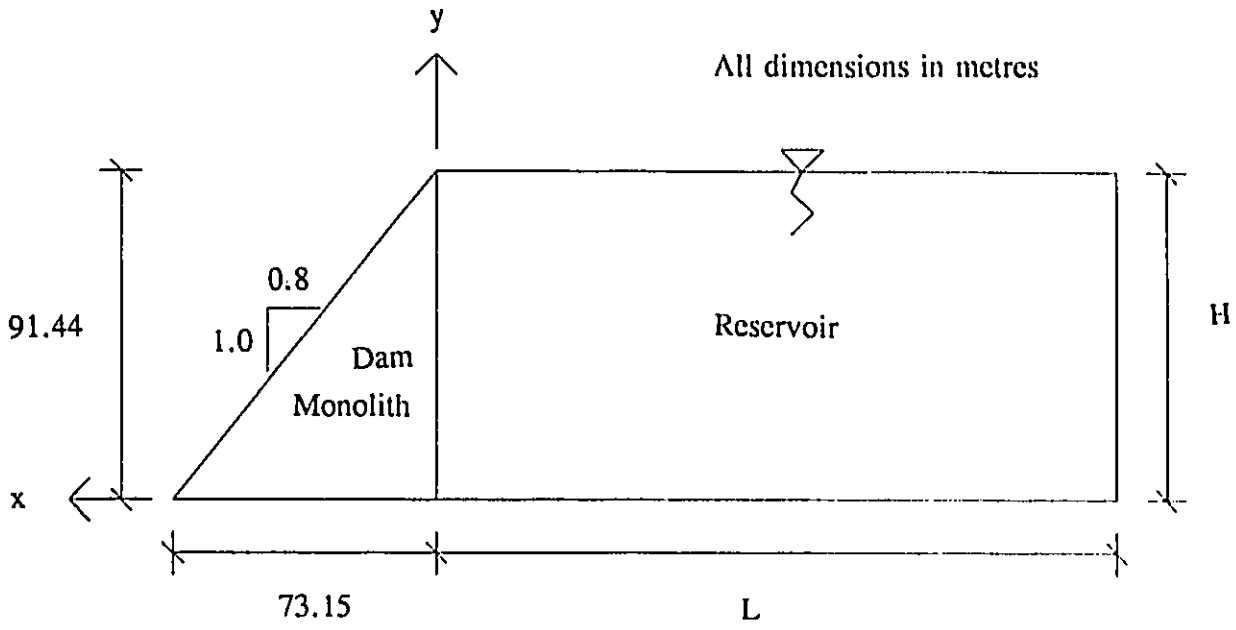

Figure 2.1 - Schematic representation of dam - finite reservoir system

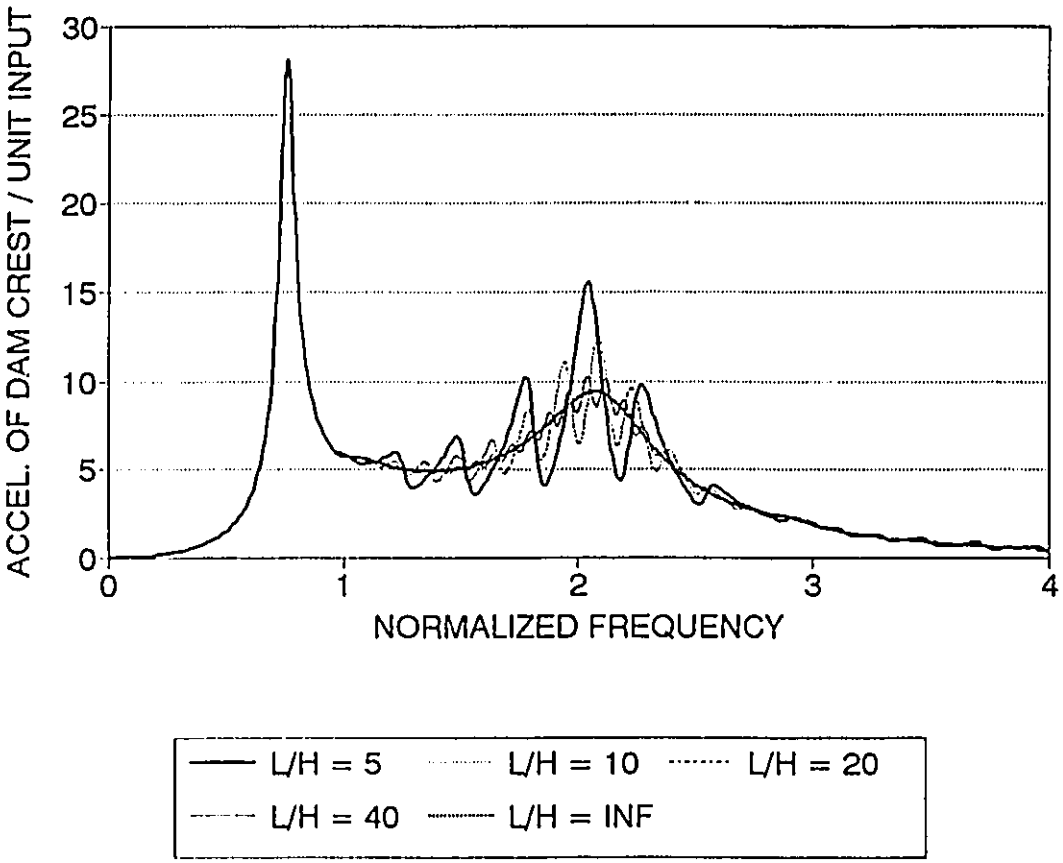

Figure 2.2 - Effect of L/H ratio on monolith response

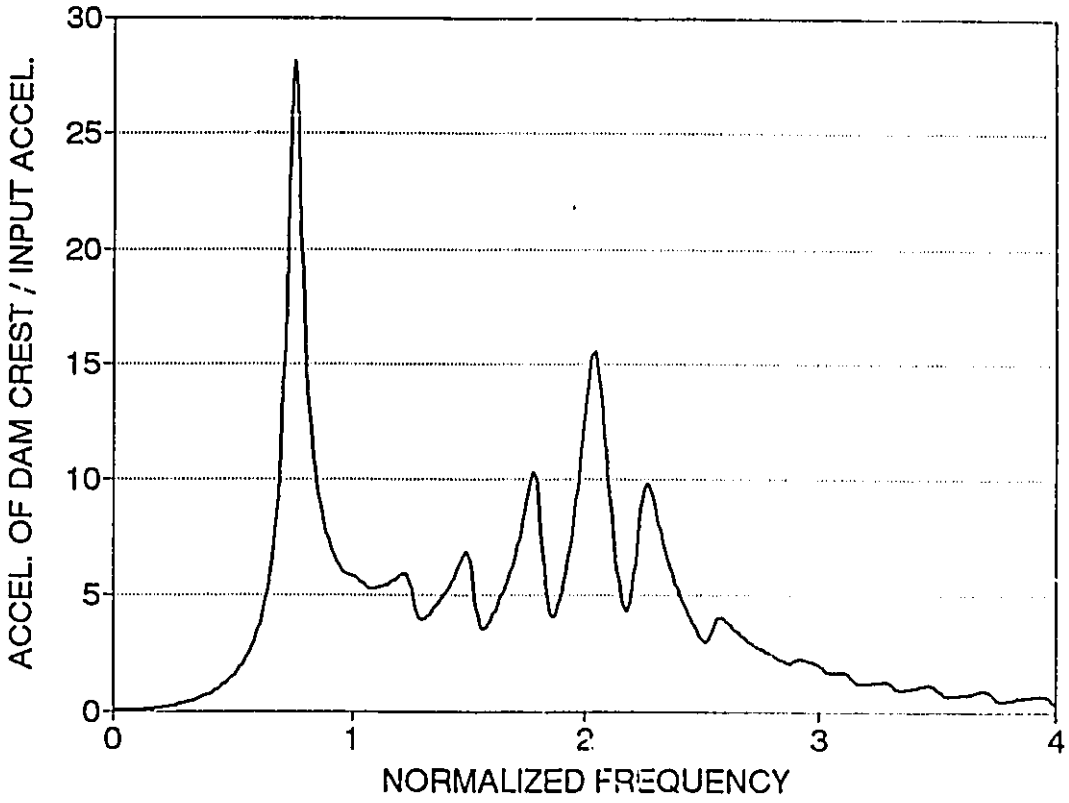

Figure 2.3 - Response of monolith - reservoir L/H = 5.0

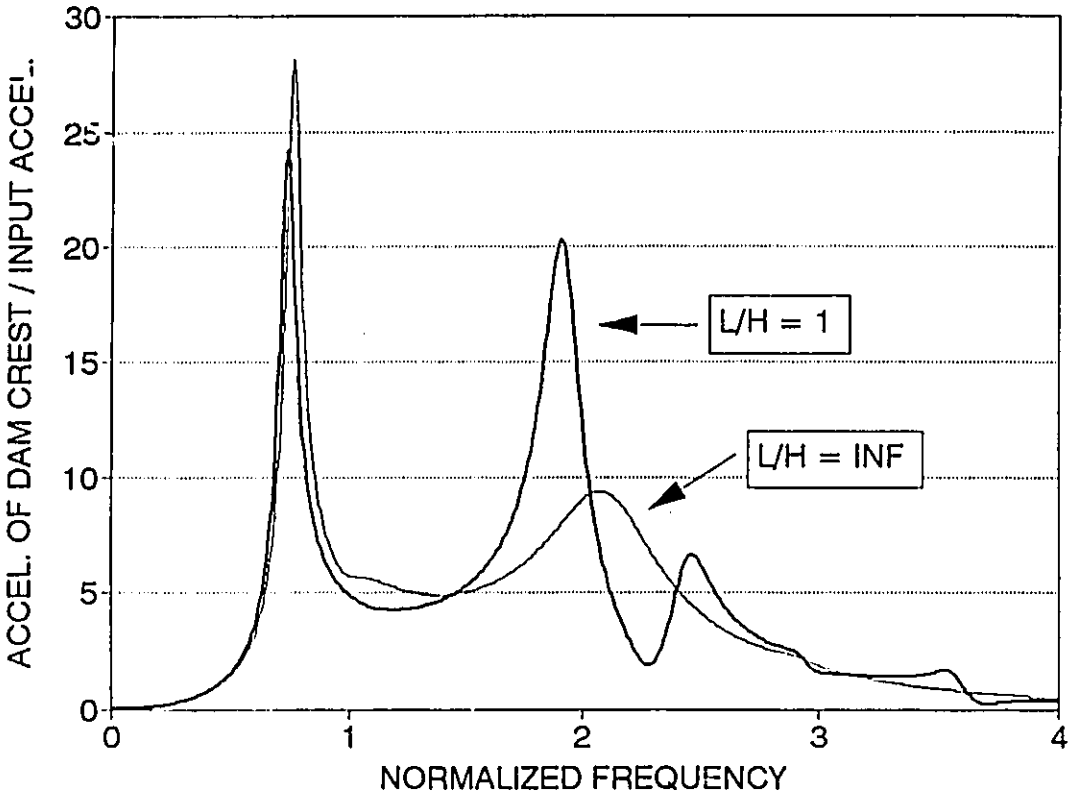

Figure 2.4 - Response of monolith impounding reservoirs of both L/H = 1 and infinite

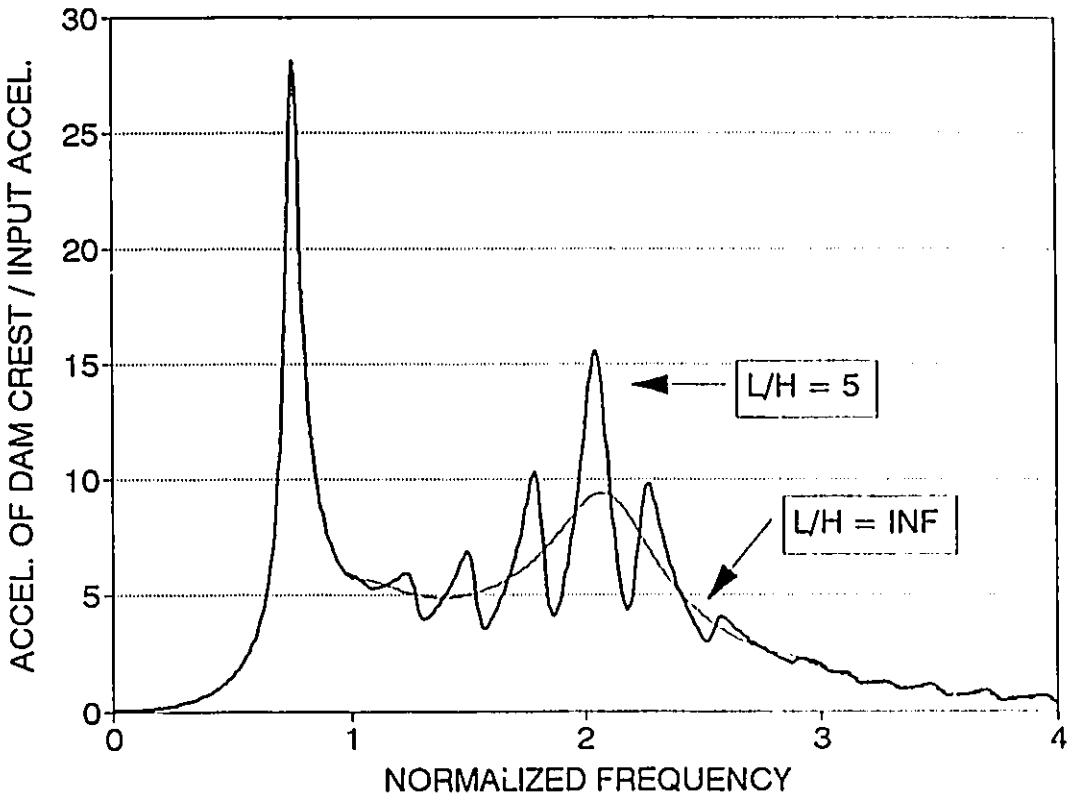

Figure 2.5 - Response of monolith impounding reservoirs of both L/H = 5 and infinite

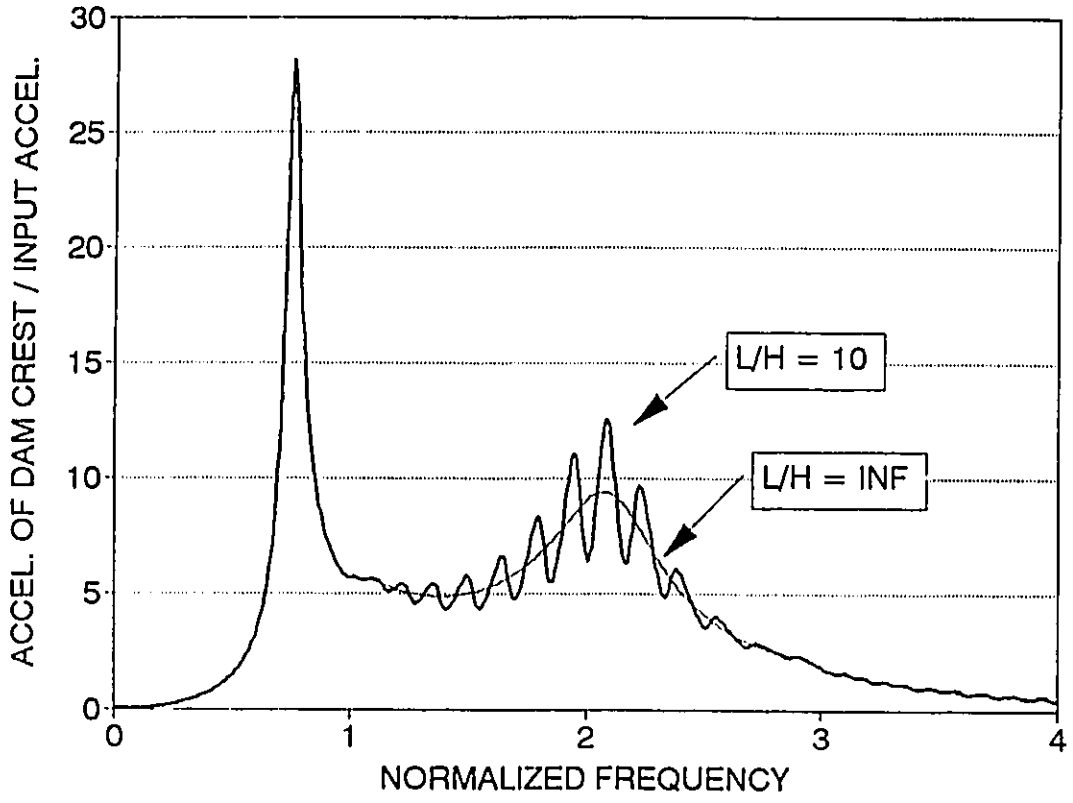

Figure 2.6 - Response of monolith impounding reservoirs of both L/H = 10 and infinite

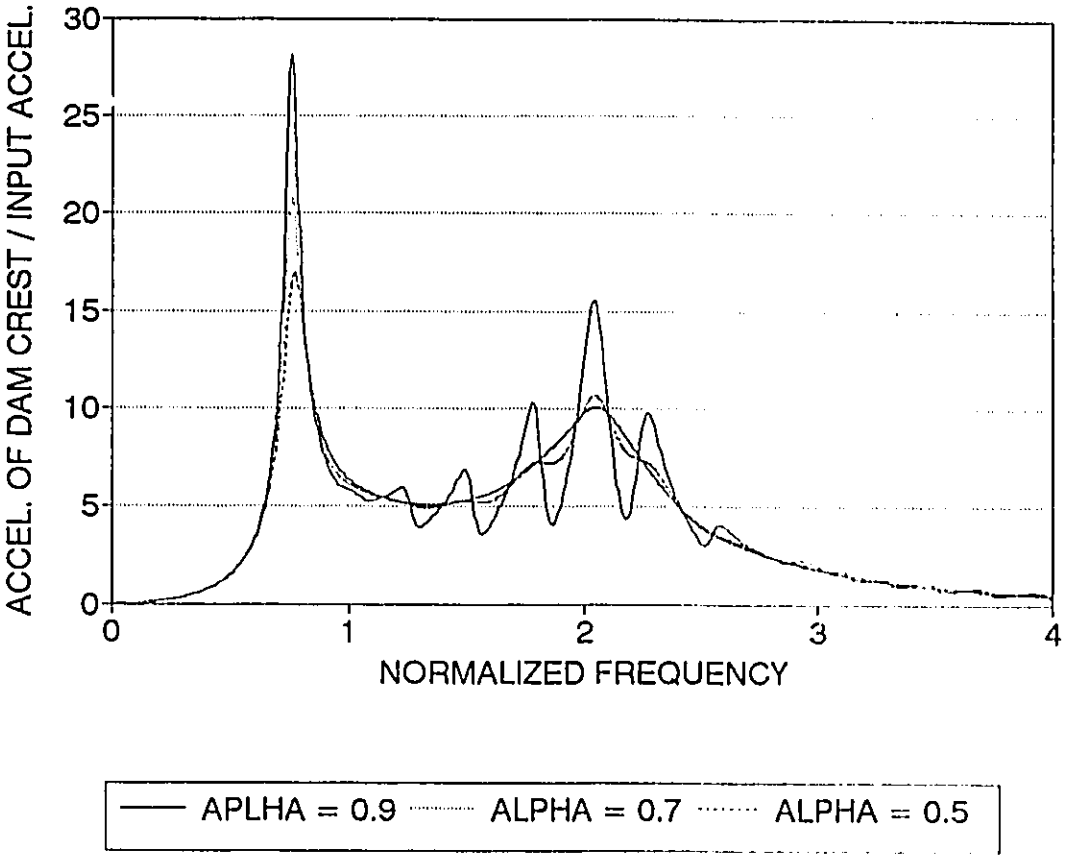

Figure 2.7 - Effect of the wave reflection coefficient - reservoir L/H = 5

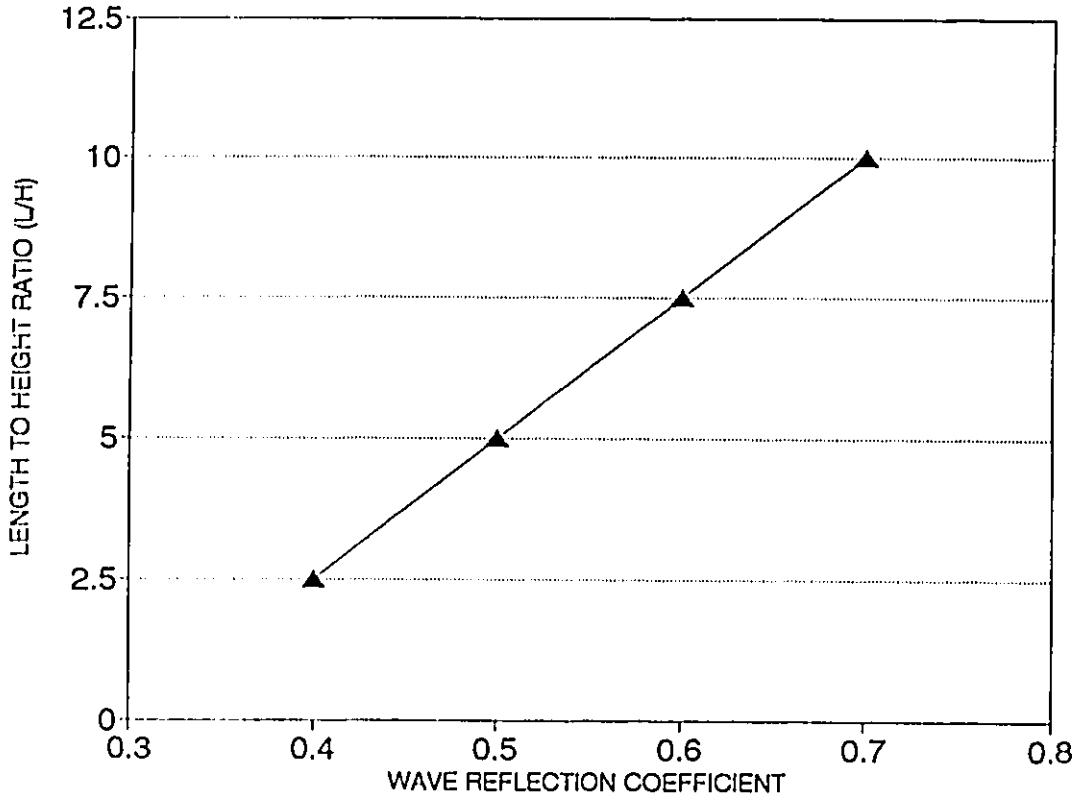

Figure 2.8 - Value of wave reflection coefficient at which finite reservoir effects are not apparent

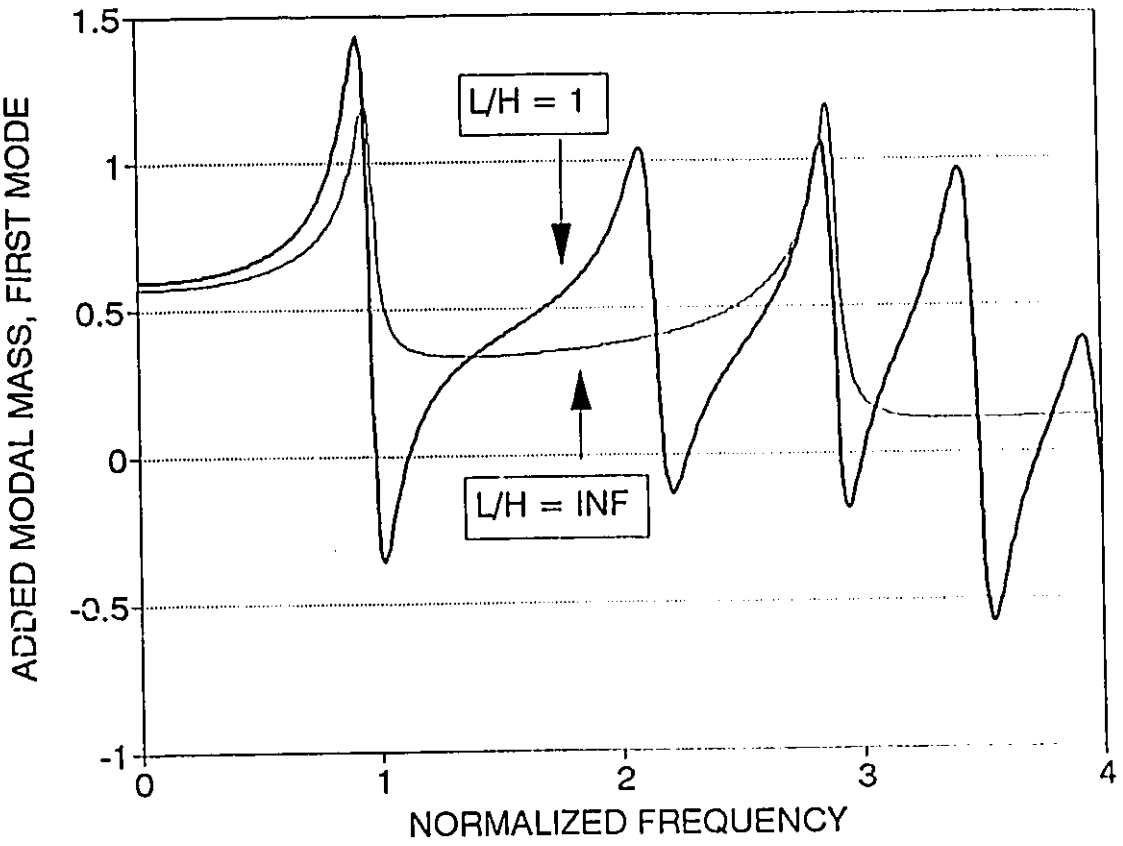

Figure 2.9 - Added modal mass for infinite and L/H = 1 cases

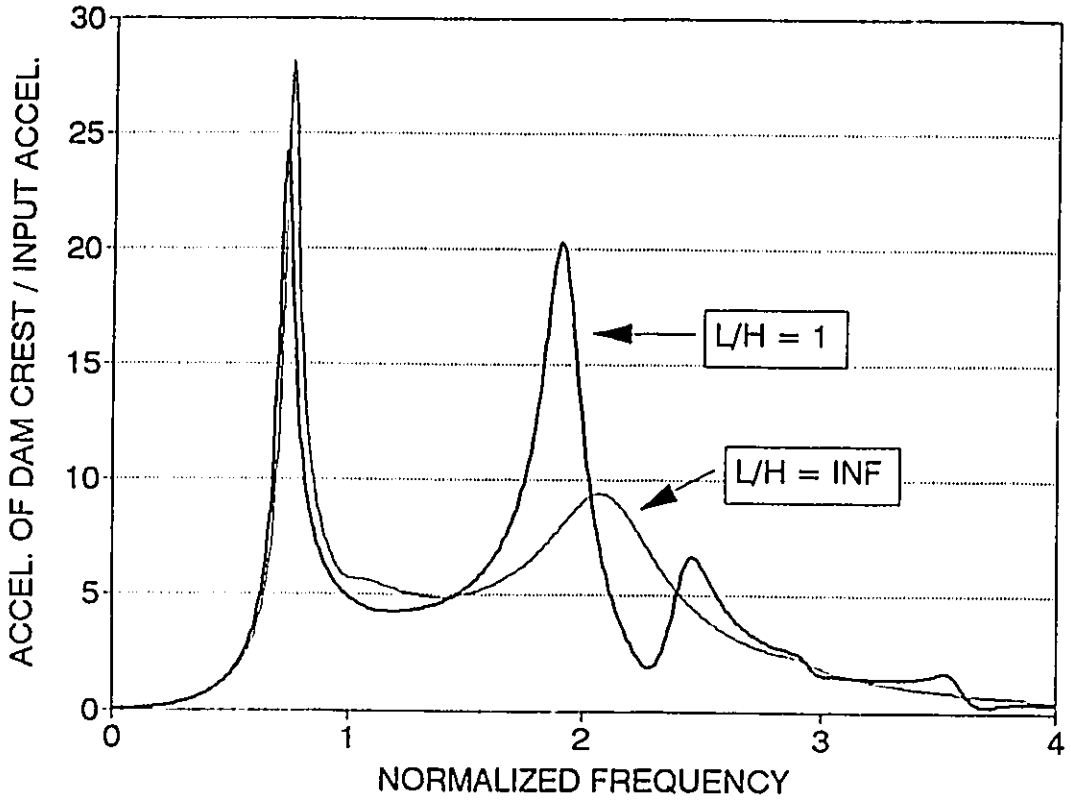

Figure 2.10 - Response of monolith,
wave reflection coefficient = 0.9

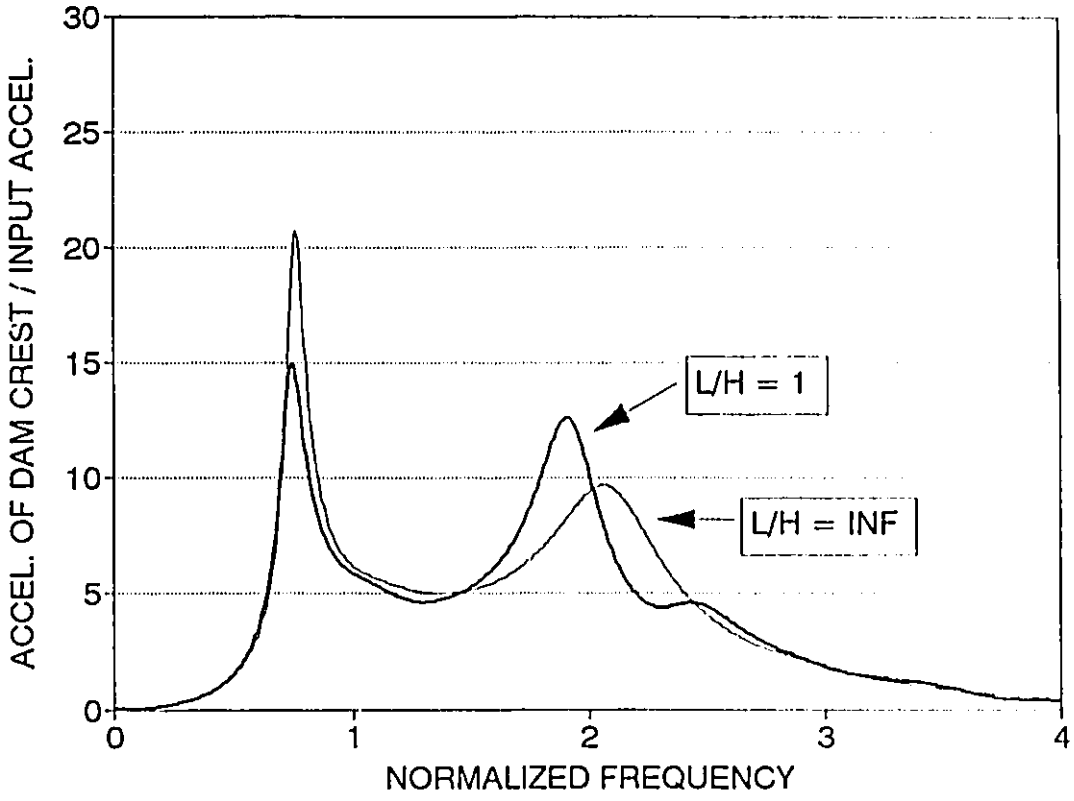

Figure 2.11 - Response of monolith,
wave reflection coefficient = 0.7

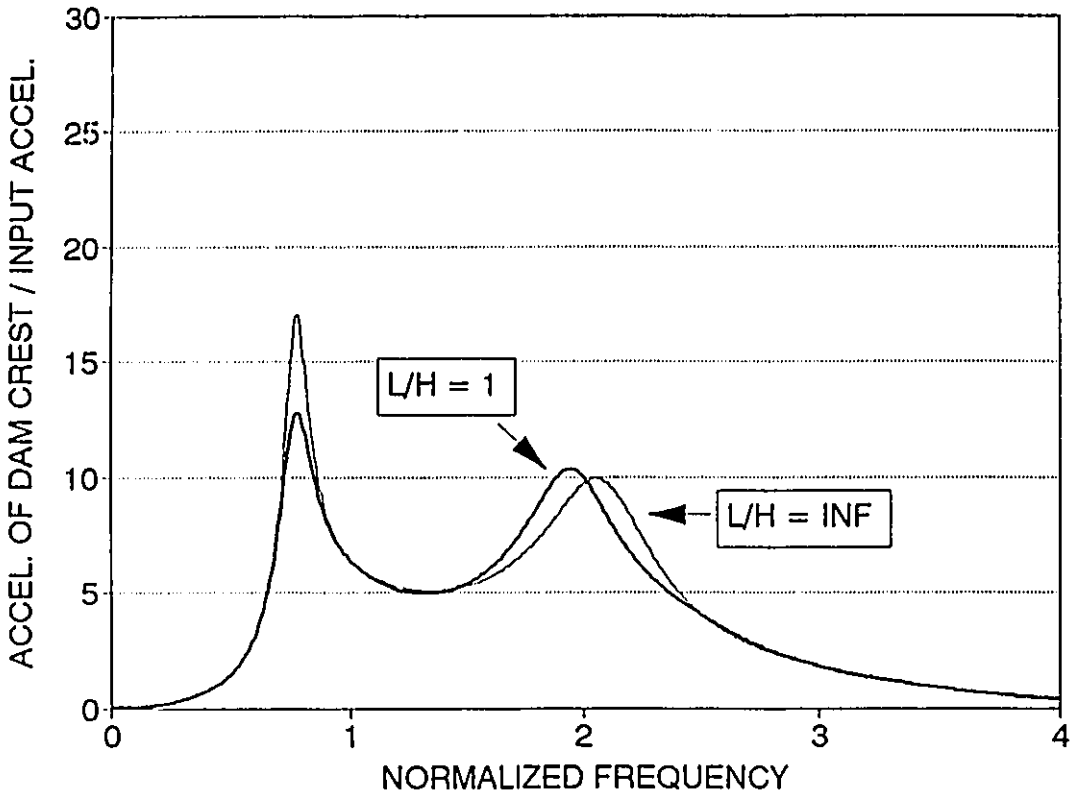

Figure 2.12 - Response of monolith,
wave reflection coefficient = 0.5

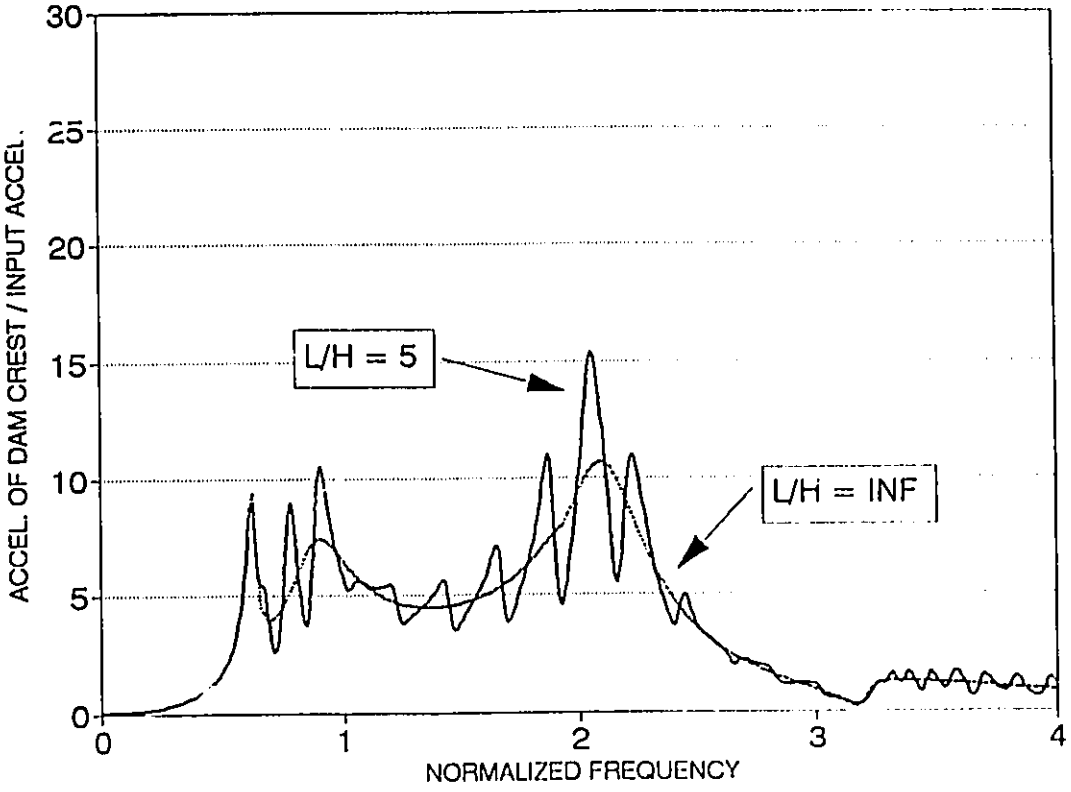

Figure 2.13 - Response of stiff monolith, $L/H = 5$

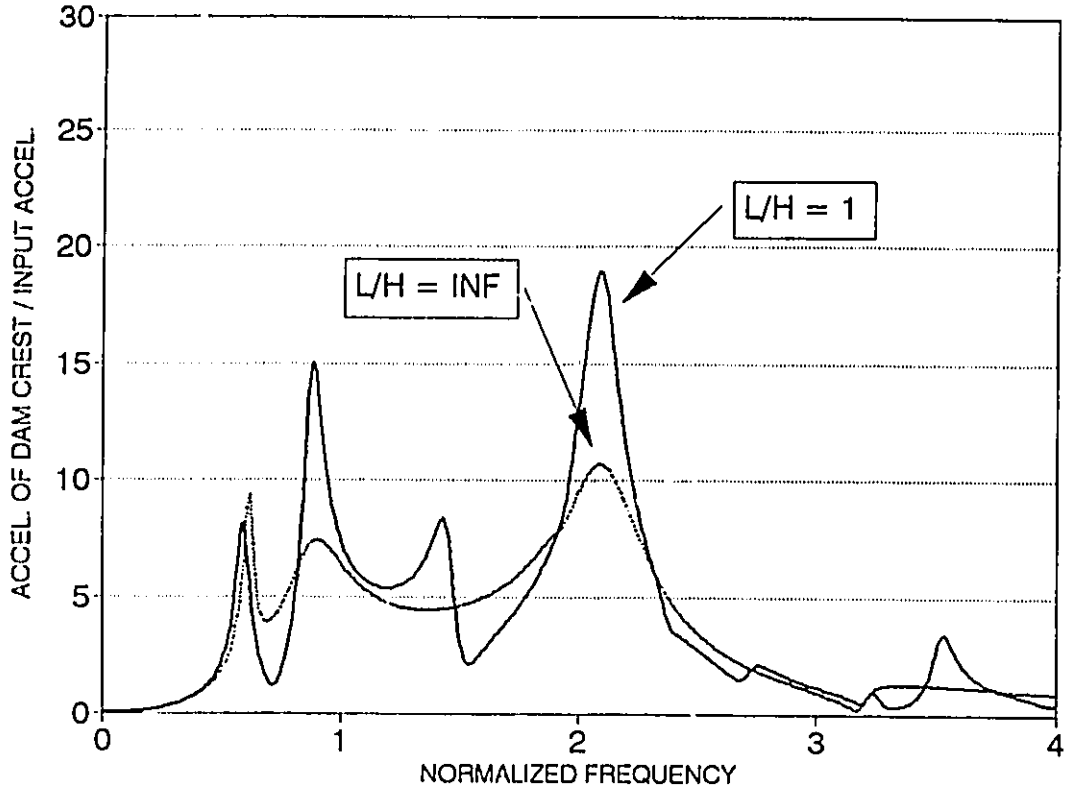

Figure 2.14 - Response of stiff monolith, L/H = 1

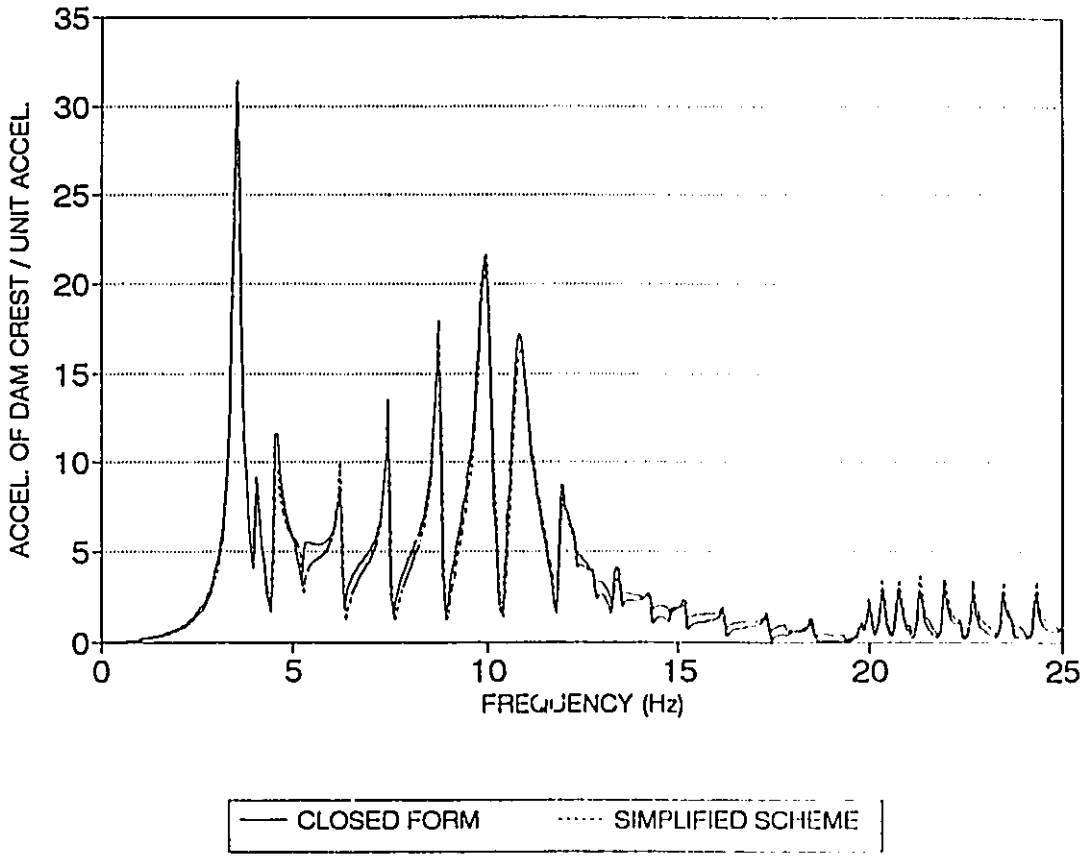

Figure 2.15 - Comparison between closed form solution and simplified analysis procedure

CHAPTER 3

DETAILED ANALYSIS OF DAM-RESERVOIR-FOUNDATION SYSTEM

3.1 INTRODUCTION

In this chapter, a more detailed analytical technique that is used to evaluate the response of the dam-reservoir-foundation system, is presented. The system is sub-divided into three substructures: the dam monolith, the dam's foundation, and the upstream reservoir. The first section in this chapter describes the three individual substructures. The dam monolith and foundation substructures are the same as those discussed in the previous chapter. A finite element analysis is utilized in solving the reservoir's equations of motion. This is different from the previous chapter where a closed form solution of these equations was obtained. The boundary condition used to model the reservoir-foundation interface is also discussed. A new two-dimensional formulation for the boundary condition was developed to model this interface. This proposed boundary condition incorporates the effects of shear stresses or soil column interaction in a simple formulation that is compatible with the present solution approaches.

The last section of this chapter is concerned with the verification of the analysis procedure. First, the effect of the size of the finite element mesh used to

model the upstream reservoir is examined. The effect of the mesh size on the hydrodynamic pressures and the modal forces is evaluated. The results obtained using the proposed analysis are then compared to those obtained using the technique involving the infinite reservoir length assumption (Hall and Chopra (1980), Fenves and Chopra (1984b)). A comparison between the closed form solution developed in the previous chapter and the detailed analytical technique is discussed. Finally, the effect of the monolith's cross sectional geometry on its response in the case of finite reservoirs is discussed.

3.2 ANALYSIS TECHNIQUE

In this section, the analysis of each substructure is discussed individually. In the reservoir substructure, the boundary condition at the reservoir-foundation interface is analyzed. Two methods are presented to model this interface. First, the one dimensional boundary condition proposed by Hall and Chopra (1980) is reviewed. Second, a modified two dimensional boundary condition which incorporates shearing effects (soil column interaction) is derived. A brief overview of the solution scheme is also presented in this section.

3.2.1 Dam Monolith

The dam monolith substructure is modelled as a two-dimensional elastic body. Each monolith is assumed to vibrate independently during strong earthquake ground

motion. This implies that the interface between neighbouring monoliths is stress free. The monoliths are therefore assumed to experience a condition of plane stress. The response of the monolith is assumed to be steady state. The transient part of the response is neglected. The damping in the monolith is assumed to be hysteretic. The equations of motion governing the dynamic behaviour of the monolith are given by equation (2.8).

The additional hydrodynamic forces, $R_{res}(\omega)$, are calculated using the principle of virtual work. The procedure for calculating these forces was given by Hall and Chopra (1980). The stresses and displacements created due to the earthquake ground motion are calculated using the procedure outlined by Fenves and Chopra (1984b). The response of the system is transformed from the frequency domain to the time domain using the Fast Fourier technique. The modal time histories are combined using a straight sum to allow for a direct comparison to the results presented by Hall and Chopra (1980) and Fenves and Chopra (1984b).

3.2.2 Dam's Foundation

The monolith's foundation is modelled as a two-dimensional visco-elastic half space. The analytical approach was originally developed by Dasgupta and Chopra (1977). It was later incorporated into the dam-reservoir-foundation system's analytical model by Chopra, Chakrabarti, and Gupta (1980). This model condenses the foundation's stiffness matrix to values occurring only at the monolith-foundation

interface. This subsystem allows the flexibility of the monolith's foundation soils to be considered in the analysis.

Taking the foundation's flexibility and the subsequent interaction effects into account will make the solution of the problem more complicated. However it will not provide new information concerning the response of the dam monolith assuming a finite length reservoir. For the purposes of this study therefore, the foundation was assumed to be rigid. In the numerical analysis, the elastic modulus of the foundation was taken to be one hundred twenty times greater than that of the monolith's elastic modulus.

3.2.3 Reservoir

The motion of the reservoir is assumed to be irrotational, inviscid, and compressible. The equations of motion of this substructure are given by equation (2.16). This equation describes the response of the pressures in the upstream reservoir. The solution of the reservoir substructure's equation is subject to four boundary conditions when the upstream reservoir is considered to have a rectangular geometry. These boundary conditions are expressed in equations (2.17) through (2.20). This system of equations is solved using the finite element technique developed by Hall and Chopra (1980). It was, however, adapted to incorporate the boundary condition at the far end of the reservoir. Details of the implementation

of the finite element technique can be found in the above mentioned reference and the adaptations will be discussed in this and later sections of this chapter.

The boundary condition at the far end of the reservoir, as given by equation (2.18), is assumed to be unaffected by the earthquake ground motion. A more realistic situation, however, is that the earthquake ground motion will also affect this far end boundary. To account for this boundary's motion in a simple form, it is assumed to vibrate only in its rigid body mode when it is excited. No attempt was made to explicitly model the foundation at the far end boundary of the reservoir. The ground motion at this far end is considered to be either in-phase or out-of-phase with that which excites the dam monolith. In this case, the far boundary condition may be presented as:

$$\frac{\partial P(-L,y,\omega)}{\partial x} = \pm \rho_o + i\ \omega\ q\ P(-L,y,\omega) \qquad (3.1)$$

The first term on the right hand side of this boundary condition represents the acceleration of the far end boundary in its rigid body mode. This acceleration is proportional to the average density of the water. A positive value of the first term on the right hand side of equation (3.1) indicates that the ground motion at the far boundary is in-phase with that at the dam monolith. A negative value indicates the case of out-of-phase ground motion.

So far the analysis has been focused on a reservoir having a rectangular geometry. In many situations, it may be more realistic to assume a sloped reservoir bottom as shown in figure 3.1. Only three boundary conditions are required when the bottom of the reservoir is assumed to be sloped. Boundary conditions (2.17) and (2.20) can be applied to this case. Equation (3.1), or equation (2.19), is applicable along the sloped bottom depending on the type of ground motion considered. The first term of equation (3.1) only applies to the horizontal component of the ground motion. The vertical component of the ground motion is neglected in this study. The bottom absorption term on the right hand side of equation (3.1) and (2.19) is applied such that it acts perpendicular to the direction of the reservoir bottom.

3.2.4 Reservoir's Foundation

The reservoir's foundation is responsible for the dissipation of a significant amount of energy from the dam-reservoir-foundation system. Pressure waves in the reservoir are generated during strong ground motion events. These pressure waves will eventually strike the interface between the reservoir and its foundation. Some of the energy from the pressure wave will be reflected back into the reservoir and the remainder will be refracted into the reservoir's foundation. This refracted energy causes a stress wave to be generated in the foundation soils. This stress wave propagates away from the reservoir-foundation interface and therefore draws the energy away from the reservoir. The energy dissipation characteristics of the

reservoir's foundation is represented by the conditions at the boundary. The one dimensional boundary condition normally used to model this interface will be reexamined in a two dimensional formulation in an attempt to develop a more representative model.

The one dimensional representation of the boundary condition at the reservoir-foundation interface assumes that the foundation soils and the reservoir both act as one dimensional elastic bodies. In this model, the reservoir's foundation is assumed to act as a series of one-dimensional elastic columns. The individual soil columns are assumed independent of one another with no interaction considered. The vertical displacement of these soil columns is the primary source of energy dissipation. The effects of the shear stresses that are developed as these columns deform relative to one another are however neglected. Full details of the derivation and the finite element formulation of this boundary condition were given by Hall and Chopra (1980). It is worthwhile to note that this boundary condition is formulated in terms of an absorptive boundary element. This was done to keep the matrices generated in the finite element method symmetric.

The amount of absorptive capacity available in each of these soil columns is described by the wave reflection coefficient, α. This parameter varies from a value of positive one to zero. A value of positive one indicates a condition of complete reflection. All the energy from the incident pressure wave is reflected off of the reservoir-foundation interface back into the reservoir. No energy is transmitted to

the foundation. A value of zero indicates a condition of maximum absorption. Most of the energy from the incident pressure wave is absorbed into the foundation substructure. This energy is then carried away from the interface by means of a stress wave which is created in the foundation.

In the one dimensional representation of the boundary effect, disregarding this interaction between the soil columns neglects an important source of energy dissipation. A boundary condition is developed which accounts for this interaction between these individual soil columns.

There are two causes for the displacements that a soil column will experience. First, the pressures acting directly on the soil column will cause displacements. This is precisely what was considered by the one dimensional boundary condition discussed previously. Second, the pressures acting on the soil column will cause displacements in the adjacent soil columns. From the theory of elasticity, a load applied at the surface of a two dimensional body will cause surface displacement in more than one soil column. The surface displacement of a two dimensional elastic body under plane strain conditions caused by a distributed load acting over a length of 2a, as shown in figure 3.2, is given by Crouch and Starfield (1983):

$$v(x_s,0) = \frac{F_y\,(1-\nu)}{2\,\pi\,G}\,\{(x_s-a)\ln((x_s-a)^2 - (x_s+a)\ln(x_s+a)^2 + (L'+a)\ln(L'+a)^2 - (L'-a)\ln(L'-a)^2\} \qquad (3.2)$$

where:

x_s	= horizontal coordinate direction
$v(x_s,0)$	= vertical displacement of soil
F_y	= distributed load
G	= shear modulus
ν	= poisson's ratio
a	= half of load length
L′	= fitted parameter

To derive the proposed boundary condition, three neighbouring soil columns are first investigated. This configuration is presented in figure 3.3. The behaviour of the centre soil column is analyzed assuming that the load is applied to each of the three soil columns individually. Each contribution is then summed to obtain the total behaviour of this soil column. The interaction between the soil columns is included when the individual contributions to the response are summed. The proposed boundary condition representing this total behaviour can therefore be written as:

$$\frac{\partial P_{oj}(x_s,0,\omega)}{\partial y} = i\ \omega\ q\ P_{oj}(x_s,0,\omega) + i\ \omega\ q\ \theta_{+1}\ P_{+1j}(x_s,0,\omega) + i\ \omega\ q\ \theta_{-1}\ P_{-1j}(x_s,0,\omega) \qquad (3.3)$$

where:

P_{oj}	= pressure acting on centre soil column
P_{+1j}	= pressure acting on soil column to the left of centre column
P_{-1j}	= pressure acting on soil column to the right of centre column
Θ_k	= displacement parameter
k	= integer indicating soil column

The first term on the right hand side of equation (3.3) represents the behaviour of the centre column due to the pressures acting directly upon it. This term has the exact same form as that of the one dimensional boundary condition discussed previously. The second and third terms on the right hand side of equation (3.3) represent the effect of the pressures acting on the two neighbouring soil columns a distance $\pm\Delta x_s$ away. These terms have the same form as the first term except for an additional parameter, Θ_k. This parameter is applied to scale the displacement of this centre column since its displacement decreases as the distance to the applied load increases. This displacement field, given by equation (3.2), is presented in figure 3.2. The parameter Θ_k is the ratio of the vertical surface displacement of the centre soil column caused by a unit pressure acting at a distance $k\Delta x_s$ away to the vertical surface displacement of this column when the same unit

pressure acts directly upon it. This parameter therefore accommodates the relative contributions of the neighbouring soil columns in a simplified form.

$$\theta_k = \frac{v(k\Delta x_s,0)}{v(0,0)} \tag{3.4}$$

where: Δx_s = width of soil column (= 2a)

Substituting equation (3.2) into equation (3.4) yields the final form of the displacement parameter.

$$\theta_k = \frac{(k\Delta x_s-a)\ln(k\Delta x_s-a)^2 - (k\Delta x_s+a)\ln(k\Delta x_s+a)^2}{-2a\ln(a^2) + (L'+a)\ln(L'+a)^2} \\ \frac{+ (L'+a)\ln(L'+a)^2 - (L'-a)\ln(L'-a)^2}{- (L'-a)\ln(L'-a)^2} \tag{3.5}$$

This displacement parameter will therefore range from a value of zero to a value of positive one. A value of positive one indicates that the pressure is applied directly over the soil column. When the pressure is no longer influencing the soil column, the displacement factor takes a value of zero. An intermediate value indicates that the pressure is applied some distance away from the soil column. The parameter L' defines the specific distance away from the soil column at which the foundation is considered to have zero displacement.

The boundary condition given by equation (3.3) can now be expanded to incorporate the interaction resulting from a larger number of soil columns. This can be written in the form:

$$\frac{\partial P_{oj}(x,0,\omega)}{\partial y} = i\ \omega\ q\ \{\sum_{k=-\infty}^{\infty} \theta_k\ P_{kj}(x+k\Delta x,0,\omega)\} \qquad (3.6)$$

This boundary condition will be implemented in a similar manner to the one dimensional boundary condition proposed by Hall and Chopra (1980). One major difference is that the boundary condition given by equation (3.6) is a function of the pressures acting at a distance $k\Delta x$ away ($k \neq 0$) as well as the pressure acting directly at the soil column in question ($k = 0$). This results in the implementation of this boundary condition to be more difficult than the one dimensional approach. This difficultly can be overcome by assuming that the pressure acting at a distance $k\Delta x$ away can be related to the pressure acting directly at the soil column and the use of an iterative solution scheme. The relationship between pressures can be expressed in the form:

$$P_{kj} = \zeta_k P_{oj} \tag{3.7}$$

where: ζ_k = pressure parameter

The proposed boundary condition therefore becomes:

$$\frac{\partial P_{oj}(x,0,\omega)}{\partial y} = i\ \omega\ q\ (\sum_{k=-\infty}^{\infty} \theta_k\ \zeta_k)\ P_{oj}(x,0,\omega) \tag{3.8}$$

The pressure parameter, ζ_k, can be evaluated for the first iteration by assuming that the pressure distribution is the same as that when the boundary condition of Hall and Chopra (1980) is utilized. A closed form of the pressures on the bottom of a finite length rectangular reservoir is given by equations (2.21) and (2.22) when the dam monolith is vibrating in its rigid body mode and its j^{th} mode of vibration, respectively. In evaluating these expressions, the first term (m = 1) in the series is considered since only a rough approximation is required. The reservoir substructure is analyzed using these approximate values for the pressure parameters. The pressure parameters are then recalculated using the updated values for the pressure along the reservoir-foundation interface. This procedure is continued until the magnitudes of the pressures do not significantly change from those of the previous iteration.

This formulation is not as rigorous as if the reservoir's foundation was modelled as an elastic half-space. This half-space is governed by the two-dimensional wave equation (Antes and Von Estorff, 1987). The proposed two-dimensional boundary condition only approximates the interaction between the vertical and horizontal displacements of the foundation sub-structure. The displacement profile assumed in the proposed boundary condition, however, is an adequate approximation of the actual displacement profile that occurs during dynamic loads. The foundation's higher modes of vibration are assumed not to be significant in its response.

The effect of using this proposed boundary condition on the monolith's response will be discussed in the following chapter. The response of the monolith using the two dimensional model for the interface at the boundary will be compared with that using the one dimensional boundary condition.

3.2.5 Numerical Solution Technique

The numerical solution technique utilized in this study is an adapted version of the computer program developed by Fenves and Chopra (1984a). This program is entitled 'Earthquake Analysis of Concrete Gravity Dams' - EAGD-84. The analysis of the dam monolith and the foundation underlying the monolith were performed using the applicable routines of the above mentioned computer program. The EAGD-84 program performs the reservoir analysis assuming an infinite length.

A new reservoir substructure routine was developed to solve the finite reservoir case. The finite element procedure outlined by Hall and Chopra (1980) was used in the analysis instead of the procedure adopted in the EAGD-84 program. This was modified to incorporate the finite length reservoir assumption. The adopted finite element procedure required that the analysis be separated into two stages. First, the dam-reservoir-foundation system was analyzed assuming that the ground motion was a series of unit harmonics of varying frequencies. Second, the dam-reservoir-foundation system was analyzed to determine the stresses and displacements that occur due to the earthquake ground motion.

The frequency domain analysis of the dam-reservoir-foundation system required that the equations of motion of the reservoir substructure be solved for each of the monolith's individual modes of vibration separately. The dam monolith-reservoir interaction is modelled using the reservoir boundary condition given by equation (2.17). This boundary condition is expressed in terms of the monoliths modal coordinates. This requires that the reservoir's equations of motion be solved separately for each term represented in this boundary condition.

When the ground motion is assumed to excite the far end boundary, the interaction between the reservoir and the foundation at the far end of the reservoir is governed by equation (3.1). The acceleration of this far end boundary is considered only when the dam monolith is vibrating in its rigid body mode. This is because the far end boundary is assumed to vibrate only in this mode. The first term

of equation (3.1) should be taken to be zero when the monolith is assumed to be vibrating in its flexible modes of vibration. The reason for this is because the motion of the dam monolith and the far end boundary of the reservoir when they are vibrating in their rigid body modes are absolute motions. The motion of the dam monolith in its modes of vibration, however, is a relative motion. These two types of motion can not be considered at the same time in a frequency domain analysis.

The calculated pressures are then converted into additional hydrodynamic forces, $R_{rcs}(\omega)$. This is accomplished by using the principle of virtual work. The procedure for this conversion is as outlined by Hall and Chopra (1980). The calculation of the additional hydrodynamic forces must be carried out for each of the monolith's modes of vibration, as well as its rigid body mode. These additional hydrodynamic forces are then introduced into the dam monolith's equation of motion (equation (2.8)). The equations of motion are solved to yield the modal response of the system for a specific frequency interval. This entire procedure must then be repeated for every frequency interval considered in the analysis. The calculated modal responses are then stored for later use in the stress analysis. To determine the Fourier representation of the system's response, the modal accelerations are combined using equation (2.27). A straight sum combination rule allows for direct comparison of the results to those reported by Hall and Chopra (1980) and Fenves and Chopra (1984b).

The dam-reservoir-foundation system may now be analyzed to determine the stresses and displacements that occur due to actual earthquake ground motion records. To perform this analysis, the modal responses calculated using the above procedure were introduced into the appropriate routines of EAGD-84.

3.3 VERIFICATION OF ANALYSIS TECHNIQUE

An attempt was made to verify the analytical technique used in this study. A discussion on the effect of the finite element mesh used to model the reservoir substructure is first presented. The results of the analytical technique are then compared to the results from the existing solution for the special case of the infinite reservoir length assumption (Hall and Chopra, 1980; Fenves and Chopra, 1984b). A comparison between the closed form technique presented in the previous chapter and the detailed analytical technique is discussed. Finally, a discussion on the effect of the dam monolith's cross sectional geometry on the response in the case of a finite reservoir is presented. Two geometries are examined: an idealized triangular cross section and the practical Pine Flat Dam type cross section.

3.3.1 Effect of Reservoir Mesh

The degree of fineness of the finite element mesh will have a direct impact on the accuracy of the analytical procedure and on the computer time needed for the analysis. The size of the finite elements must be small enough that sufficient

accuracy is obtained in the numerical results. Concurrently, the number of elements must be limited such that the computational time required to perform the analysis is minimized. To determine the optimum size of the finite element mesh, a 91.44 m (300 ft.) tall gravity dam having a triangular cross section and impounding a reservoir having an L/H ratio of 5.0 is analyzed. The reservoir-foundation interface is assumed to have a wave reflection coefficient of 0.9. The dam's elastic modulus is 13 790 MPa (2 X 10^6 psi).

Three finite element meshes were selected as shown in figure 3.4. The effect of having four, eight, and twelve elements along the height of the dam face was examined. This necessitated having 20, 40, and 60 elements, respectively, along the reservoir's bottom to keep the elements equally proportioned. The six node isoparametric element that is used in the reservoir substructure performs its best when the two legs of the triangle are equal in length.

(a) Hydrodynamic Pressures and Modal Forces

The pressure distribution that is created along the dam face is dependent upon the number of elements used to define the reservoir substructure. Table 3.1 presents the real component of the pressures acting along the dam face created by the vibration of the monolith in its fundamental mode for the three finite element meshes considered. The frequency of excitation is 3 Hz and the pressures are normalized to the value of the hydrostatic pressure at the bottom of the reservoir.

The pressures generated at this frequency of excitation do not change significantly with the use of an increasing number of elements.

The magnitudes of the calculated modal forces are however dependent upon the number of elements used in the finite element mesh. Table 3.2 presents the real component of the modal forces acting on the dam face when the monolith is vibrating in its fundamental mode. The frequency of excitation is again taken as 3 Hz. The modal forces are calculated by integrating the pressure distribution over the height of the dam and multiplying by the transpose of the mode shape. The modal forces are normalized to the value of the hydrostatic force acting on the dam face. As evident from this table, the magnitudes of the modal forces change with an increasing number of finite elements used. An increased number of elements are required to determine the shape of the pressure distribution more accurately.

A finer finite element mesh is required to calculate the response of the reservoir substructure at higher frequencies of excitation or when excited by higher modes of vibration of the monolith. The pressure distribution is again not significantly affected by the finite element mesh. However, the effect of the fineness of the finite element mesh on the forces is quite significant. Table 3.3 presents the modal forces created by the vibration of the monolith in its fundamental mode at a frequency of excitation 10 Hz. An increased number of nodal points are required to define the pressure distribution and the loaded area more accurately. This will allow the modal forces to be calculated more accurately.

(b) Response of Monolith

The response of the monolith, which is of interest in dam design, is affected by the size of the finite element mesh used in several ways. The mesh size of the reservoir substructure determines the accuracy of the modal hydrodynamic forces that affect the monolith. This was discussed in the previous section. The finite element discretization of the reservoir also influences the monolith's response. This discretization is done in such a manner that the nodal points along the dam face align with those of the reservoir substructure. As the number of nodal points along the dam face increases for the reservoir substructure, the number for the monolith substructure will therefore also increase. The response of a monolith impounding a reservoir having an L/H ratio of 5 and a wave reflection coefficient of 0.9 are plotted in figure 3.5 for various finite element meshes. Meshes of four, eight, and twelve elements were used for the reservoir along the dam face. The response of the monolith increases with an increased number of elements used in the analysis. Table 3.4 presents the peak response at the fundamental frequency for the case of a finite reservoir and an infinite reservoir (Fenves and Chopra, 1984b) when all three reservoir meshes are considered. As evident from this table, the peak for the infinite length case also increases with an increasing number of elements used in the reservoir substructure (monolith mesh size is made compatible to that of the reservoir mesh size). The magnitude of the fundamental response is therefore dependent on the discretization of the reservoir. This is expected as the modal

forces created by the reservoir substructure were shown in the previous section to be dependent on the mesh size. It should be noted that there is no significant difference in the prediction of the magnitude of the fundamental response for the same monolith discretization when both a finite and infinite reservoir length is assumed.

The response of the monolith at higher frequencies of excitation is underestimated using a coarse finite element mesh. This can also be seen in figure 3.5. A finer finite element mesh is required to capture both the magnitude of the pressures and the shape of the pressure distribution at these higher excitation frequencies. This is especially true when the monolith is vibrating in its higher modes of vibration. The finite element mesh having eight elements along the dam face underestimates the response at a frequency of 8.3 Hz by 11.7%. The four element mesh underestimates the response by 28.8%. The response of the monolith when a finite length reservoir is assumed is therefore dependent on the mesh size used to model the reservoir substructure.

(c) Computational Time Required

The fineness of the finite element mesh will also have a significant impact on the time required to perform the complete analysis. The solution time increases as the number of elements used in the analysis is increased. Table 3.5 presents the times required to solve for the response of a monolith impounding a reservoir having an L/H ratio of 5 and a wave reflection coefficient of 0.9. The solution time is

determined using a 386-40 MHz microcomputer with a mathematical coprocesser. The solution time drastically increases as the number of elements used increases. Pressures must be calculated at an increasing number of nodal points as the mesh size increases. This increases the computational effort required to carry out the analysis. The desired accuracy of the solution technique must therefore be balanced with the time required to perform the analysis. A reasonable level of accuracy must be obtained as well as a reasonable length of time required to perform the analysis.

In this study, the reservoir mesh having eight elements along the dam height and 40 elements along the reservoir length was used. The accuracy of this reservoir mesh was considered to be adequate. The magnitudes of the hydrodynamic pressures and forces are determined quite accurately. The response of the finite reservoir system at its fundamental frequency is predicted to be the same as for the infinite reservoir system having a compatible finite element mesh for the monolith. This is presented in Table 3.4. The underestimation of this response peak relative to the finer reservoir mesh (12 X 60 elements) was approximately 12.5%. As this study is more concerned with comparing the finite and infinite reservoir length assumptions, the underestimation of the fundamental response peak is acceptable. The required solution time of 32 hours was also deemed to be reasonable.

3.3.2 Comparison with Infinite Reservoir Assumption

The results of the analytical procedure was compared with the existing solutions for the infinite length reservoir case to verify the accuracy of the solution. The results from the finite element procedure assuming an increasing L/H ratio should approach that of when the reservoir is considered infinite in length. Three values for the ratio of the reservoir length to dam height (L/H) were used: 5.0, 10.0, and 20.0. The analysis was conducted using the finite element procedure outlined in the previous section. The results were compared against those obtained using the computer program EAGD-84 (Fenves and Chopra, 1984a) where the reservoir was assumed infinite in length. These analyzes were performed using a 91.44 m (300 ft) tall dam monolith. This monolith was assumed to have a triangular cross section with a downstream slope of 0.8:1.0. The dam's elastic modulus was taken as 13 790 MPa (2 X 10^6 psi). The first six modes of vibration were considered in this analysis. Only the horizontal component of the ground motion was taken as the input motion. The reservoir's wave reflection coefficient was assumed to be 0.975.

Figures 3.6 (a), (b), and (c) present the response of a dam monolith impounding reservoirs having L/H ratios of 5, 10, and 20 (thin solid lines), respectively. The response of the monolith when the reservoir is assumed to be infinite in length is presented as the heavy solid line in these figures. The response of the finite length reservoir system can be seen to approach that of the infinite length reservoir system as the L/H ratio increases. As this ratio increases, the

number of the supplementary response peaks increase. At the same time, the magnitudes of these peaks decrease with increasing L/H ratio. For very large L/H ratios, the two solutions give identical results. It can be concluded that the analytical procedure used to investigate the effects of a finite length reservoir on the response of the monolith does reproduce the results of the infinite length reservoir case in the limit.

3.3.3 Comparison between Closed Form Solution and Finite Element Procedure

In order to verify the accuracy of the closed form solution, a comparison is made between the response obtained using this solution with the response obtained using the finite element procedure. The response of the monolith obtained by using both approaches are plotted in figure 3.7. The monolith was assumed to have a triangular cross section. The first two modes of vibration of the monolith only were considered in the analysis. The reservoir length was assumed to be five times the height of the monolith. The modulus of elasticity of the monolith's concrete was assumed to be 27 580 MPa. The wave reflection coefficient was taken as 0.975. The foundation underneath the monolith was assumed to be completely rigid.

The response of the monolith that is predicted by the finite element procedure was found to be similar to that predicted by the closed form solution technique. The closed form solution overestimates the magnitudes of the monolith's response. The magnitude of the fundamental response peak is predicted by the closed form solution

to be 31.4 whereas the finite element procedure predicts it to be 23.9. The closed form solution correctly predicts the frequencies at which the supplementary response peaks occur. The magnitudes of the supplementary response peaks are also overestimated but not as significantly. The supplementary response peak occurring at a frequency of 4.54 Hz for the reservoir having an L/H ratio of 5.0 is predicted by the closed form solution to be 11.66 whereas the detailed analysis predicts the magnitude to be 11.13.

This difference in the magnitude of the fundamental response peak between the closed form solution and the finite element procedure was previously reported by Fenves and Chopra (1984b). These authors performed a closed form solution of the dam-reservoir problem for an infinite length reservoir with a completely reflective reservoir bottom. The monolith was idealized as triangular in shape. One mode of vibration was considered and the elastic modulus of the concrete was taken as 28 959 MPa (4.2 X 10^6 psi). The magnitude of the fundamental response peak was determined to be 40.4 using this technique. They also conducted a finite element analysis using the program EAGD-84. The same monolith cross section was used and the reservoir was assumed to be infinite in length. One mode of vibration was included in the analysis and the reservoir bottom was again assumed to be completely reflective. The monolith's elastic modulus was taken as 27 580 MPa (4 X 10^6 psi). Fenves and Chopra (1984b) determined the magnitude of the fundamental response peak to be approximately 28.2 using the finite element procedure. The slight

difference in the modulus of elasticity does not significantly affect the difference in the two responses.

The same overestimation of the fundamental response peak's magnitude between that predicted by the closed form solution and that predicted by the finite element procedure occurs for this study as reported by Fenves and Chopra (1984b). Excellent agreement was noted in this study between the frequencies at which the fundamental and supplementary response peaks occur when the two techniques were used. The finite element procedure developed in Chapter 3 therefore predicts the behaviour of the system to be similar to that predicted by the closed form solution technique that was presented in Chapter 2. The closed form solution therefore satisfactorily predicts the behaviour of the dam-finite reservoir system.

3.3.4 Monolith Cross Sectional Geometry

Two cross sectional geometries were examined. The first cross section examined was triangular in shape and usually termed the structural section. The second cross sectional shape used was one similar to that of the Pine Flat Dam located in California, and will be referred to as the practical cross section. Schematics of the two cross sectional geometries are presented in figure 3.8. The triangular cross section obviously neglects the effects of the mass located at the top of the dam monolith. This top structure is used to allow for a road to be located on the dam's crest or to support services for the dam itself.

The cross sectional geometry significantly affected the frequencies of vibration of the monolith when the reservoir was considered to be empty. The increased mass of the practical cross section resulted in the lowering of the monolith's frequencies of vibration (Chopra, 1987). The frequencies of the first four horizontal modes are presented in Table 3.6 for both cross sections when a finite length upstream reservoir is considered. The other two modes (modes 3 and 6) are primarily vertical modes.

The decreased frequencies of vibration of the monolith in turn caused the response of the overall dam-reservoir-foundation system to be altered. The cross sectional geometry had the primary effect of lowering the frequencies at which all the response peaks occurred.

The solution for the case of a finite reservoir was conducted for the two monolith cross sections. The reservoir being impounded was assumed to have an L/H ratio of 5.0 and the reservoir was assumed to have a wave reflection coefficient of 0.975. The height of the dam was taken to be 91.44 MPa (300 ft) and its elastic modulus was taken to be 13 790 MPa (2 X 10^6 psi). Figure 3.9 represents the responses of the overall system when the monolith is assumed to have a triangular cross section (heavy solid line) and a practical cross section (thin solid line). The resonance of the monolith interacts with the resonance of the reservoir at different frequencies for both of the cross section considered. This is a result of the decreased frequencies of vibration of the practical cross section relative to that of the triangular

cross section. The fourier representation of the system's response therefore is significantly different for the two cross sectional geometries.

The effect of the change in the monoliths cross section becomes significant when a finite length reservoir is assumed. All major response peaks that are present in the fourier representation of the response are shifted to lower frequencies when the practical cross section is analyzed. For example, the supplementary response peak marked by the single headed arrow in figure 3.9 has a greater frequency shift than the fundamental response peak. Depending on the frequency content of the actual ground motion, significant changes in the monolith response may occur due to cross section variation.

The monolith's cross sectional geometry has an important influence on the system's response. This is especially true when the reservoir length is assumed to be finite. In order to realistically estimate the monolith's response when impounding a finite length reservoir, the monolith's geometry must therefore be modelled as closely as possible. It was decided that the monolith considered in this study should have a practical cross sectional geometry. This will ensure that a more realistic response of the monolith will be obtained in the analysis.

Table 3.1 - Pressures due to fundamental mode at $\omega = 3$ Hz

Y/H	Normalized pressures at dam face		
	4 Elements	8 Elements	12 Elements
0	0.0534	0.0537	0.0537
0.125	0.0545	0.0546	0.0546
0.250	0.0562	0.0564	0.0564
0.375	0.0584	0.0585	0.0585
0.500	0.0598	0.0600	0.0600
0.625	0.0595	0.0596	0.0596
0.750	0.0552	0.0550	0.0551
0.875	0.0386	0.0420	0.0418
1.000	0.0000	0.0000	0.0000

Table 3.2 - Modal forces due to fundamental mode, $\omega = 3$ Hz

Mode	Normalized modal forces		
	4 Elements	8 Elements	12 Elements
1	2.983	3.102	3.126
2	-0.978	-0.820	-0.782
3	-0.438	-0.543	-0.566
4	-0.530	-0.681	-0.727
5	0.271	0.156	0.116
6	-0.143	-0.214	-0.221

Table 3.3 - Modal forces due to fundamental mode, ω = 10 Hz

MODE	Normalized Modal Force		
	4 Elements	8 Elements	12 Elements
1	27.307	28.793	29.086
2	1.339	3.050	3.470
3	-7.381	-8.164	-8.339
4	2.356	0.697	0.216
5	2.741	-0.179	-0.922
6	-4.851	-5.587	-5.567

Table 3.4 - Peak monolith response at 3 Hz for various mesh sizes

Reservoir case	4 Elements	8 Elements	12 Elements
Finite	19.66	21.93	25.05
Infinite	20.71	22.01	24.78

Table 3.5 - Time required for analysis of complete system

Number of Elements	Time Required (hours)
4 x 20	8
8 x 40	32
12 x 60	72

Table 3.6- Frequencies of monolith (Hz) with varying geometry (after Chopra, 1987)

Mode	Structural section	Pine Flat section	% decrease
1	21.962	19.997	8.95
2	50.001	41.915	16.17
4	85.229	72.837	14.54
5	123.434	108.341	12.15

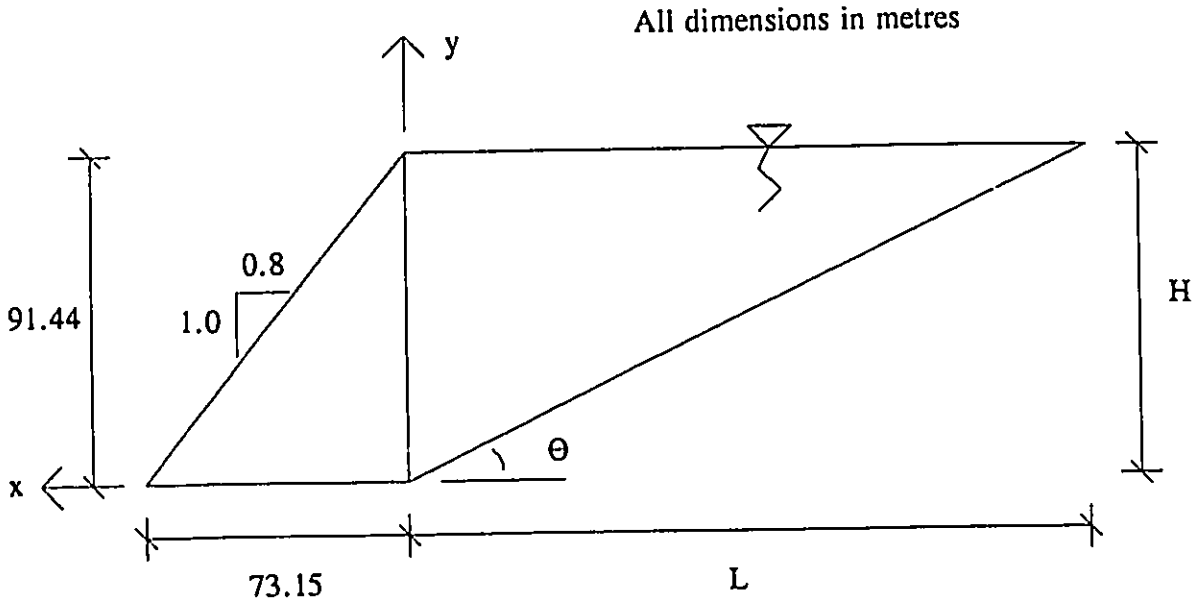

Figure 3.1 - Schematic of monolith impounding triangular shaped reservoir

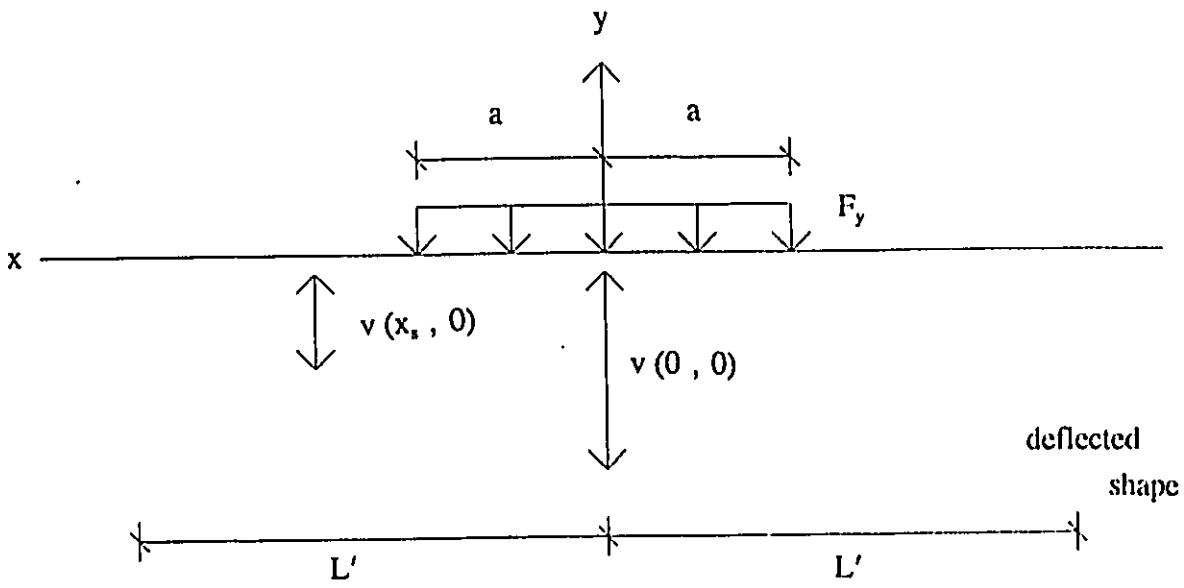

Figure 3.2 - Displacement of surface of elastic body due to distributed load of length 2a

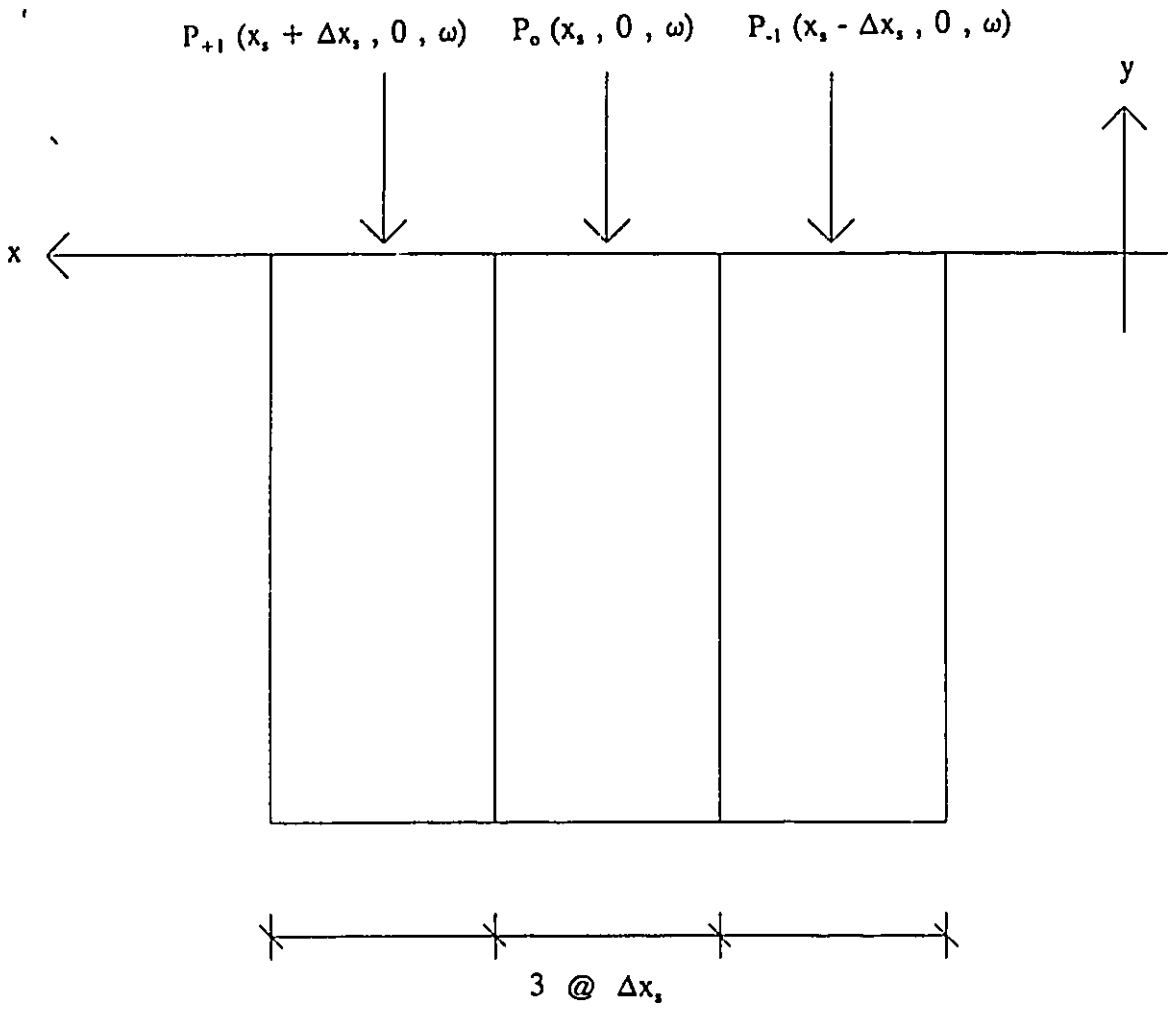

Figure 3.3 - Configuration of neighbouring soil columns

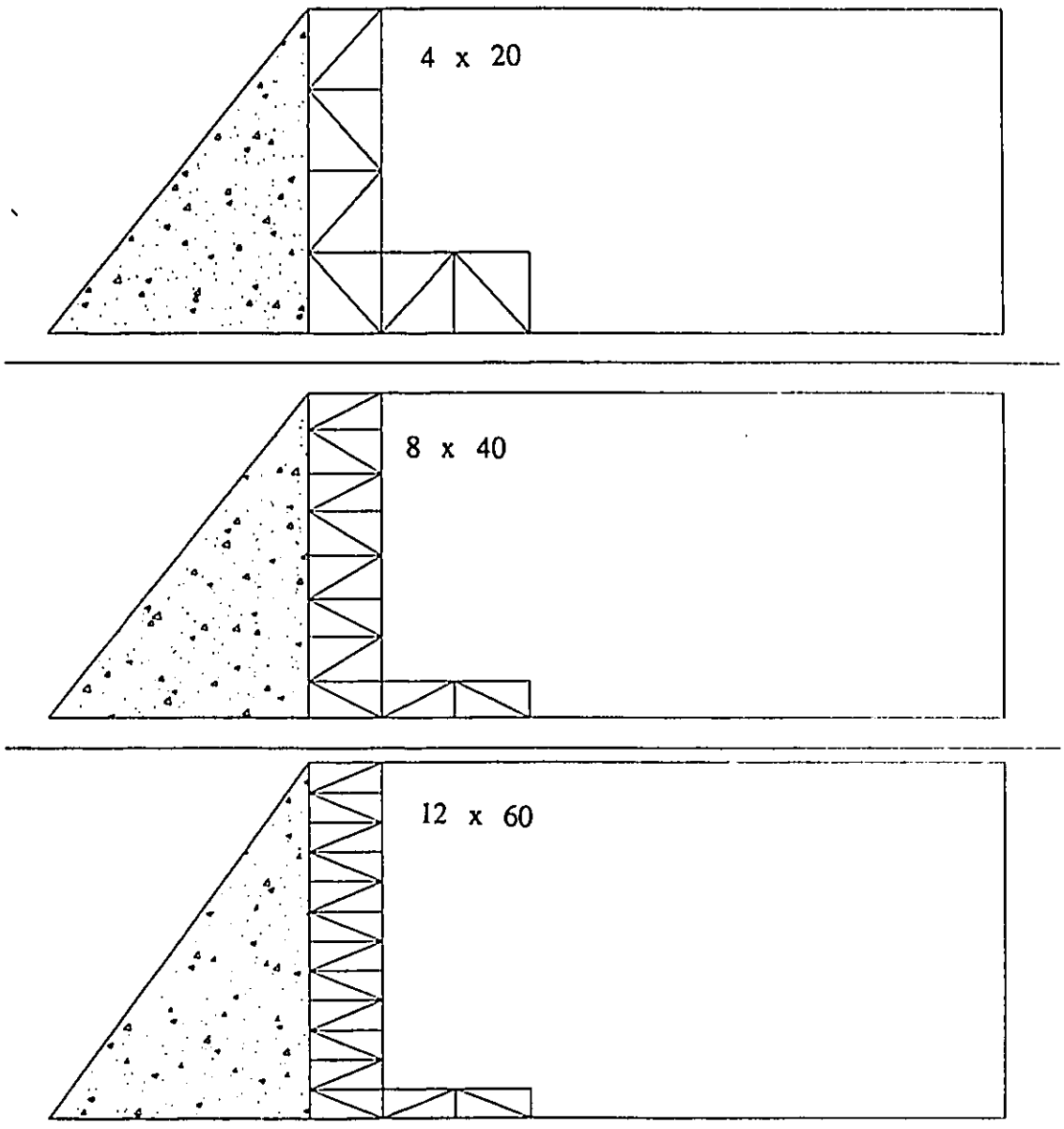

Figure 3.4 - Finite element meshes considered in the reservoir substructure

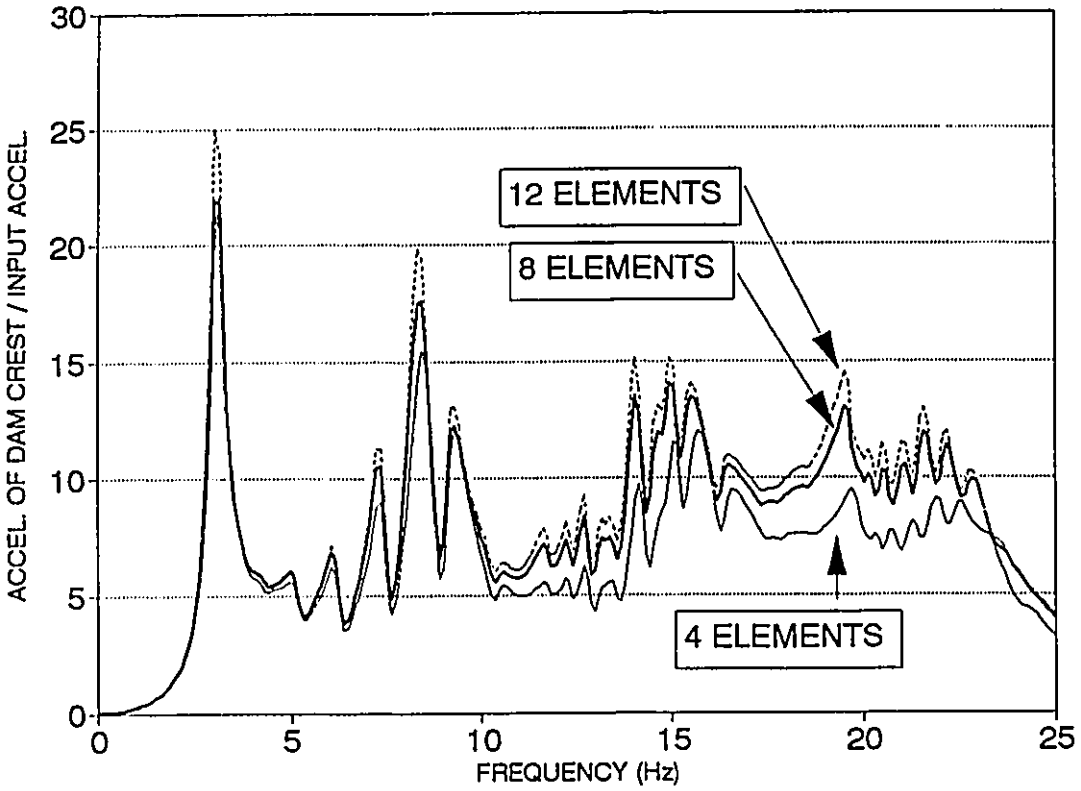

Figure 3.5 - Response of monolith for different reservoir finite element meshes (monolith mesh size increases with reservoir mesh size)

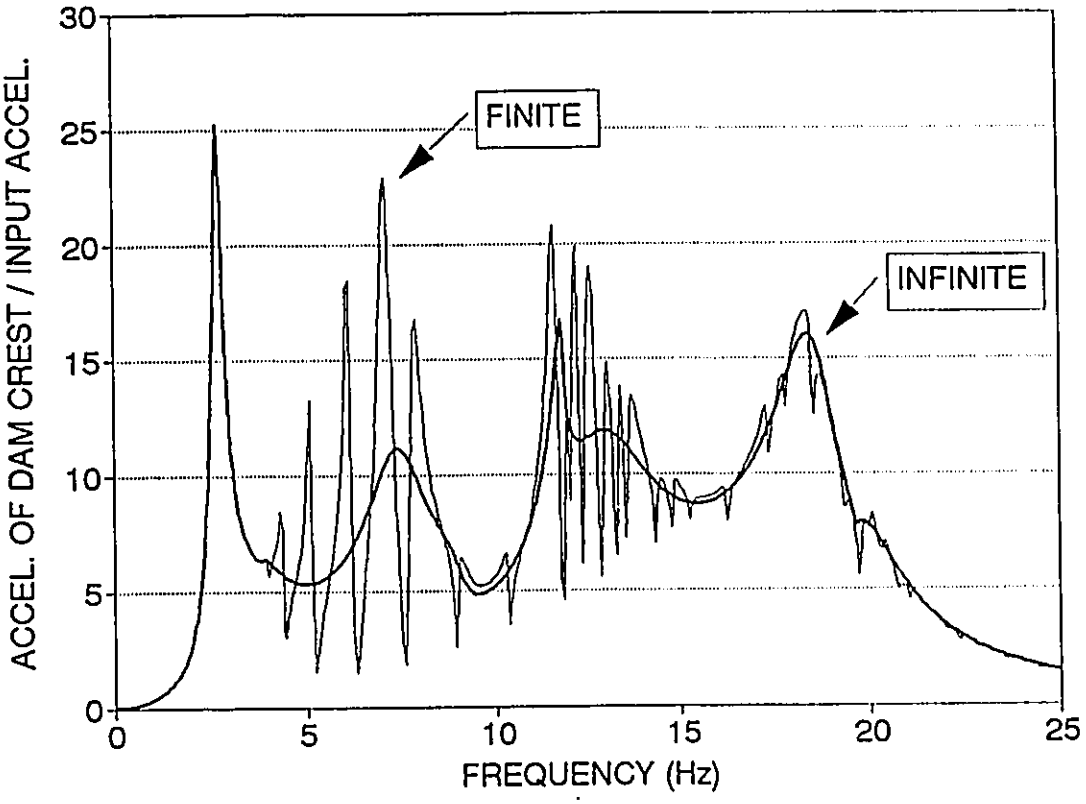

Figure 3.6(a) - Response of structural section when impounding reservoir of L/H = 5

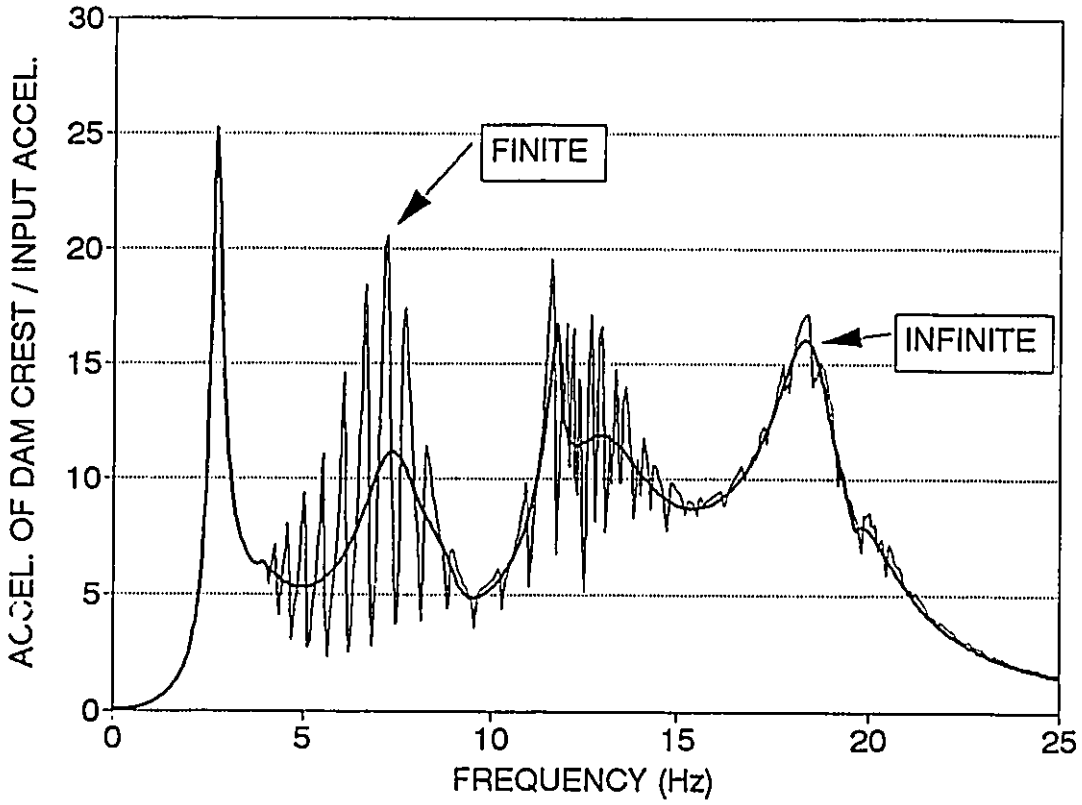

Figure 3.6(b) - Response of structural section when impounding reservoir of L/H = 10

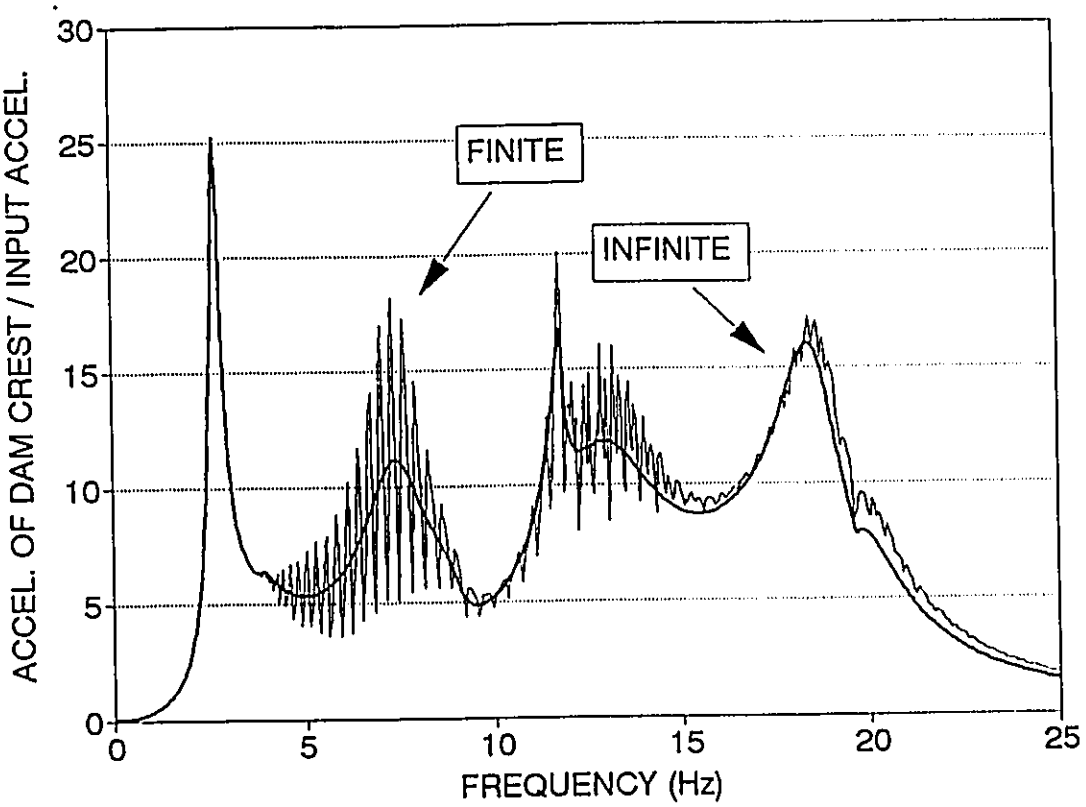

Figure 3.6(c) - Response of structural section when impounding reservoir of L/H = 20

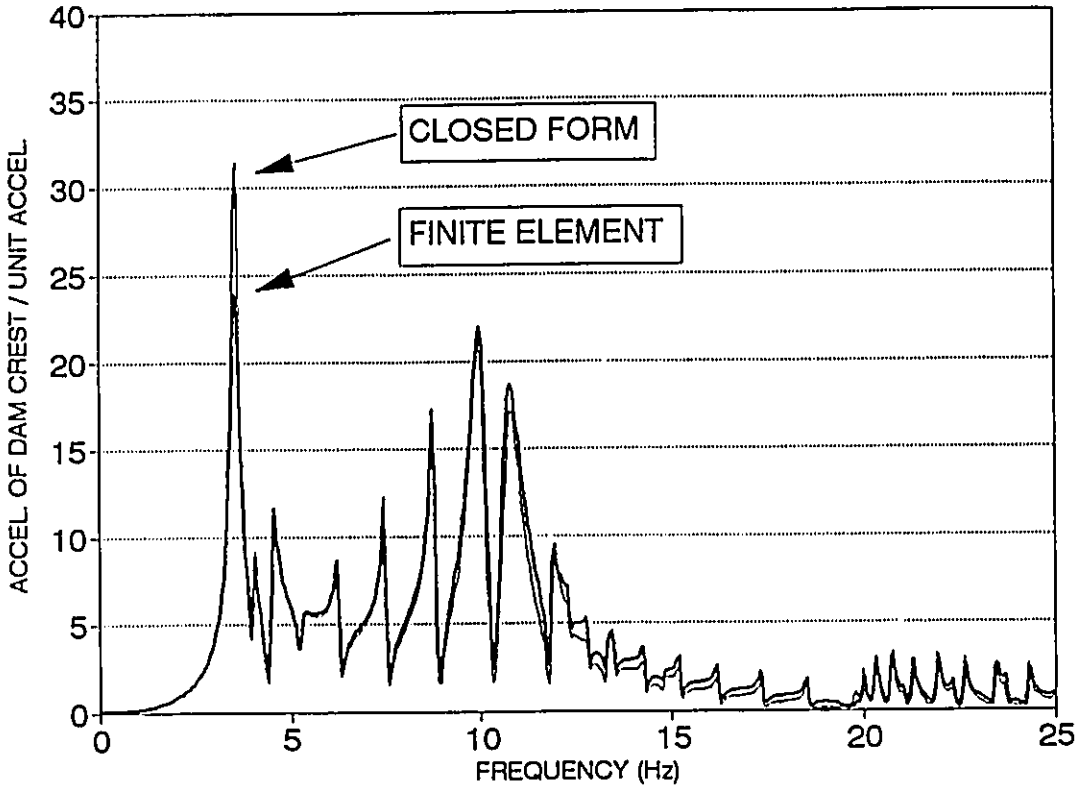

Figure 3.7 - Comparison between closed form solution and detailed analysis procedure (L/H = 5.0)

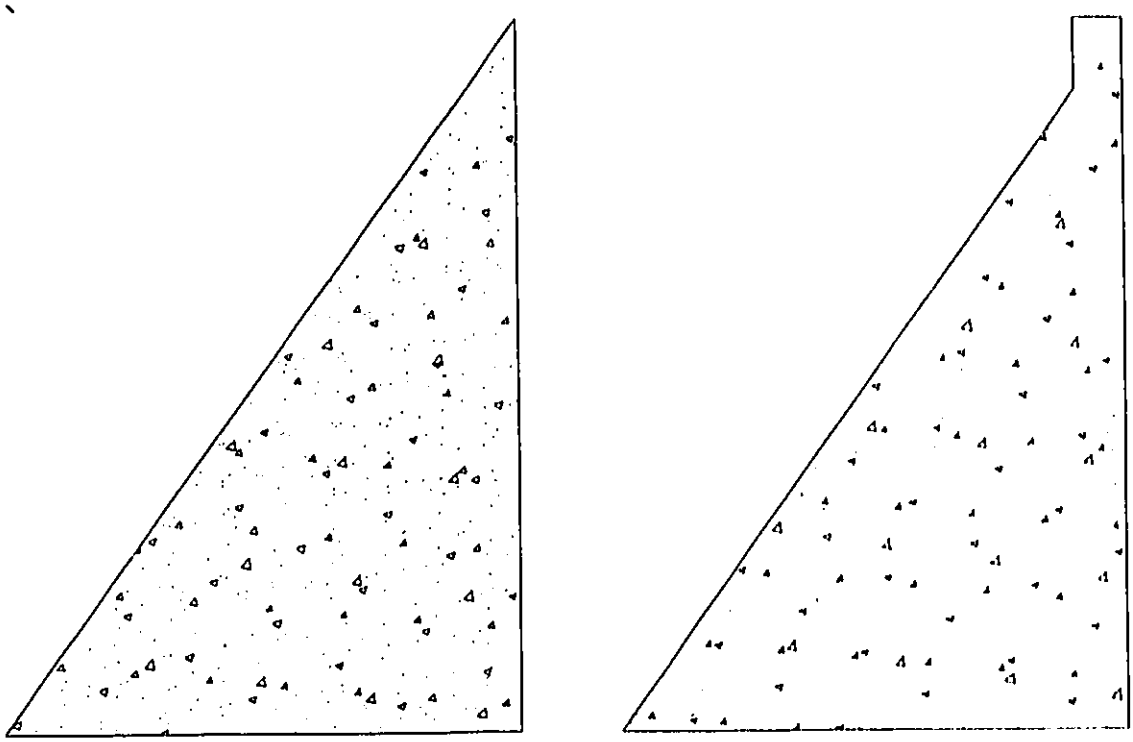

Figure 3.8 - Dam monolith geometries

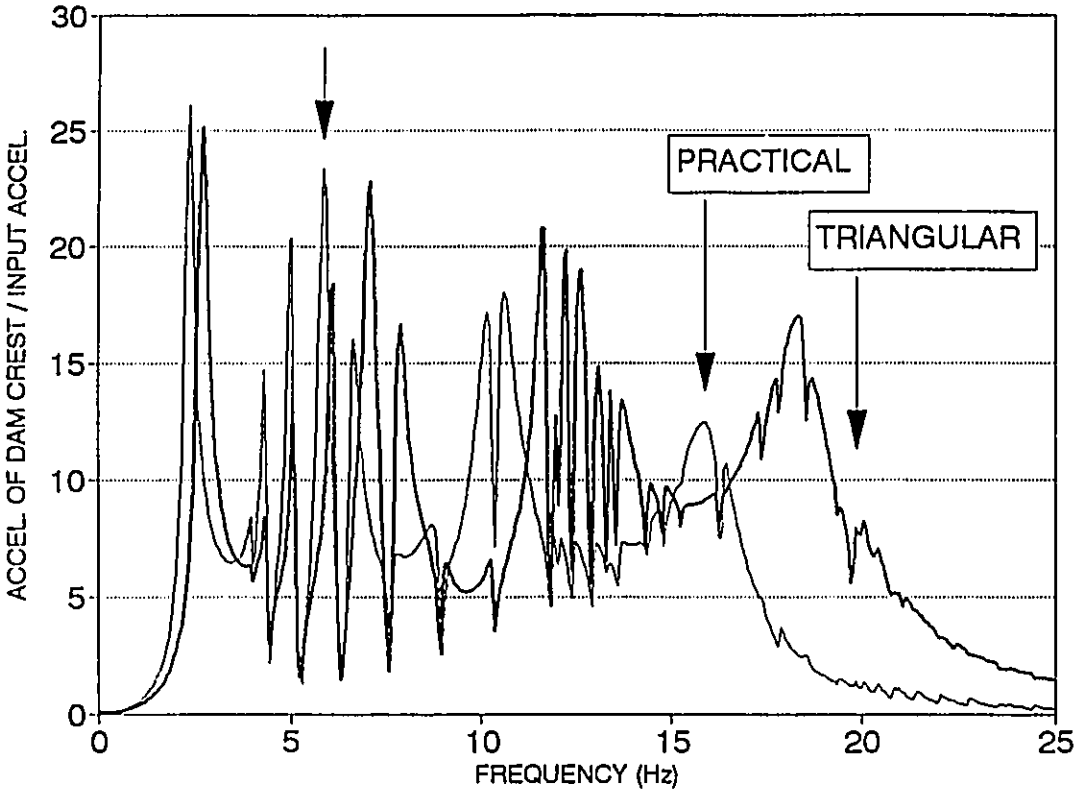

Figure 3.9 - Comparison of response of system when using both triangular and practical monolith geometries

CHAPTER 4

DAM MONOLITH RESPONSE

4.1 INTRODUCTION

In this chapter, the response and behaviour of a dam monolith impounding a finite length reservoir is investigated. The ground motion is assumed to be applied at both the monolith and the far end boundary of the reservoir. Two cases of ground motion excitation are examined. The first case is a special case where the far end boundary is assumed to be unaffected by the ground motion. The second case is the general case when this far boundary is excited by either in-phase or out-of-phase ground motion. This analysis was performed using the finite element procedure that was outlined in Chapter 3. The effect of the finite reservoir length, the wave reflection properties of the reservoir bottom, and the geometry of the upstream reservoir on the monolith's response are evaluated.

4.2 DAM-RESERVOIR SYSTEM

A concrete gravity dam with a practical cross sectional geometry was selected for the dynamic analysis. The monolith was taken to be 91.44 m (300 ft) high and 71.85 m (235.75 ft) wide at the base. The upstream reservoir was assumed to be

completely full so that the height of the reservoir is equal to the height of the dam monolith. The downstream flow channel was assumed to be completely empty. This represents the case of maximum horizontal force on the dam monolith which governs the earthquake design. A schematic of the selected dam-reservoir system when the reservoir is idealized to have both a rectangular and a triangular geometry is presented in figure 4.1.

A range of values was assigned to the various important reservoir parameters in order to evaluate their effect on the response of the monolith. These parameters are: the ratio of the reservoir's length to the dam's height (L/H), the reservoir-foundation interaction and the upstream reservoir's geometry. The L/H ratio was considered to have three values: 1.0, 2.5, and 5.0. The reservoir-foundation interaction was modelled using the one and two dimensional boundary conditions that were described in the previous chapter. The wave reflection coefficient's value (denoted as α) was taken as 0.975, 0.7, and 0.5 for both models of this boundary condition. The response of the monolith was also examined for cases when the bottom of the upstream reservoir was considered horizontal or inclined in the form of a rectangular and triangular reservoir geometry, respectively (figure 4.1). The reservoir-foundation interface was modelled using the one dimensional boundary condition developed by Hall and Chopra (1980) unless otherwise stated. Table 4.1 presents a summary of all the combinations of the above mentioned parameters that were considered in this study. In all cases, the system was subjected to three cases

of ground motion excitation: the monolith only excited, the far end boundary excited in-phase with the monolith, and the far end boundary excited out-of-phase with the monolith.

The concrete used in the monolith was assumed to have a unit weight of 24.3 kN/m^3 (155.0 lb/ft^3) and a Poisson's ratio of 0.2. The monolith's elastic modulus was taken to be 20 685 MPa (3 x 10^6 psi). All the monolith's modes of vibration were assumed to have a damping ratio of 5% of critical. The monolith's foundation was assumed rigid. The ground motion considered in this frequency domain analysis was assumed to be a unit harmonic. The frequency of this unit harmonic was varied from 0 to 25 Hz.

In the dam-reservoir-foundation problem, the monolith's response is coupled to the hydrodynamic forces that are created in the reservoir. The response of the system and the applied loads are not truly independent of one another. For this reason, it is not possible to present the results as true frequency response functions. The response of the monolith is therefore presented in the form of a Fourier representation. This permits the effects of the forces created by the monolith's inertia as well as the forces created by the response of the reservoir to be included in the monolith's response. In this chapter, the acceleration of the top upstream corner at the crest of the monolith was taken as a representative quantity for comparison. These accelerations are non-dimensionalized with respect to the input ground motion.

4.3 GROUND MOTION AT DAM MONOLITH AND FAR BOUNDARY

In Chapter 2, the ground motion was assumed applied only at the dam monolith. A more realistic situation, however, is that the ground motion will affect both the dam monolith and the far end boundary of the reservoir. In this section, the ground motion is applied at the far end boundary and is considered to have either a 0 (in-phase) or 180 (out-of-phase) degree phase difference to that applied at the monolith. The analysis of the monolith's response with various L/H ratios was performed using the finite element procedure developed in Chapter 3.

The two models for the reservoir-foundation interface are evaluated. For the one dimensional boundary condition, the effect of the wave reflection coefficient is discussed when the general excitation case is assumed. The proposed two dimensional boundary condition is studied. The response of the monolith using this boundary condition is compared to the response of the monolith using the one dimensional boundary condition. Lastly, the response of the system is investigated when the reservoir's geometry is varied. The reservoir's geometry is assumed to be either rectangular or triangular in cross section.

4.3.1 Reservoir Length to Dam Height (L/H) Ratio

The effect of the ratio of the reservoir's length to dam height (L/H) on the response of the dam monolith is investigated. The special case of the monolith alone being excited by the ground motion is first discussed. The general case of the far

boundary being excited by ground motion that is either in-phase or out-of-phase with that at the monolith is then examined.

(a) Special Case - Dam Monolith Excited Alone

The responses of a dam monolith that impounds a reservoir with a length of five times the monolith's height and a length that is infinite are compared in figure 4.2. The response of the monolith assuming a finite length is presented as the solid line. The wave reflection coefficient was taken as 0.975. The response of the monolith assuming a finite length reservoir is increased significantly in the frequency range of 4 to 8 Hz from that when the reservoir is assumed infinite in length. For example, the non-dimensional acceleration of the top upstream corner of the monolith at an excitation frequency of 6.01 Hz is increased from 6.59 to 22.08 when the reservoir length is shortened to five times the monolith's height from an infinite length. This is an increase of 235%. The other three major supplementary response peaks are also increased as significantly.

The presence of the far end boundary causes the creation of additional response peaks in the dam's overall response. These additional response peaks, termed supplementary response peaks, occur at frequencies greater than that of the fundamental frequency of the dam-reservoir-foundation system. The existence of these peaks is primarily due to the finite geometry of the reservoir. The presence of the far end boundary causes the pressures in the reservoir to resonate both in the

vertical and horizontal directions. This coupled vertical and horizontal resonance of the reservoir creates additional hydrodynamic forces on the face of the dam. These additional hydrodynamic forces in turn, cause the monolith to respond at frequencies of excitation which correspond to the resonance of the reservoir. These additional resonances therefore result in the creation of the supplementary response peaks in the Fourier representation of the monolith's response.

These supplementary response peaks occur at frequencies which correspond to the frequency content of actual earthquake ground motion events that are characterized as having a high ratio of the maximum ground acceleration to maximum ground velocity (a/v). If the earthquake ground motion has significant energy at these particular frequencies, the response of the monolith will be underestimated by the analysis assuming an infinite length reservoir.

The overall dynamic response of a dam impounding a reservoir having an L/H ratio of 1.0 is plotted in figure 4.3. The response of a dam having an infinite length reservoir is again presented as a dashed line and that having a finite length reservoir is presented as a solid line. The wave reflection coefficient was taken as 0.975. In this example, the response of the monolith at a frequency of 6.69 Hz is increased by 192%. The magnitude of this response increases from 8.21 to 23.96 when the L/H ratio is shorten to a value of one from an infinite value. This will again result in an increase in the monolith's response if the actual earthquake ground motion has significant energy at this particular frequency.

The supplementary response peaks are primarily generated due to the resonance of the reservoir substructure. At these particular resonant frequencies, the monolith will still show some level of response, although not large. An example of this type of supplementary response peak is labelled 'A' in figure 4.4. Figure 4.4 presents the response of a dam monolith impounding a reservoir having an L/H ratio of 5.0 when it is decomposed into the contributions of its individual modes. The wave reflection coefficient was again taken as 0.975. This peak has significant contributions from both the first and second modes of vibration of the monolith.

Supplementary response peaks are also generated through the combined resonance of the monolith and reservoir substructures. This type of supplementary response peak is labelled 'B' in this figure. Note that the actions of the second mode are the most significant in the generation of this peak. The monolith's motion is increased due to its own resonant behaviour. This increased motion of the monolith causes pressures to be created in the reservoir. The resonant frequency of the monolith however coincides with one of the resonant frequencies of the reservoir. The motion of the reservoir is therefore enhanced. This increased motion amplifies the pressures that are created. This in turn affects the motion of the monolith. These combined resonance response peaks typically have larger magnitudes than those generated sol :y by the resonance of the reservoir.

(b) General Case - Dam Monolith and Far Boundary Excited

The relative phase of the ground motion that affects the far end boundary of the reservoir influences the magnitude of the supplementary response peaks. The response of a dam monolith impounding a reservoir having an L/H ratio of 5.0 when subjected to in-phase ground motion (phase difference of 0 degrees), is presented in figure 4.5. The wave reflection coefficient is taken as 0.975. The ground motion at the far end boundary either increases or decreases the magnitudes of the supplementary response peaks depending on the frequency of excitation. This can be seen in comparing figures 4.2 and 4.5. Figure 4.2 is the response of the same system when the ground motion only affects the monolith. The supplementary response peak that occurs at a frequency of 4.30 Hz is increased considerably in magnitude. This peak's magnitude increases from 14.77 (monolith excited only) to 35.66 (far boundary and monolith excited in-phase). This is an increase of 141.4%. The supplementary response peak at a frequency of 6.01 Hz is increased to a value of 38.44 for the in-phase case from a value of 22.08 for the monolith only case. This is an increase of 74.1%.

Supplementary response peaks that occur at frequencies of 4.89 Hz and 6.89 Hz are decreased by 86.5% and 52.9%, respectively. The peak at 4.89 Hz decreases from a value of 19.01 to 2.56 for the monolith only case. The magnitude of the peak at 6.89 Hz decreases from a value of 19.66 to a value of 9.25 when the ground motion is applied to the far end boundary.

The motion of the two boundaries, when subjected to in-phase ground motion, is such that it accentuates the unsymmetric eigen modes of the reservoir. Symmetry of the reservoir's eigen modes is measured about the mid-point of the reservoir's length in the horizontal direction. Symmetry in the vertical direction does not exist. As the monolith is moving away from the reservoir, the far end boundary is moving towards the reservoir. This causes a reduction in the hydrodynamic pressures at the monolith and an increase at the far end boundary. These unsymmetric eigen modes occur at excitation frequencies of 4.30 Hz and 6.01 Hz in the above mentioned example. Resonance of these reservoir modes therefore occurs and the resulting pressures will have significant magnitude.

Response peaks that are associated with symmetric eigen modes of the reservoir are decreased in magnitude for this case of ground motion excitation. The symmetric eigen modes occur at excitation frequencies of 4.89 Hz and 6.89 Hz in this example. These particular modes do not satisfy the boundary conditions at the ends of the reservoir. They are not excited by the ground motion and therefore their magnitudes are decreased relative to the case where only the monolith is excited.

When the ground motion is considered to be out-of-phase, the exact opposite occurs. Response peaks that were accentuated in the in-phase case are now diminished and visa versa. This can be seen by comparing figures 4.5 and 4.6. Figure 4.6 represents the response of a monolith impounding a reservoir having an L/H ratio of 5.0 when the ground motion at the far end boundary is out-of-phase

with the ground motion at the monolith. The wave reflection coefficient is taken as 0.975. The supplementary response peaks that occur at excitation frequencies of 4.30 Hz and 6.01 Hz have their magnitudes reduced by 45.8% and 73.1%, respectively. The response peak that occurs at a frequency of 4.30 Hz decreases from a non-dimensional acceleration of 14.77 when the monolith is excited alone to 8.02 when the far boundary is excited out-of-phase. The response peak at a frequency of 6.01 Hz is similarly decreased from an acceleration of 22.08 to an acceleration of 5.93.

The response peaks that occur at frequencies of 4.89 Hz and 6.89 Hz have their magnitudes increased. The supplementary response peak that occurs at a frequency of 4.89 Hz increases from a magnitude of 19.01 to a magnitude of 36.44 when the far boundary is excited out-of-phase. This is an increase of 91.5% over the case where the monolith is excited alone. The other response peak increases from a value of 19.66 to a value of 30.07; an increase of 53.0%. These same two peaks increase 1323.4% and 225.1%, respectively, when the out-of-phase response is compared to the in-phase response.

The supplementary response peaks that are associated with the unsymmetrical eigen modes of the reservoir are decreased in magnitude when the ground motion at the far end boundary is considered to be out-of-phase. Peaks that are associated with the symmetrical reservoir eigen modes have their magnitudes increased. As the monolith is moving in towards the reservoir, so does the far end boundary. The hydrodynamic pressures at the two ends of the reservoir will increase. This will tend

to excite the symmetric reservoir eigen modes rather than the unsymmetric ones. Significant differences in the magnitudes of these supplementary response peaks are observed depending on the phase of the ground motion at the far end boundary of the reservoir. The response of the system is therefore significantly dependent on the phase of the ground motion that affects this far end boundary. An inaccurate estimate of the monolith's response will be obtained if the ground motion at the far end boundary in a finite reservoir is neglected in the dynamic analysis.

The response of the system when actual ground motion records are used in the analysis depends on the relative phase difference between the ground motion at the monolith and that at the far end boundary of the reservoir. The peaks that are the most significantly affected occur in the frequency range of 4 to 8 Hz. Earthquake ground motion events that are classified as having a high a/v ratio also have significant energy in this frequency range. The dam-reservoir-foundation system will therefore have dramatically different responses depending on the energy content of the ground motion to which it is subjected.

The response of a dam impounding a reservoir having an L/H ratio of 1.0 is presented in figure 4.7. The ground motion at the far end boundary was considered to be in-phase with the ground motion at the dam monolith. The wave reflection coefficient was taken as 0.975. For this ground motion case, the magnitude of the fundamental peak decreases significantly. When the reservoir is considered long (L/H = 5.0), this peak has a magnitude of 28.84. It is reduced to a value of 21.33

when the reservoir is shortened to an L/H ratio of 1.0. This can be seen in comparing figures 4.5 and 4.7. The pressures in the reservoir caused by the rigid body mode of the monolith decrease as the reservoir becomes increasingly shorter in length, when subjected to in-phase ground motion. It was shown by Werner and Sundquist (1949) that the pressures inside a tank having rigid vertical walls affected by in-phase ground motion will decrease as the length of the tank decreases. That appears to be similar to what occurs in the case of a short reservoir. As the length of the reservoir decreases, the pressures acting on the dam face decrease in magnitude. The additional hydrodynamic forces created by the reservoir are therefore also decreased in magnitude. This results in the reduction of the magnitude of the system's fundamental response peak.

For the case when the ground motion affecting the dam monolith and the far end boundary is considered to be out-of-phase, the magnitude of the fundamental response peak is increased as the L/H ratio decreases. The magnitude of this response peak is increased from a value of 28.84 to a value of 37.76 when the reservoir's L/H ratio is decreased from 5.0 to 1.0. This can be seen by comparing figures 4.6 and 4.8. Figure 4.8 presents the response of a monolith impounding a reservoir having an L/H ratio of 1.0. The ground motion at the far boundary was considered to be out-of-phase with that at the monolith. The wave reflection coefficient was taken as 0.975. This occurs because the pressures created by the rigid

body mode are increased as the reservoir's length decreases as demonstrated by Werner and Sundquist (1949).

This change in the magnitude of the fundamental response peak will alter the response of the system when it is subjected to both intermediate and high a/v ratio earthquake ground motion events when the reservoir is assumed to be short in length. This response peak occurs at a frequency of 2.63 Hz. These two types of earthquake ground motion both have significant energy at this frequency. The response of the system can be substantially increased or decreased, as compared to the long reservoir case, depending on the relative phase of the ground motion at the far end of the reservoir. The length of the reservoir therefore has an important impact on the overall response of the system when the ground motion is assumed to affect the far end boundary as well as the monolith.

4.3.2 Reservoir-Foundation Interaction

In this section, the response of the dam monolith is investigated when the system is analyzed using the one and two dimensional boundary conditions for the reservoir-foundation interface. These boundary conditions were discussed in section 3.2.4. The first sub-section is concerned with the effect of the wave reflection coefficient (denoted as α) on the response of the finite reservoir system when the far end boundary is excited. The interface is modelled using the one dimensional boundary condition of Hall and Chopra (1980). This boundary condition excludes

the effects of soil column interaction, or shear effects. The second sub-section deals with the effect of including the soil column interaction in the boundary condition for the reservoir-foundation interface. The proposed two dimensional boundary condition that incorporates the effects of soil column interaction is used in this analysis. The response determined using this proposed boundary condition is compared to that determined using the one dimensional boundary condition developed by Hall and Chopra (1980).

(a) One Dimensional Boundary Condition

The response of a dam monolith impounding a reservoir having an L/H ratio of 5.0 is presented in figure 4.9. The ground motion at the far end boundary is in-phase with that at the dam monolith. The thin solid line in the figure presents the response when the wave reflection coefficient is 0.975 and the heavy solid line is the response when the coefficient is 0.7. The supplementary response peaks at excitation frequencies of 4.30 Hz and 6.01 Hz are significantly decreased in magnitude by the decreased value of the wave reflection coefficient as shown in this figure. The response peak at a frequency of 4.30 Hz is reduced in magnitude from a value of 35.66 to 7.20 when the wave reflection coefficient is decreased from 0.975 to 0.700. This is a decrease of 79.8% relative to the case of more reflective reservoir bottom (α = 0.975). The response peak at a frequency of 6.01 Hz is decreased by 74.8%, changing in magnitude from 38.44 to 9.68.

The fundamental response peak experiences a small decrease in magnitude from 28.84 to 24.39, or of 15.4%. This reduction is the same as predicted when the analysis assumes an infinite length reservoir (Hall and Chopra, 1980; Fenves and Chopra, 1984b).

The response of the dam-reservoir-foundation system impounding a reservoir having an L/H ratio of 5.0 no longer exhibits finite reservoir length effects when the wave reflection coefficient has a value of 0.5. Reservoirs having smaller L/H ratios ($\leq$ 2.5) are more susceptible to finite reservoir effects. All values of the wave reflection coefficient should be considered for these reservoirs when the general case of ground motion excitation is used.

The value of the wave reflection coefficient has a significant impact on the dam-reservoir-foundation system when a finite reservoir length is assumed. It has a particularly dramatic effect on the magnitudes of the supplementary response peaks. These response peaks have their magnitudes significantly reduced when the value of this coefficient is changed only slightly. The reservoir-foundation interface dissipates energy directly form the reservoir substructure. Response peaks that are generated primarily by the resonance of the reservoir are therefore significantly reduced. Peaks that are generated through the combined resonance of the monolith and the reservoir have their magnitudes decreased by a lesser amount. The reservoir-foundation interface does not dissipate energy directly from the monolith substructure. The

choice of a coefficient value therefore is very important in the analysis of the overall dam-reservoir-foundation system when a finite length reservoir is assumed.

(b) Proposed Two Dimensional Boundary Condition

The behaviour of a monolith impounding a reservoir having an L/H ratio of 1.0 and a wave reflection coefficient of 0.975 is plotted in figure 4.10. The length parameter, L′, in equation (3.8) is taken as 150 m (500 ft). The ground motion at the far end boundary was considered to be in-phase with that at the dam monolith. The proposed two dimensional boundary condition which takes into account the interaction between soil columns was used in this analysis. The proposed boundary condition has the effect of reducing the magnitude of the fundamental response peak. This response peak is reduced 7.7% from a value of 21.33 to a value of 19.69 when the boundary condition is switched from being one dimensional to two dimensional.

This is true of the supplementary response peaks as well. The response peaks that occur at frequencies of 4.15, 6.69, and 9.28 Hz are decreased by 41.5%, 7.9%, and 40.1%, respectively, relative to the case where the one dimensional boundary condition is used. The proposed boundary condition permits more energy to be drawn out of the reservoir substructure than the boundary condition developed by Hall and Chopra (1980) when the same value of the wave reflection coefficient is assumed.

The two response peaks that occur at frequencies of 4.15 and 9.28 Hz are generated primarily through the resonance of the reservoir. This boundary condition dissipates energy primarily from the reservoir substructure. Very little energy is dissipated directly from the monolith. These two peaks are therefore affected significantly by the proposed boundary condition.

The supplementary response peak that occurs at a frequency of 6.69 Hz is not reduced as significantly. This particular peak is generated from the combined resonance of the monolith and reservoir substructures. Peaks that are generated solely by the resonance of the reservoir will be the most significantly affected by this boundary condition.

The shape of the Fourier representation of the monolith's response however remains the same for both the proposed two dimensional and the one dimensional (Hall and Chopra, 1980) boundary conditions. This is because the two boundary conditions are similar in form. The interaction that exists between individual soil columns has the primary effect of increasing the damping provided by the reservoir-foundation interface. This increased damping in turn reduces the magnitude of the monolith's response to the earthquake ground motion. The resonant characteristics of the reservoir itself are not altered by the proposed boundary condition.

The behaviour of the system when the wave reflection coefficient is reduced to a value of 0.7 is somewhat similar to the case with a coefficient value of 0.975. The response of a dam monolith impounding a reservoir having an L/H ratio of 1.0

and a wave reflection coefficient of 0.7 is presented in figure 4.11. The length parameter, L′, was again taken as 150 m (500 ft). The ground motion at the far end boundary was assumed in-phase with that at the dam monolith. The proposed boundary condition reduces the magnitudes of the supplementary response peaks as compared to the one dimensional boundary condition. The supplementary response peak occurring at a frequency of 6.69 Hz is decreased by 29.7%. Its magnitude is reduced from a value of 21.53 to 15.14 when the soil column interaction is considered. This reduction of the magnitude again can be explained by the additional damping provided by the proposed boundary condition.

The proposed two-dimensional boundary condition that has been developed is equivalent to the one-dimensional boundary condition (Hall and Chopra, 1980) with an increased damping value at the reservoir-foundation interface. The amount of additional damping that is provided is dependent on the frequency of excitation, the mode shape of the monolith that excites the reservoir substructure, and the specific location along the reservoir-foundation interface that is considered.

The interaction between the reservoir and its foundation is an important characteristic of the dam-reservoir-foundation system when a finite length reservoir is assumed. The manner by which this reservoir-foundation interface is modelled will significantly affect the response of the monolith to earthquake ground motion. The monolith's response has been shown to decrease in magnitude when the soil column interaction, or shear effects, are included in the dynamic analysis. It is important to

model this interface as properly as possible in order to obtain an accurate estimate of the response of the monolith.

4.3.3 Reservoir Shape

The response of a monolith impounding a triangular shaped (heavy solid line) and a rectangular shaped (thin solid line) reservoir are shown in figure 4.12. The L/H ratio of this configuration is 5.0, the wave reflection coefficient is taken as 0.975, and the ground motion is considered to be in-phase. The response of this configuration when subjected to out-of-phase ground motion is presented in figure 4.13. The different reservoir geometries cause the frequencies of excitation at which the reservoir responds to be different for the triangular reservoir geometry than for the rectangular reservoir geometry. The additional hydrodynamic forces, and therefore the supplementary response peaks, for the triangular reservoir geometry occur at different excitation frequencies than those of the rectangular reservoir geometry.

The phase of the ground motion affects the reservoir's eigen modes in the case of a triangular reservoir geometry in a similar fashion to the case of a rectangular reservoir. In-phase and out-of-phase ground motion that affects the reservoir's bottom (or the far end boundary in a rectangular reservoir) excites different eigen modes of the reservoir. This can be seen in comparing figures 4.12 and 4.13. The response peak at a frequency of 4.69 Hz is increased in magnitude

from a value of 18.40 for the in-phase case to a value of 47.31 for the out-of-phase case. This is an increase of 157.1%. The increase is calculated relative to the in-phase ground motion case. The supplementary response peak occurring at a frequency of 6.49 Hz is decreased by 54.0%. This peak decreases from a magnitude of 31.50 for the in-phase case to 14.48 for the out-of-phase case.

The geometry of the upstream reservoir is an important parameter in defining the monolith's response. It has been shown to alter the frequencies at which the supplementary response peaks occur in the Fourier representation of the monolith's response. As a result, the actual earthquake ground motion may cause significant response of the monolith at different frequencies for different assumed geometries. The response of the monolith when it impounds a triangular shaped reservoir will be very much different from that when the reservoir is rectangular in shape. It is important therefore that the reservoir's geometry be modelled as accurately as possible.

The phase of the ground motion is also an important parameter in the monolith's response when the reservoir geometry is idealized as triangular as it is when the reservoir geometry is idealized as rectangular. The phase of the ground motion has been shown to influence the magnitudes of the supplementary response peaks. This will in turn affect the monolith's response to actual earthquake ground motion. The phase difference between the ground motion affecting the monolith and

that affecting the reservoir bottom must be considered at the same time as the particular reservoir geometry is considered.

4.4 SUMMARY

The effect of a finite length reservoir has been shown to be very important in the dynamic analysis of a dam monolith. The finite length reservoir resonates in the horizontal as well as the vertical directions. This results in the creation of additional supplementary response peaks at excitation frequencies larger than that of the fundamental mode of the dam-reservoir-foundation system. The magnitude of these response peaks are significantly greater than that of the response of a monolith that impounds an infinite length reservoir. The response of the monolith will therefore be significantly underestimated if the reservoir length is assumed infinite when the actual reservoir length is finite.

The ratio of the reservoir length to dam height (L/H) is a significant parameter that affects the monolith's response. The value of this ratio determines the number and magnitude of these supplementary response peaks that are created. As the L/H ratio decreases, the number of these supplementary response peaks decreases and their magnitudes increase.

The phase of the ground motion was also found to affect the magnitudes of the supplementary response peaks. The specific response peaks that are increased or decreased in magnitude depend directly on the phase of the ground motion. In-

phase motion excites the unsymmetric eigen modes of the reservoir. Out-of-phase ground motion excites the symmetric eigen modes of the reservoir. The L/H ratio of the reservoir will determine the specific frequencies at which these symmetric and unsymmetric eigen modes occur.

The model that is used for the reservoir-foundation interface has an impact on the monolith's response when a finite reservoir length is assumed. Supplementary response peaks generated primarily through the sole resonance of the reservoir are affected more by the value of the wave reflection coefficient than those generated through the combined resonance of the reservoir and monolith substructure. The effect of the soil column interaction, or shear effects, further reduces the magnitudes of the response peaks when the proposed two dimensional boundary condition is used. This boundary condition allows more energy to be dissipated from the reservoir substructure than the one dimensional boundary condition of Hall and Chopra (1980).

The reservoir geometry is a significant parameter in the response of the dam-reservoir-foundation system when a finite length reservoir is assumed. The geometry of the reservoir determines the resonant frequencies of this substructure. These in turn determine the frequencies at which the supplementary response peaks occur in the monolith's response.

Finite reservoir effects will be the most significant when the dam-reservoir-foundation system is being subjected to earthquake ground motion that is classified

as having an intermediate to high a/v ratio. These types of ground motion have significant energy contents in the frequency range of 0 to 10 Hz. The most significant supplementary response peaks are located in this frequency range for most of the practical finite length reservoir geometries. All the above mentioned parameters must be considered simultaneously in order that a reasonable estimate of the dynamic behaviour of the dam-reservoir-foundation system be obtained when a finite length upstream reservoir is assumed.

Table 4.1 - Cases of Dam-Reservoir-Foundation Systems Analyzed

Case	L/H	Wave Reflection Coefficient	Boundary Condition	Reservoir Geometry	Ground Motion
1	5.0	0.975	1-D	Rectangular	Monolith only
2	2.5	0.975	1-D	Rectangular	Monolith only
3	1.0	0.975	1-D	Rectangular	Monolith only
4	5.0	0.700	1-D	Rectangular	Monolith only
5	2.5	0.700	1-D	Rectangular	Monolith only
6	1.0	0.700	1-D	Rectangular	Monolith only
7	5.0	0.975	1-D	Rectangular	In-Phase
8	2.5	0.975	1-D	Rectangular	In-Phase
9	1.0	0.975	1-D	Rectangular	In-Phase
10	5.0	0.700	1-D	Rectangular	In-Phase
11	2.5	0.700	1-D	Rectangular	In-Phase
12	1.0	0.700	1-D	Rectangular	In-Phase
13	5.0	0.975	1-D	Rectangular	Out-of-Phase
14	2.5	0.975	1-D	Rectangular	Out-of-Phase
15	1.0	0.975	1-D	Rectangular	Out-of-Phase
16	5.0	0.700	1-D	Rectangular	Out-of-Phase
17	2.5	0.700	1-D	Rectangular	Out-of-Phase
18	1.0	0.700	1-D	Rectangular	Out-of-Phase
19	5.0	0.975	2-D	Rectangular	Monolith only
20	1.0	0.975	2-D	Rectangular	Monolith only
21	5.0	0.700	2-D	Rectangular	Monolith only
22	1.0	0.700	2-D	Rectangular	Monolith only
23	5.0	0.975	2-D	Rectangular	In-Phase
24	1.0	0.975	2-D	Rectangular	In-Phase
25	5.0	0.700	2-D	Rectangular	In-Phase
26	1.0	0.700	2-D	Rectangular	In-Phase
27	5.0	0.975	2-D	Rectangular	Out-of-Phase
28	1.0	0.975	2-D	Rectangular	Out-of-Phase
29	5.0	0.700	2-D	Rectangular	Out-of-Phase
30	1.0	0.700	2-D	Rectangular	Out-of-Phase
31	5.0	0.975	1-D	Triangular	Monolith only
32	2.5	0.975	1-D	Triangular	Monolith only
33	1.5	0.975	1-D	Triangular	Monolith only

Table 4.1 - Cases of Dam-Reservoir-Foundation Systems Analyzed (cont'd)

Case	L/H	Wave Reflection Coefficient	Boundary Condition	Reservoir Geometry	Ground Motion
34	1.0	0.975	1-D	Triangular	Monolith only
35	5.0	0.700	1-D	Triangular	Monolith only
36	2.5	0.700	1-D	Triangular	Monolith only
37	1.5	0.700	1-D	Triangular	Monolith only
38	1.0	0.700	1-D	Triangular	Monolith only
39	5.0	0.500	1-D	Triangular	Monolith only
40	2.5	0.500	1-D	Triangular	Monolith only
41	1.5	0.500	1-D	Triangular	Monolith only
42	1.0	0.500	1-D	Triangular	Monolith only
43	5.0	0.975	1-D	Triangular	In-Phase
44	2.5	0.975	1-D	Triangular	In-Phase
45	1.5	0.975	1-D	Triangular	In-Phase
46	1.0	0.975	1-D	Triangular	In-Phase
47	5.0	0.700	1-D	Triangular	In-Phase
48	2.5	0.700	1-D	Triangular	In-Phase
49	1.5	0.700	1-D	Triangular	In-Phase
50	1.0	0.700	1-D	Triangular	In-Phase
51	5.0	0.500	1-D	Triangular	In-Phase
52	2.5	0.500	1-D	Triangular	In-Phase
53	1.5	0.500	1-D	Triangular	In-Phase
54	1.0	0.500	1-D	Triangular	In-Phase
55	5.0	0.975	1-D	Triangular	Out-of-Phase
56	2.5	0.975	1-D	Triangular	Out-of-Phase
57	1.5	0.975	1-D	Triangular	Out-of-Phase
58	1.0	0.975	1-D	Triangular	Out-of-Phase
59	5.0	0.700	1-D	Triangular	Out-of-Phase
60	2.5	0.700	1-D	Triangular	Out-of-Phase

Table 4.1 - Cases of Dam-Reservoir-Foundation Systems Analyzed (cont'd)

Case	L/H	Wave Reflection Coefficient	Boundary Condition	Reservoir Geometry	Ground Motion
61	1.5	0.700	1-D	Triangular	Out-of-Phase
62	1.0	0.700	1-D	Triangular	Out-of-Phase
63	5.0	0.500	1-D	Triangular	Out-of-Phase
64	2.5	0.500	1-D	Triangular	Out-of-Phase
65	1.5	0.500	1-D	Triangular	Out-of-Phase
66	1.0	0.500	1-D	Triangular	Out-of-Phase

Monolith only = the ground motion was applied at monolith only

In-phase = the ground motion applied at the far boundary was in-phase with the ground motion at the monolith

Out-of-phase = the ground motion applied at the far boundary was out-of-phase with the ground motion at the monolith

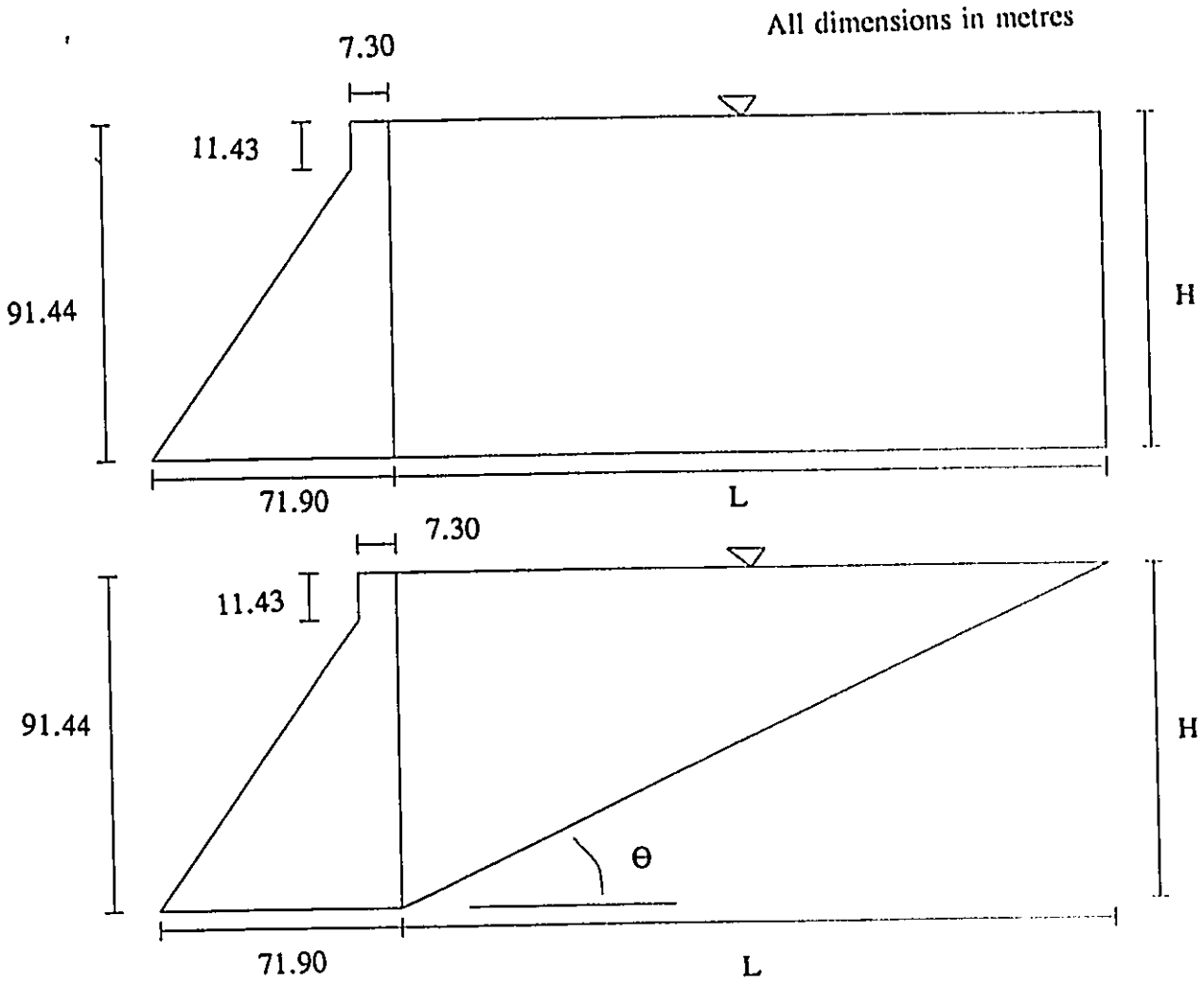

Figure 4.1 - Schematic of dam-reservoir-foundation system

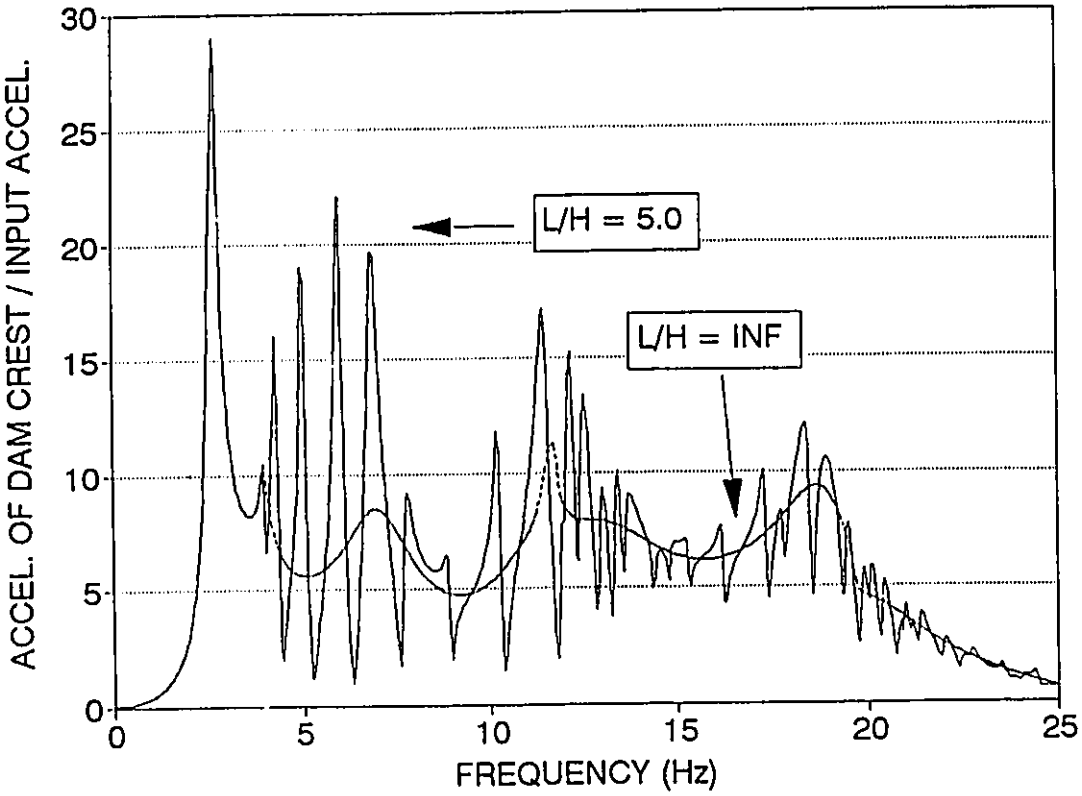

Figure 4.2 - Response of long reservoir (L/H = 5.0), monolith only excited

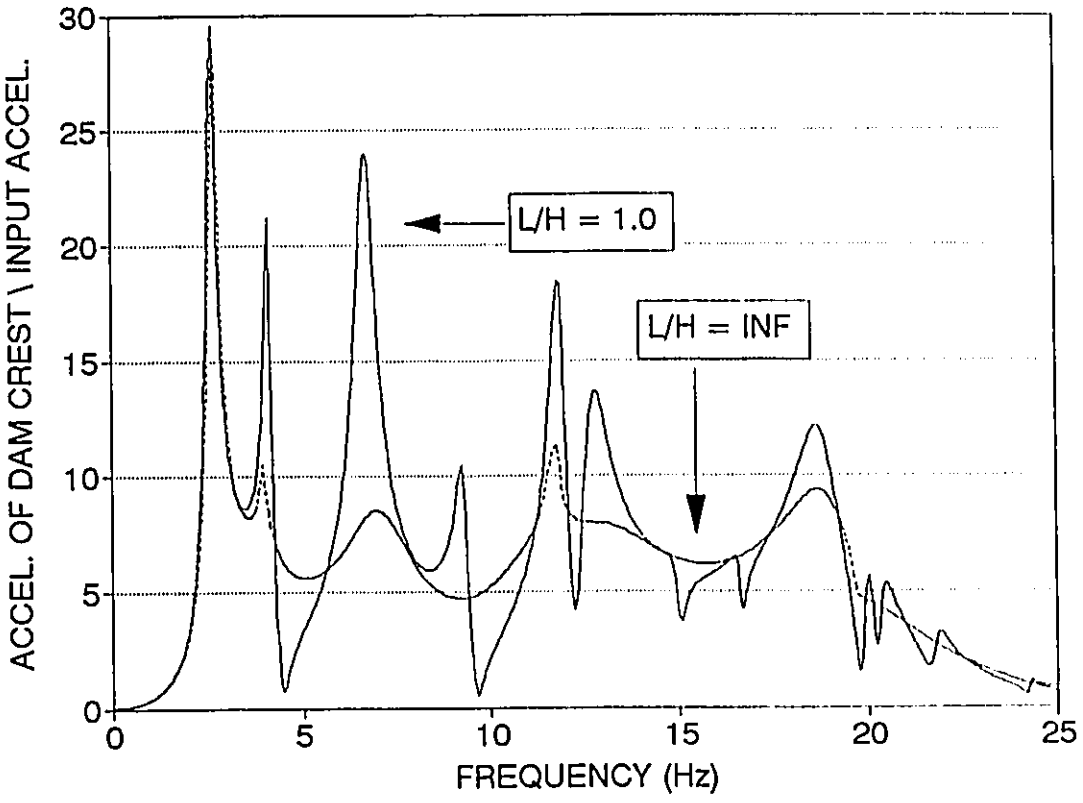

Figure 4.3 - Response of short reservoir (L/H = 1.0), monolith only excited

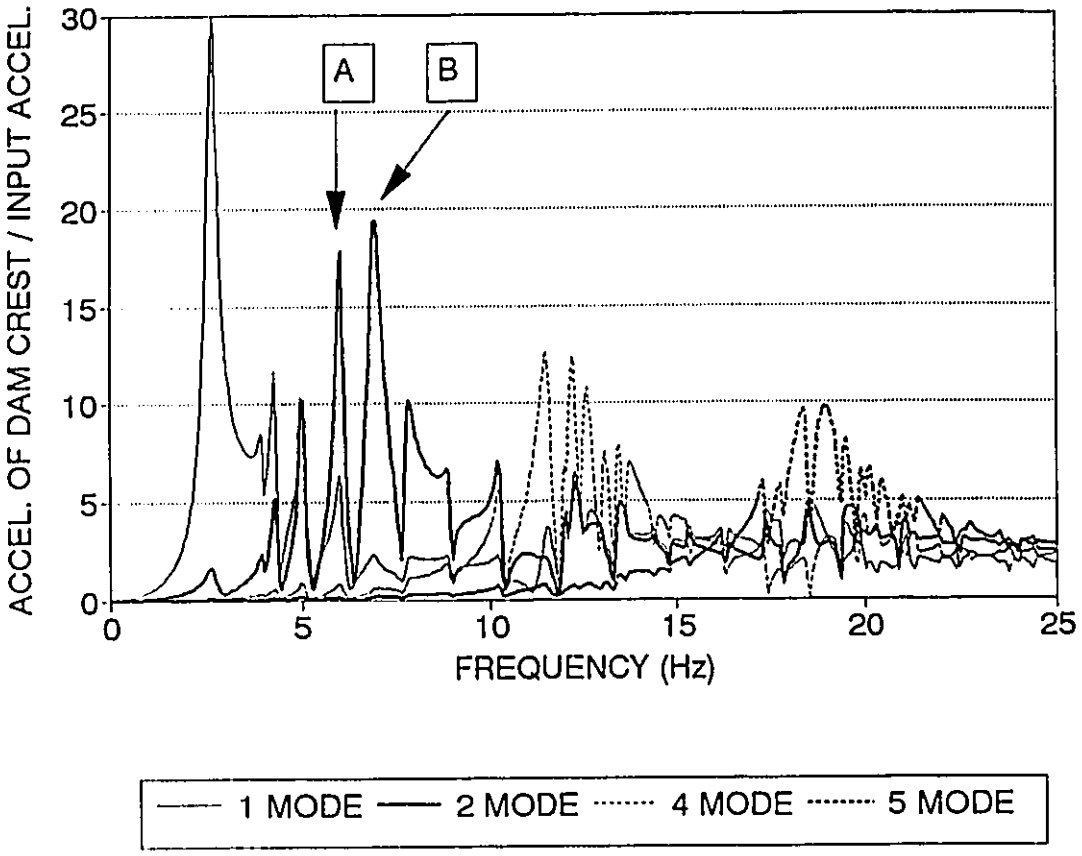

Figure 4.4 - Modal contributions for long reservoir (L/H = 5.0)

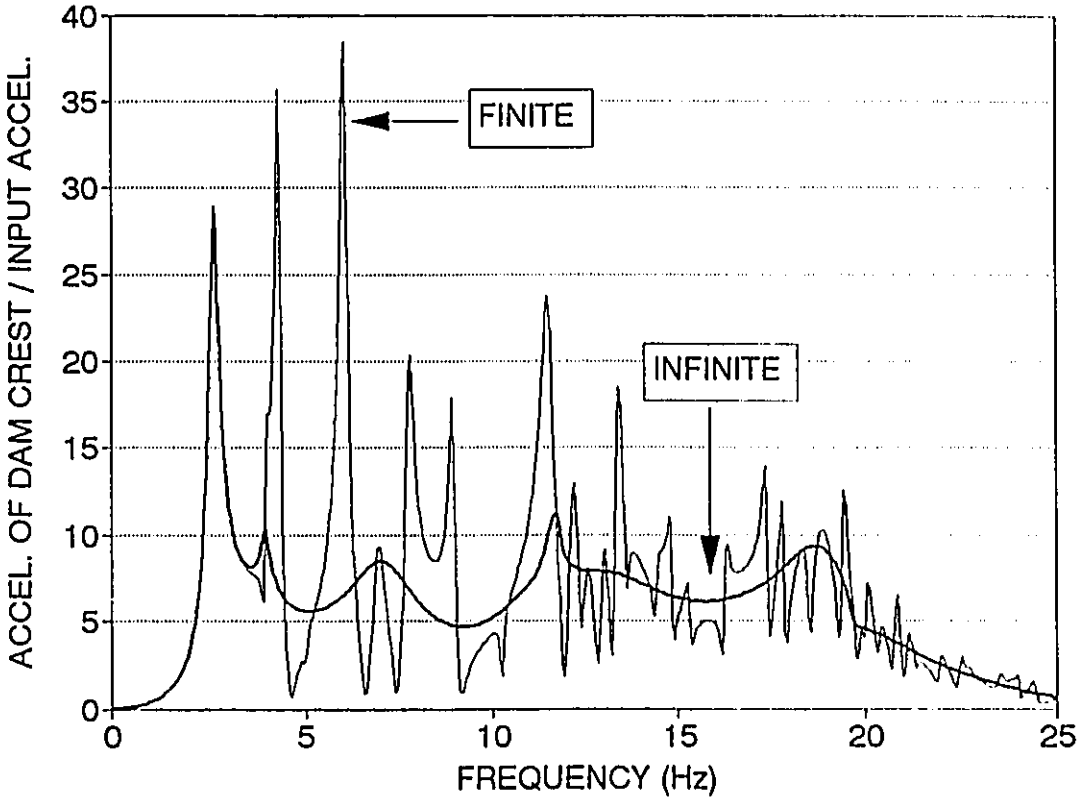

Figure 4.5 - Monolith response for long (L/H = 5.0) reservoir when ground motion is considered in-phase

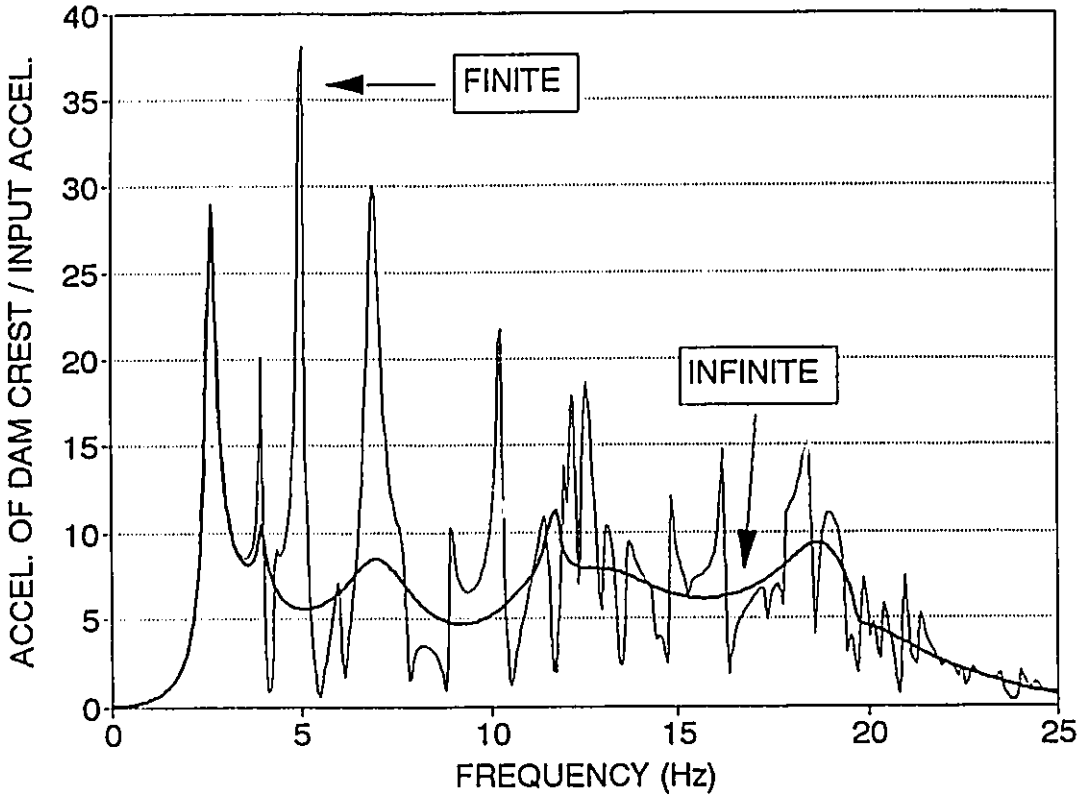

Figure 4.6 - Monolith response for long (L/H = 5.0) reservoir when ground motion is considered out-of-phase

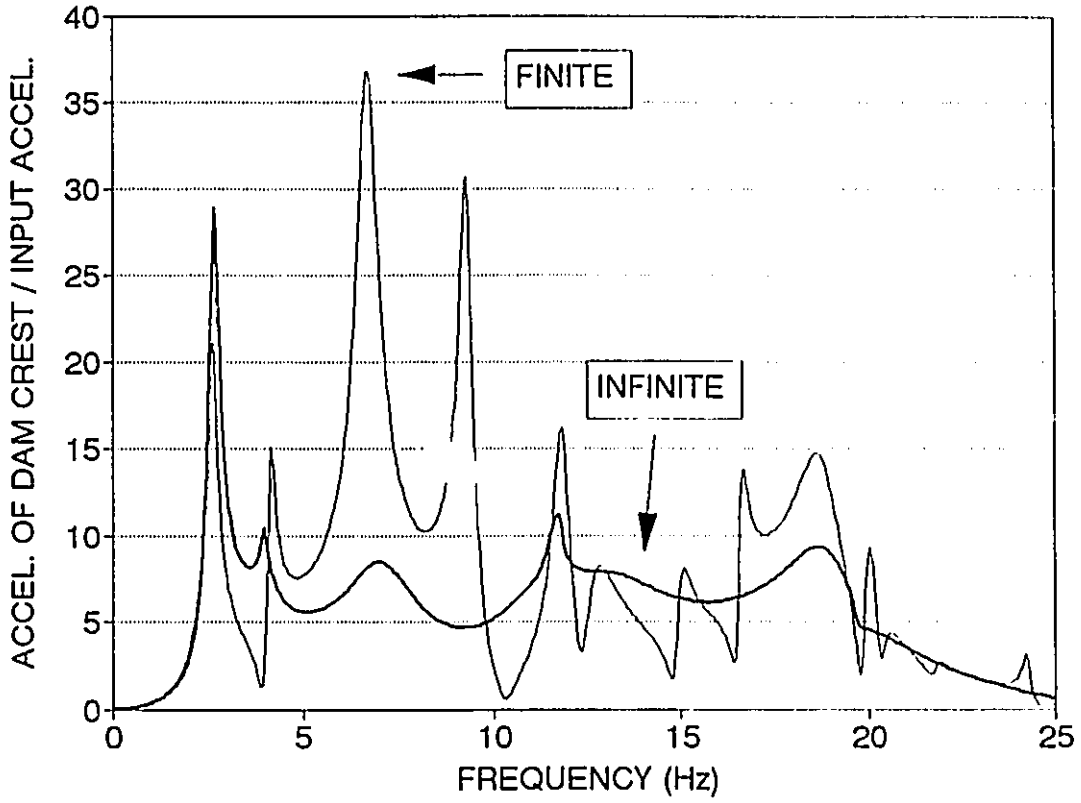

Figure 4.7 - Monolith response for short (L/H = 1.0) reservoir when ground motion is considered in-phase

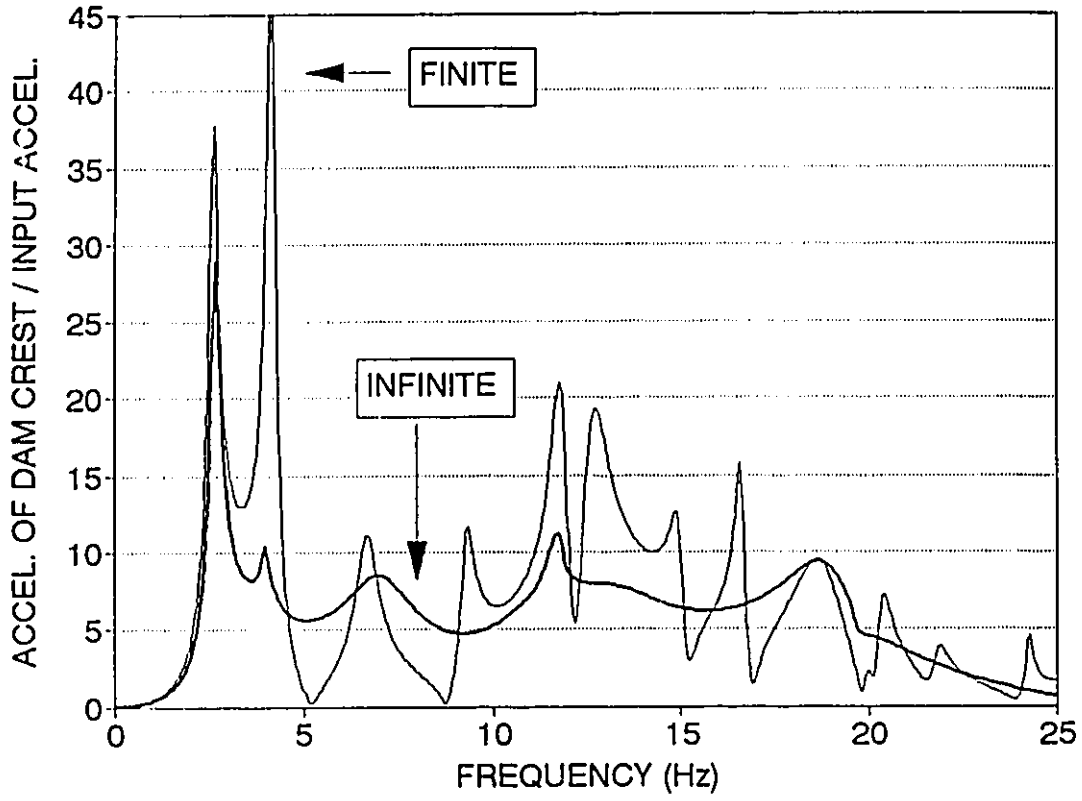

Figure 4.8 - Monolith response for short (L/H = 1.0) reservoir when ground motion is considered out-of-phase

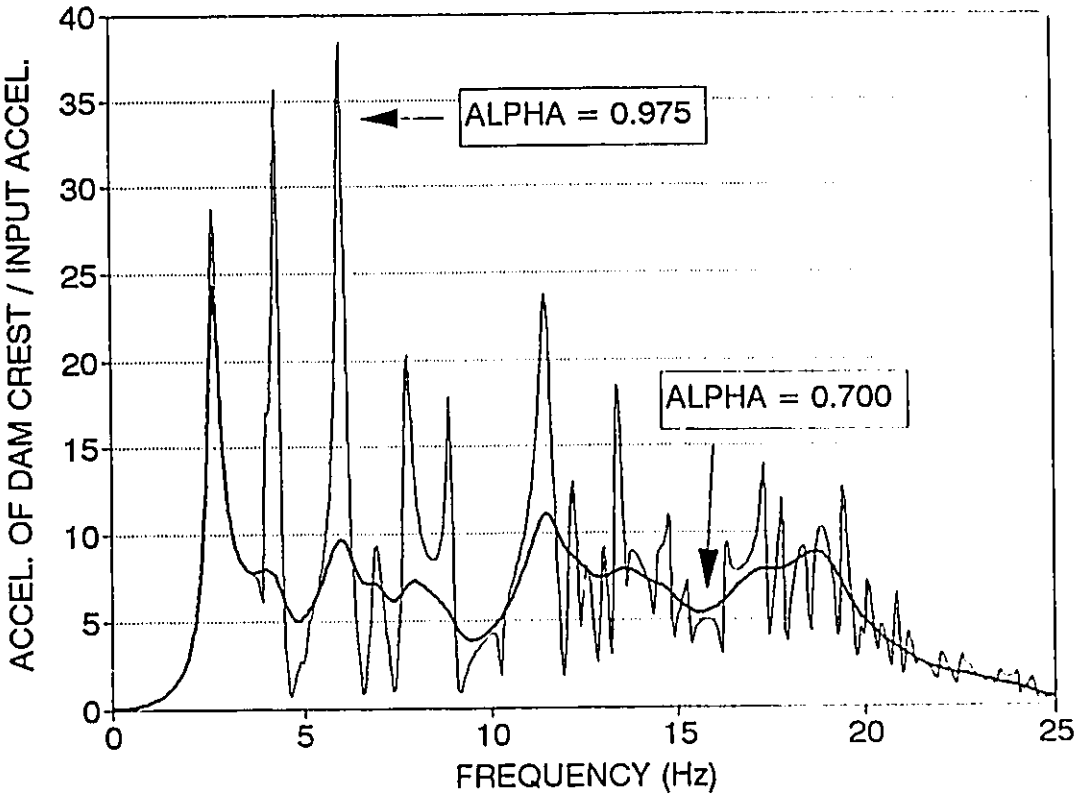

Figure 4.9 - Effect of wave reflection coefficient on monolith response for in-phase ground motion

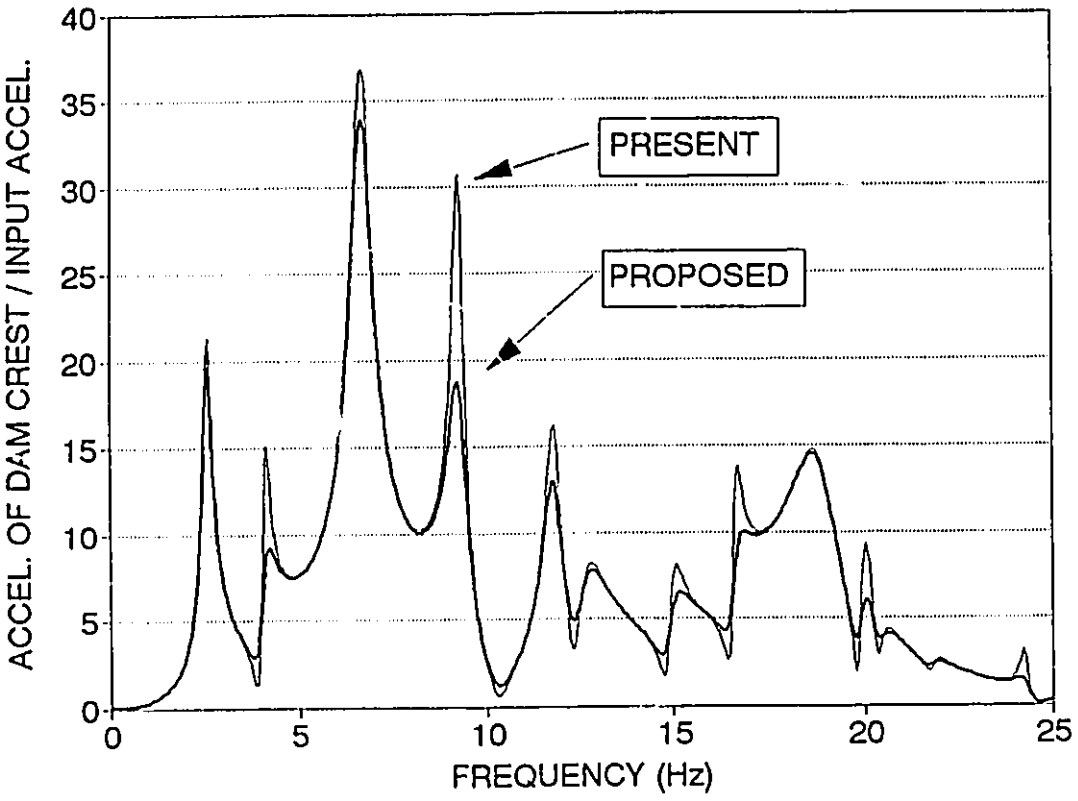

Figure 4.10 - Comparison of present and proposed boundary conditions for in-phase ground motion and wave reflection coefficient of 0.975 (L/H = 1.0)

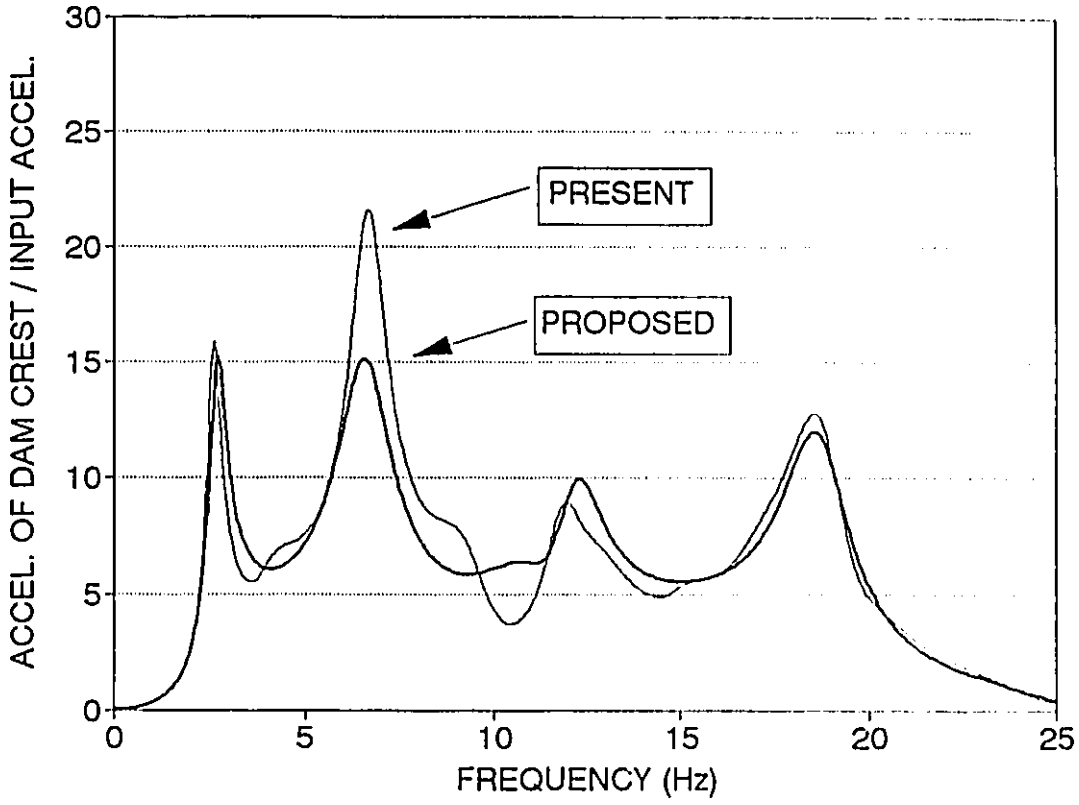

Figure 4.11 - Comparison of present and proposed boundary condition for in-phase ground motion and wave reflection coefficient of 0.700 (L/H = 1.0)

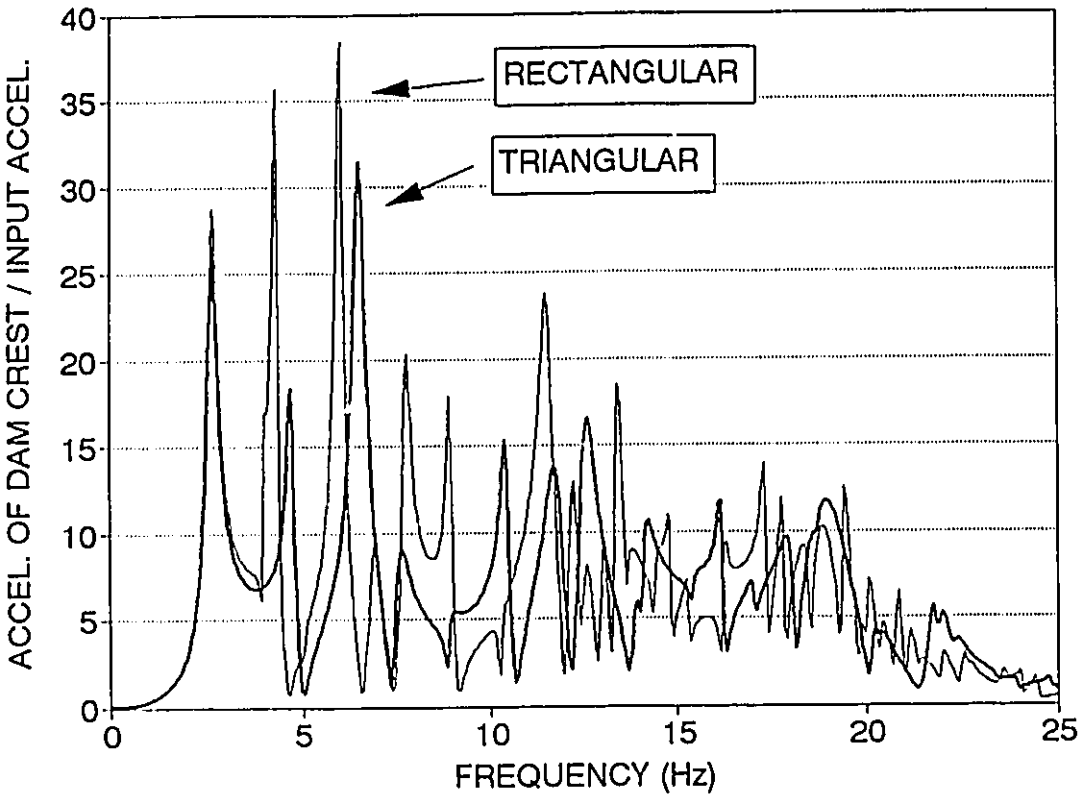

Figure 4.12 - Monolith response for rectangular and triangular geometry (L/H = 5.0) assuming in-phase ground motion

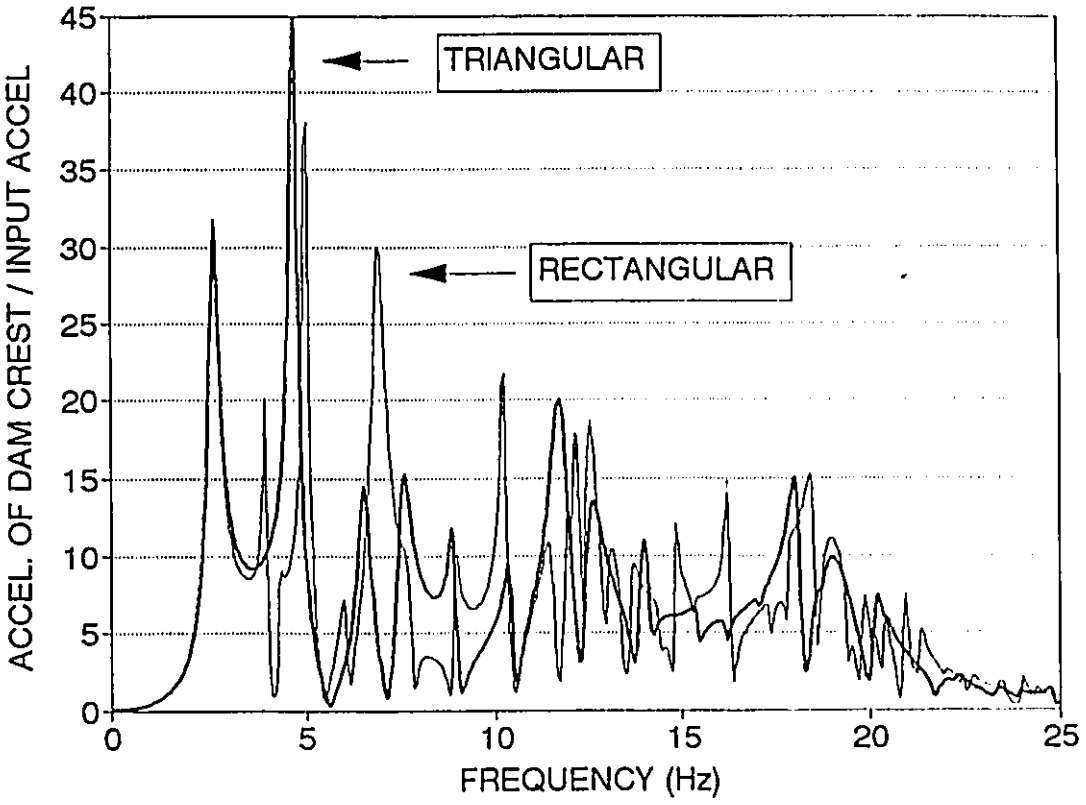

Figure 4.13 - Monolith response for rectangular and triangular geometry (L/H = 5.0) assuming out-of-phase ground motion

CHAPTER 5

STRESS ANALYSIS

5.1 INTRODUCTION

In this chapter, the dam-reservoir-foundation system is analyzed using actual earthquake ground motion records when a finite reservoir length is assumed. The effect of the finite length reservoir characteristics (L/H ratio, phase of ground motion, and reservoir geometry) on the tensile stresses that the monolith experiences is investigated when the system is subjected to earthquake ground acceleration records. The tensile stress experienced by the dam monolith is of interest because this is the critical stress during earthquake excitation. Experience at the Koyna Dam during the 1967 earthquake (Chopra and Chakrabarti, 1972) showed that cracking of the concrete is more critical than crushing of the concrete during strong shaking. The system configurations adopted for analysis in Chapter 4 are also used in this chapter. Four actual earthquake ground motion records are used. Two are classified as having an intermediate ratio of their maximum ground acceleration (in g's) to their maximum ground velocity (in m/s) (a/v) ($0.8 \leq a/v \leq 1.2$) and two that are classified as having a high a/v ratio ($a/v \geq 1.2$) (Naumoski, et. al., 1988).

In this chapter, the ground motion records used in the stress analysis are described. The normalization of the acceleration records is discussed. The effect of the ratio of the reservoir's length to dam height on the magnitude of the maximum dynamic tensile stress is evaluated. The ground motion is assumed to only excite the dam monolith. The effect of the phase of the ground motion that excites the far end boundary of the reservoir is analyzed. Again, the magnitude of the maximum dynamic tensile stress is of interest. The last section of this chapter examines the effect of varying the reservoir geometry on the dynamic tensile stresses. Two reservoir geometries are examined: rectangular and triangular.

5.2 EARTHQUAKE GROUND MOTION

Four earthquake ground motion records were used in this analysis. Two records with an intermediate a/v ratio were selected. These are the Imperial Valley (S00E; May 18, 1940; El Centro) and the Kern County (N21E; July 21, 1952; Taft Lincoln School Tunnel) records. The acceleration time histories of these two earthquake events are presented in figures 5.1 and 5.2 for the Imperial Valley and Kern County events, respectively. These two records have significant accelerations in the frequency range from 0 to 4 Hz. The records have low accelerations at frequencies greater than 4 Hz. The Fourier representation of the actual earthquake ground motions are presented in figures 5.3 and 5.4 for the Imperial Valley and the

Kern County events, respectively. Table 5.1 presents the recorded ground motion characteristics of these records.

Two records having a high a/v ratio were also used. These records are the San Francisco (S80E; March 22, 1957; Golden Gate Park) and the Saguenay (Longitudinal component; November 25,1988;St.-Ferreol) earthquake events (Wang, 1988). The acceleration time histories of these two earthquake events are presented in figures 5.5 and 5.6 for the San Francisco and Saguenay records, respectively. These records have significant accelerations in the frequency range from 0 to 15 Hz. The Fourier representations of the ground acceleration for the San Francisco and the Saguenay events are presented in figures 5.7 and 5.8, respectively. The recorded ground motion characteristics for these records are also listed in table 5.1.

All records have been scaled such that their maximum ground velocity is equal to that of the Imperial Valley record. This record has a maximum ground velocity of 0.334 m/s. This required that the acceleration records of the Kern County, San Francisco, and Saguenay records be scaled by factors of 2.13, 7.26, and 12.32, respectively. Their maximum unscaled ground velocities are 0.155,0.046,and 0.027 m/s, respectively. The maximum scaled ground accelerations for the four records are 0.348 g, 0.332 g, 0.762 g, and 1.490 g for the Imperial Valley, Kern County, San Francisco, and Saguenay records, respectively.

The dam-reservoir-foundation system assuming a finite length reservoir is a high frequency system. The fundamental frequency of the complete system is

approximately 2.6 Hz. This occurs near the extreme end of the frequency range at which the Imperial Valley and the Kern County records show significant acceleration. The absence of high frequency motion in these two records may be due to two distinct reasons. First, the Kern County record was recorded 56 kilometres from the epicentre. Some of the high frequency motion is likely to have attenuated as the ground motion event travelled away from the epicentre. The second probable reason for the absence of high frequency accelerations may be because of the type of accelerometer used to record the Imperial Valley ground motion. The Imperial Valley record was recorded just 8 kilometres from the epicentre. Such near field events typically have significant high frequency components in the ground acceleration record (Naumoski, et. al., 1988). The accelerometer used to record this motion most probably had a low Nyquist frequency and was thus unable to record the high frequency components of the ground motion.

The ground motion records were scaled to a common maximum ground velocity to obtain a quantitative estimate of the effect of the frequency content of the earthquake ground motion on the monolith's response. It is not the intent of this section of the study to compare the dynamic tensile stresses obtained from one ground motion record with those from the other records. It is of more interest to compare how the dynamic tensile stresses vary for each record separately when the dam-reservoir-foundation system's characteristics are altered. The ground motion records were therefore scaled to the maximum ground velocity of the Imperial Valley

record but their frequency content and a/v ratio were not altered. The number of ground motion records used is too small for a meaningful statistical analysis to be conducted.

5.3 FINITE RECTANGULAR RESERVOIR

The stresses in this analysis are determined at the centroid of each element. The Fourier representation of the system's response is combined with the Fourier representation of the earthquake ground motion to obtain the system's frequency domain response. An inverse Fourier transform is performed to obtain a time history of the monolith's displacements. These time histories are converted to strains at the centroid and combined with the elasticity matrix of the element. This yields the three components of stress that the element experiences. The maximum and minimum principle stresses are then determined. Figure 5.9 presents the finite element discretization of the monolith used in the analysis. The modulus of elasticity used in the analysis is 20 685 MPa. The compressive strength of the concrete is assumed to be 17 MPa. The modulus of rupture of the concrete is assumed to be 2.5 MPa.

The tensile stress profiles for the dam monolith impounding a reservoir of L/H ratio of infinity and 5.0 are presented in figure 5.10. The monolith alone is excited by the Imperial Valley event. The stresses in the monolith assuming a long finite length reservoir (L/H = 5.0) do not change significantly as compared to the

infinite length case when the monolith is subjected to the Imperial Valley ground motion record. This earthquake ground motion event has high input energy at excitation frequencies below 4 Hz. The Fourier representation of the monolith's response in this frequency range when the reservoir length is assumed finite is identical to that of when the reservoir length is assumed infinite. This can be seen in figure 4.2. This figure presents the response of a monolith impounding a reservoir having an L/H ratio of 5.0 when the ground motion is only exciting the monolith. The earthquake ground motion will not significantly excite the higher frequencies of the dam-reservoir-foundation system. The two resulting stress profiles shown in figure 5.10 are virtually identical. The same results are obtained using the other three ground motion records considered in this study. The maximum value of the dynamic tensile stress experienced by the dam monolith when subjected to the four earthquake ground motion records used in this study are listed in table 5.2. The maximum tensile stress that results from the infinite reservoir length assumption is also presented. The monolith alone is assumed to be excited by the earthquake ground motion. The numbers in the parenthesises are the element numbers at which this maximum tensile stress is located as shown in figure 5.9.

As the reservoir length becomes increasingly shorter, the maximum value of the dynamic tensile stress begins to differ from that when the reservoir length is assumed infinite when high a/v ratio ground motion records are used. The maximum dynamic tensile stress caused by the Saguenay earthquake event is 24.6% greater

when the reservoir has an L/H ratio of 2.5 than when the L/H ratio is infinite. The maximum dynamic tensile stress is 11.51 MPa when the reservoir is assumed infinite in length and is 14.34 MPa when the L/H ratio is 2.5.

Figure 5.11 presents the tensile stress profiles for the cases when the L/H ratio of the upstream reservoir is both infinite and 1.0. The Saguenay earthquake event is used and is assumed only to excite the dam monolith. The dynamic tensile stresses are increased as the reservoir length decreases, as evident in this figure. The maximum tensile stress experienced by the monolith is increased by 67.1% to a value of 19.23 MPa. This increase in tensile stress is a result of the supplementary response peak that is prominent in this configuration's dynamic response (figure 4.3). The Saguenay ground motion record has significant accelerations at the same frequency as this supplementary response peak. The combination of the large response peak and the high accelerations results in the increase in the dynamic tensile stress.

Dam monoliths are susceptible to high frequency content earthquakes when the upstream reservoir is assumed to be finite in length. These types of earthquake ground motion have high energy contents in the frequency range of 4 to 15 Hz. This is also the frequency range at which the supplementary response peaks occur in the monolith's response. Dam monoliths which impound a reservoir of short length ($L/H \leq 2.5$) are affected the most.

It should be noted here that some of the dynamic tensile stress values are greatly in excess of the modulus of rupture of the concrete. These higher stress values occur primarily due to the scaling of the earthquake ground motion records. The stresses increase proportionally with the scaling as the analysis is assumed linear elastic. The objective of this section of the study is to obtain the location of the highest tensile stress. This section therefore is the most likely to fail. It is also of interest to compare the tensile stress distributions when the reservoir characteristics are varied rather than obtain a qualitative estimate of the stresses experienced by the monolith.

5.4 PHASE OF GROUND MOTION

The maximum dynamic tensile stresses that the monolith experiences when the far end boundary of the reservoir is assumed to be excited by ground motion that is in phase with that at the monolith are listed in table 5.3. The same information, but for the case where the ground motion at the far end boundary is out of phase with that at the monolith is listed in table 5.4. As evident from these two tables, the phase of the ground motion that affects the far boundary significantly influences the magnitude of the maximum dynamic tensile stress that occurs. The location of the maximum stress is occasionally altered as well.

The dynamic tensile stress profile for the case of a monolith impounding a reservoir having an L/H ratio of 5.0 when subjected to the Imperial Valley

earthquake record is plotted in figure 5.12. The far boundary of the reservoir is assumed to be both unexcited and excited in-phase with the monolith. The maximum dynamic tensile stress increases by 9.3%; increasing to a value of 5.42 MPa for the in-phase case from a value of 4.96 MPa for the unexcited case. The Fourier representation of the monolith's dynamic response when the far boundary is excited in-phase with that at the monolith (figure 4.5) has a large supplementary response peak at a frequency of 4.30 Hz. This is at the extreme of the frequency range at which this particular earthquake event has significant accelerations. This large response peak increases the monolith's response. The dynamic tensile stresses that are induced into the monolith are therefore subsequently increased.

The case of a monolith impounding a reservoir having an L/H ratio of 5.0 when the motion at the far boundary of the reservoir is considered to be out-of-phase with that at the monolith is compared to the case where only the monolith is excited. The Imperial Valley ground motion record is used. The maximum dynamic tensile stress does not change significantly in magnitude as compared to the monolith only excited case. The location of the maximum stress does however change. As evident from table 5.4, the location drops to the base of the monolith (element 121, figure 5.9). This is a result of the large supplementary response peak that exists at a frequency of 5.03 Hz (figure 4.6) participating strongly in the dynamic response of the monolith. This response peak is due to the actions of the second mode of vibration of the monolith. Although the ground motion does not have high

accelerations at this particular frequency, its combination with the large supplementary response peak results in the monolith having significant accelerations at this frequency. The lowering of the location of maximum stress is therefore a result of the contribution of the response at the monolith's fundamental frequency (2.64 Hz, hydrodynamic effects included) and this supplementary frequency (5.03 Hz).

The response of a monolith impounding a short reservoir (L/H = 1.0) excited by the Imperial Valley ground motion record is plotted in figure 5.13. In this example, the far boundary of the reservoir is assumed to be both unexcited and excited out-of-phase with the dam monolith. The increase in the dynamic tensile stresses, relative to the unexcited case, can be seen in this figure. The maximum tensile stress that occurs is increased by 47.4%, as evident from comparing tables 5.2 and 5.4. The magnitude of the fundamental response peak is increased significantly for the out-of-phase case as can be seen in comparing figures 4.3 and 4.8. This increased magnitude of the fundamental response peak has the effect of increasing the dynamic tensile stress levels in the monolith.

The increase in dynamic tensile stresses is even more significant when the ground motion that excites the monolith and the far boundary has a high a/v ratio. This type of ground motion has significant accelerations in the frequency range of the supplementary response peaks that occur in the monolith's dynamic response. The maximum dynamic tensile stress is increased by approximately 15% for all the long reservoir cases considered. This can be seen in comparing both tables 5.3 and 5.4

to table 5.2. The high a/v ratio ground motion events used in this study have significant accelerations in the frequency range of 5 to 10 Hz. This is evident in figures 5.7 and 5.8 for the San Francisco and Saguenay ground motion records, respectively. The monolith response also has large supplementary response peaks in this frequency range (figures 4.5 and 4.6 for the in-phase and out-of-phase cases, respectively). These large dynamic responses and ground accelerations will result in the monolith having a larger response at these frequencies as compared to both the infinite length case and the same finite length case but where only the dam monolith is excited by the ground motion.

Figure 5.14 presents the dynamic tensile stress profile for the case when the monolith impounds a reservoir having an L/H ratio of 1.0 when the San Francisco earthquake ground motion record is used. The far end boundary is assumed to be both unexcited and excited out-of-phase with the monolith. The maximum dynamic tensile stress is increased by 53.2%. This can also be observed in comparing tables 5.2 and 5.4. The Fourier representation of the dynamic response of the monolith has a significant response peak at a frequency of 4.10 Hz as shown in figure 4.8. This ground motion record also has significant accelerations at this particular frequency. This, together with the increase in the fundamental response peak's magnitude, results in a large increase in the dynamic tensile stresses that the monolith experiences.

The dam monolith, when finite reservoir effects are considered, is susceptible to both intermediate and high a/v ratio events. The phase of the ground motion at the far boundary of the reservoir increases the sensitivity of the overall system to the earthquake ground motion. The dam-reservoir-foundation system is however more sensitive to high a/v ratio ground motion than to intermediate a/v ratio ground motion. The phase of the ground motion that excites the far end boundary of the reservoir must also be considered in conjunction with the L/H ratio of the upstream reservoir. The dynamic tensile stresses are typically increased in magnitude when the motion of this boundary is considered. However, some specific combinations of L/H ratio, phase of the ground motion, and the ground motion characteristics may result in a decrease in the dynamic tensile stresses. The upstream reservoir's characteristics must be carefully considered in order that an accurate estimate of the monolith's response to the earthquake ground motion can be obtained.

5.5 GEOMETRY OF UPSTREAM RESERVOIR

The maximum dynamic tensile stress that the monolith experiences when the reservoir geometry is idealized as triangular are listed in table 5.5. The ground motion is assumed only to excite the dam monolith in this table. The primary effect of varying the upstream reservoir's geometry is to increase the value of the maximum dynamic tensile stress that the monolith experiences. This can be seen in comparing tables 5.2 and 5.5 for the rectangular and triangular reservoir geometry cases,

respectively. The supplementary response peaks that occur in the Fourier representation of the monolith's response are typically larger in magnitude when the reservoir geometry is triangular than when it is rectangular. For example, consider the case of a reservoir that has an L/H ratio of 5.0 when the Kern County ground motion record is used. The ground motion only excites the monolith. The maximum dynamic tensile stress increases from a value of 6.05 MPa for the rectangular reservoir case to a value of 6.97 MPa for the triangular case. This represents an increase of 15.2%. Figure 5.15 presents the Fourier representation of the monolith's dynamic response for the cases of both a triangular and a rectangular reservoir geometry both having an L/H ratio of 5.0. The wave reflection coefficient is taken as 0.975. Figure 5.16 presents the Fourier representation of the dynamic response of the same monolith when impounding both a triangular and a rectangular reservoir both having an L/H ratio of 1.0. The larger supplementary response peaks for the triangular reservoir geometry can be seen in these two figures.

The maximum dynamic tensile stress that the monolith experiences when the reservoir is idealized as triangular and the ground motion that excites the bottom of the reservoir is in-phase with that at the monolith are listed in table 5.6. The maximum dynamic tensile stress for the triangular geometry is generally reduced as compared with the tensile stress that occurs when the upstream reservoir geometry is idealized as rectangular. This occurs for all earthquake ground motion records considered in this study. High a/v ratio events tend to cause larger decreases in

tensile stress than the intermediate a/v ratio events. This can be seen in comparing tables 5.3 and 5.6.

The response peaks in the frequency range of 0 to 10 Hz are reduced in magnitude when the ground motion is considered to be in-phase. This can be seen in both figures 4.12 and 5.17. Figure 4.12 presents the Fourier representation of a monolith's response when impounding both a triangular and a rectangular reservoir. These reservoirs both have an L/H ratio of 5.0 and are excited by in-phase ground motion. Figure 5.17 is the Fourier representation of the monolith's dynamic response when both the triangular and rectangular reservoirs have an L/H ratio of 1.0. The reduced magnitude of these response peaks interact with the earthquake acceleration record to produce a reduced monolith response.

The maximum tensile stress for the monolith impounding a triangular upstream reservoir geometry are listed in table 5.7. The ground motion that excites the far end boundary is assumed to be out-of-phase with that at the monolith. The maximum dynamic tensile stress that is generated when the reservoir geometry is triangular increases in magnitude as compared with that when the reservoir geometry is rectangular. This occurs for all earthquake ground motion records considered in this study. High a/v ratio events tend to produce larger increases in tensile stresses than the intermediate a/v ratio ground motion records. This can be seen in comparing tables 5.4 and 5.7. For example, the maximum dynamic tensile stress caused by the San Francisco ground motion record for the case of a reservoir having

an L/H ratio of 5.0 is increased by 28.5%. The tensile stress is increased from a value of 11.58 MPa for the rectangular reservoir case to a value of 14.88 MPa for the triangular reservoir case.

The geometry of the upstream reservoir is an important factor and should be considered in the analysis of the dam-reservoir-foundation system at the same time as the L/H ratio, the phase of the ground motion, and the specific ground motion characteristics. The reservoir geometry significantly affects the magnitude of the maximum dynamic tensile stress that the monolith experiences. The dynamic tensile stresses are typically increased for the triangular reservoir geometry over those for the rectangular geometry. The dam monolith is therefore more sensitive to earthquake ground motion, especially when the event is characterized as having a high a/v ratio, and the geometry of the upstream reservoir is assumed triangular. The main exception to this is when the earthquake ground motion is assumed to be in-phase with that at the monolith, where the tensile stresses are reduced.

Table 5.1 - Recorded ground motion characteristics

Earthquake Event	Magnitude	Epicentral Distance (km)	Maximum Accel. (g)	Maximum Vel. (m/s)	a/v (gs/m)
Imperial Valley (1940)	6.6	8	0.348	0.334	1.04
Kern County (1952)	7.6	56	0.156	0.157	0.99
San Francisco (1957)	5.25	11	0.105	0.046	2.28
Saguenay (1988)	5.7	114	0.121	0.027	4.46

Table 5.2 - Maximum dynamic tensile stress (MPa), monolith only excited case

	Earthquake record			
L/H	Imperial Valley	Kern County	San Francisco	Saguenay
∞	4.59(121)*	5.97(121)	9.19 (24)	11.51 (24)
5.0	4.96(121)	6.05 (24)	9.29 (24)	12.86 (24)
2.5	4.87(121)	6.81 (24)	9.08 (24)	14.34 (24)
1.0	5.11 (24)	5.81(121)	11.79(24)	19.23 (24)

* location - element number (ref. Figure 5.9)

Table 5.3 - Maximum dynamic tensile stress (MPa), far boundary in-phase with monolith

	Earthquake record			
L/H	Imperial Valley	Kern County	San Francisco	Saguenay
∞	4.54(121)*	5.97(121)	9.19 (24)	11.51 (24)
5.0	5.42 (24)	6.73 (24)	11.92(24)	15.90 (24)
2.5	5.24 (24)	6.93 (24)	15.50(24)	14.46 (24)
1.0	5.52 (24)	4.62 (24)	12.54(24)	24.47 (24)

* location - element number (ref. Figure 5.9)

Table 5.4 - Maximum dynamic tensile stress (MPa), far boundary out-of-phase with monolith

	Earthquake record			
L/H	Imperial Valley	Kern County	San Francisco	Saguenay
∞	4.54(121)*	5.97(121)	9.19 (24)	11.51 (24)
5.0	5.19(121)	7.17 (24)	11.58(24)	14.81 (24)
2.5	5.38 (24)	6.69 (24)	13.43(24)	19.93 (24)
1.0	7.53 (24)	7.46 (24)	18.06(24)	14.87 (24)

* location - element number (ref. Figure 5.9)

Table 5.5 - Maximum dynamic tensile stress (MPa), monolith excited alone and triangular reservoir geometry

	Earthquake record			
L/H	Imperial Valley	Kern County	San Francisco	Saguenay
5.0	5.28 (24)*	6.97 (24)	11.66(24)	12.97 (24)
1.0	5.60(121)	7.36 (24)	14.44(24)	16.56 (24)

* location - element number (ref. Figure 5.9)

Table 5.6 - Maximum dynamic tensile stress (MPa), far end excited in-phase and triangular reservoir geometry

	Earthquake record			
L/H	Imperial Valley	Kern County	San Francisco	Saguenay
5.0	4.49 (24)*	6.21 (24)	8.86(24)	16.56 (24)
1.0	3.95(121)	4.41(121)	7.62(24)	11.70 (24)

* location - element number (ref. Figure 5.9)

Table 5.7 - Maximum dynamic tensile stress (MPa),
far end excited out-of-phase and triangular reservoir geometry

	Earthquake record			
L/H	Imperial Valley	Kern County	San Francisco	Saguenay
5.0	6.21 (24)*	7.92 (24)	14.88(24)	12.70 (24)
1.0	7.81 (24)	11.13(24)	24.27(24)	31.14 (24)

* location - element number (ref. Figure 5.9)

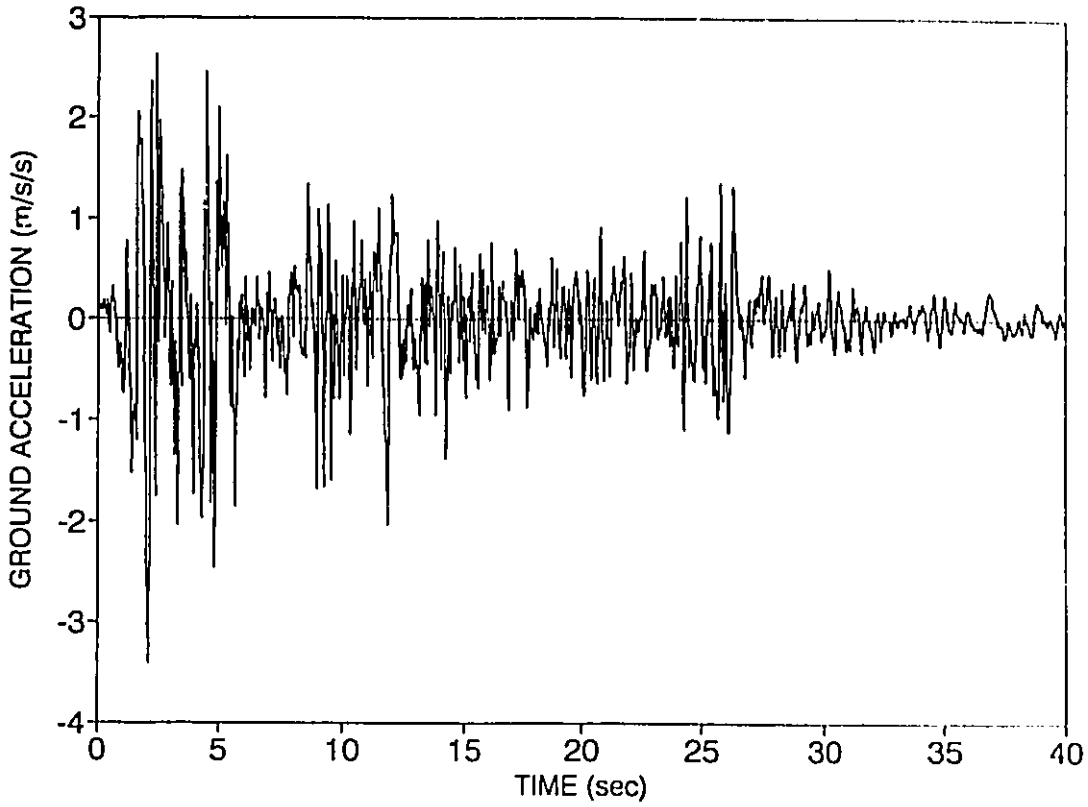

Figure 5.1 - Acceleration time history of the Imperial Valley earthquake event

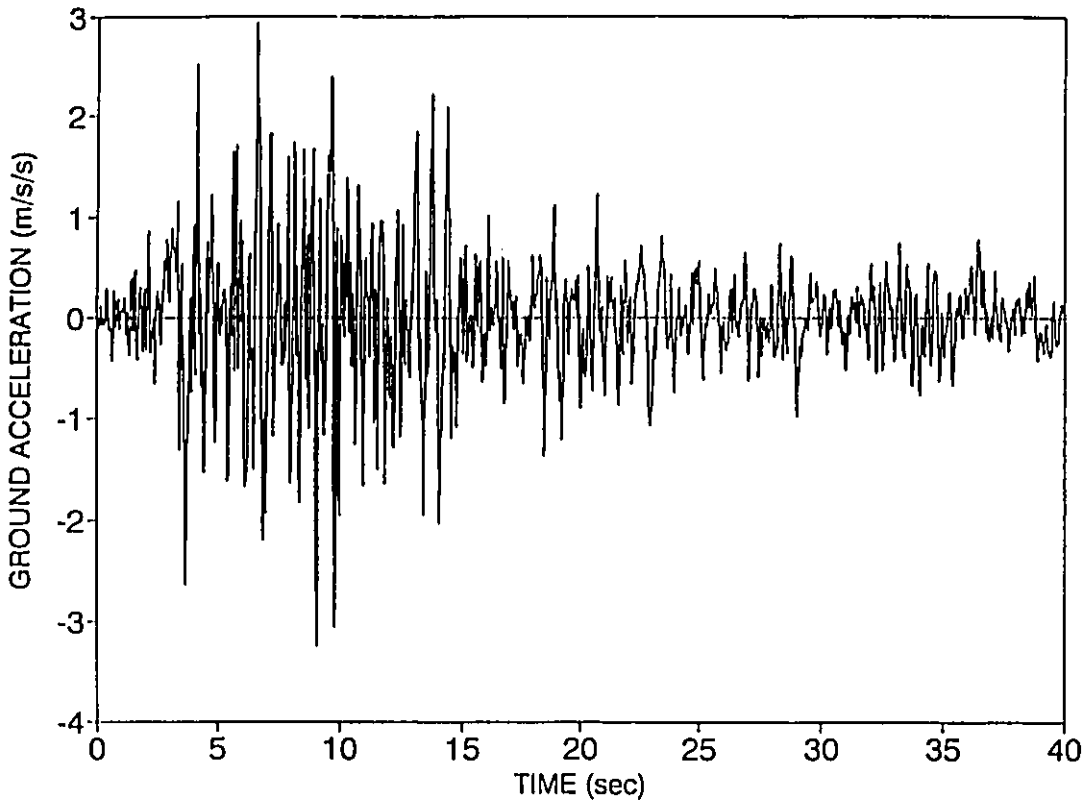

Figure 5.2 - Acceleration time history of the Kern County earthquake event

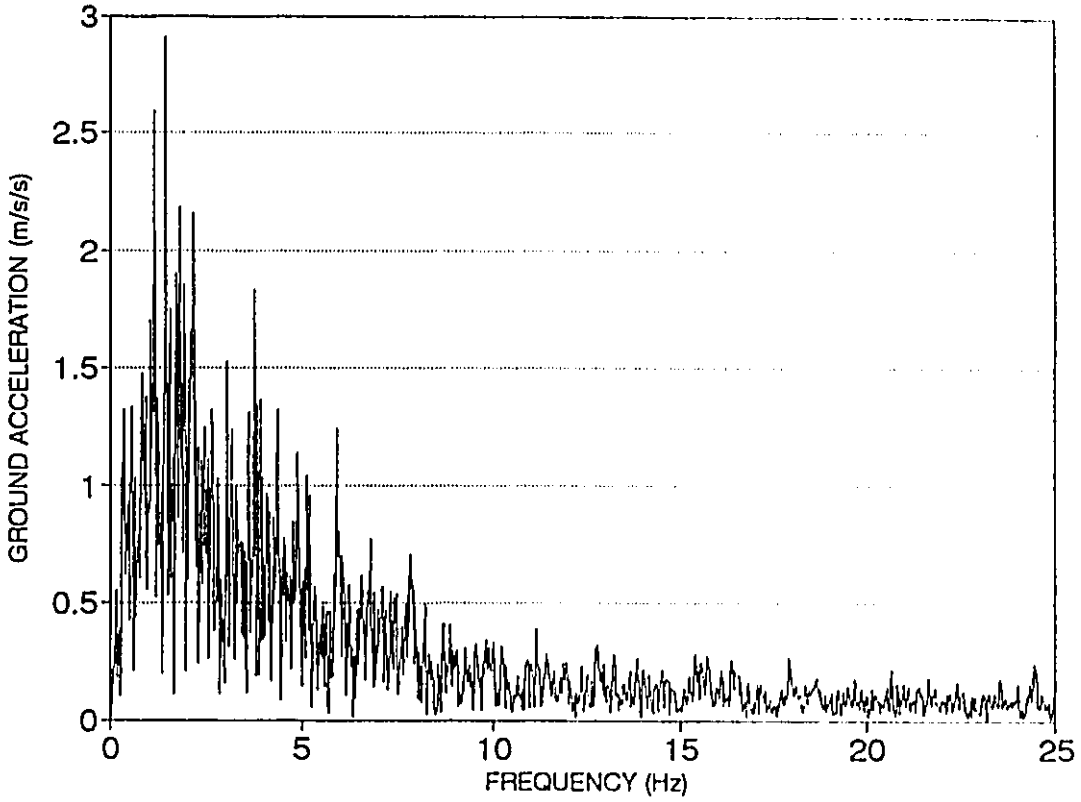

Figure 5.3 - Fourier representation of the Imperial Valley (May 18, 1940) earthquake event

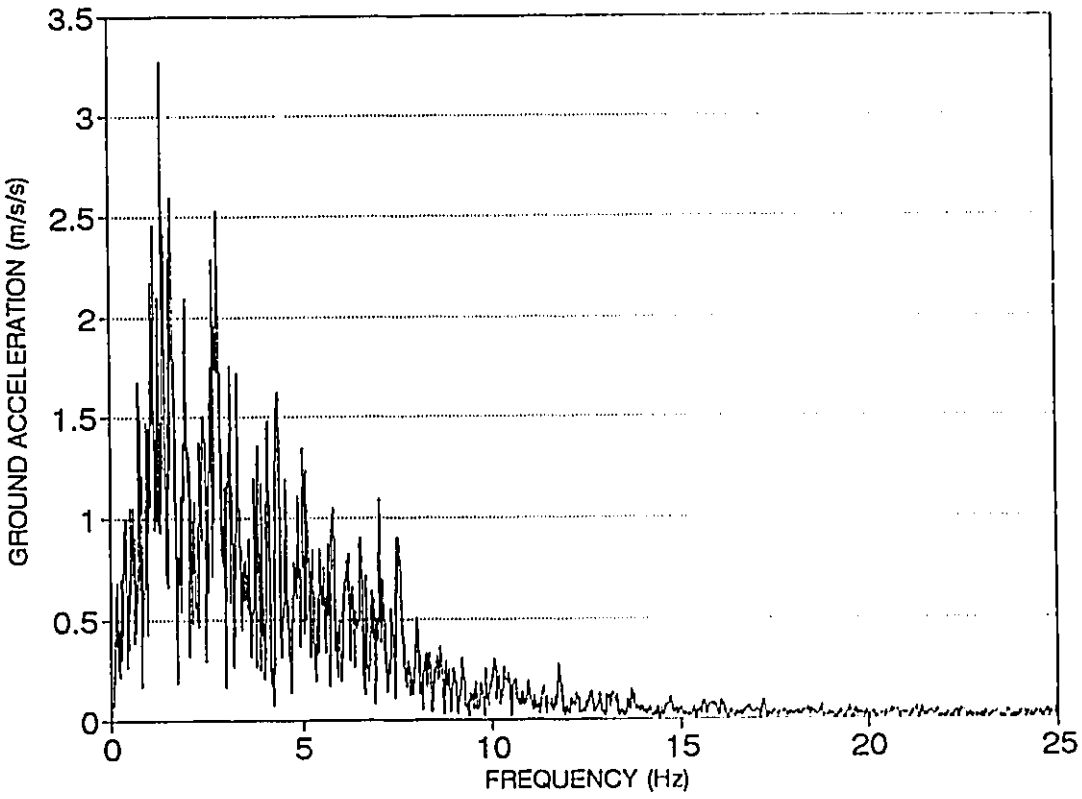

Figure 5.4 - Fourier representation of the Kern County (July 21, 1952) earthquake event

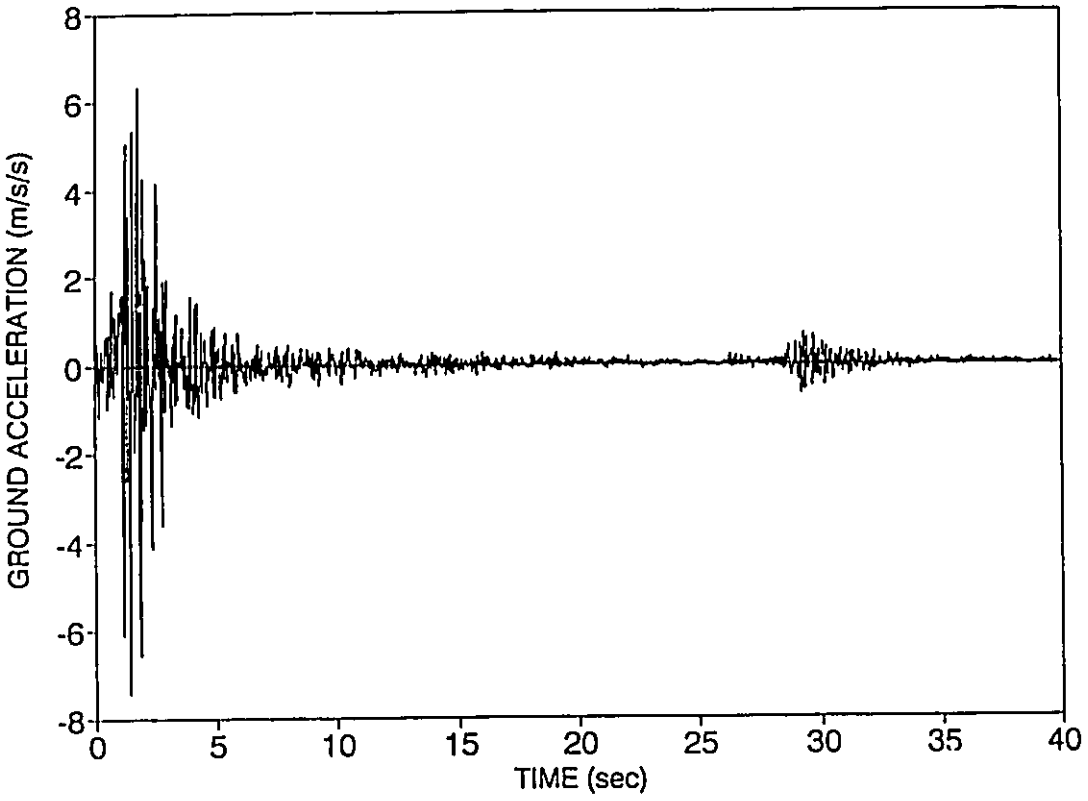

Figure 5.5 - Acceleration time history of the San Francisco earthquake event

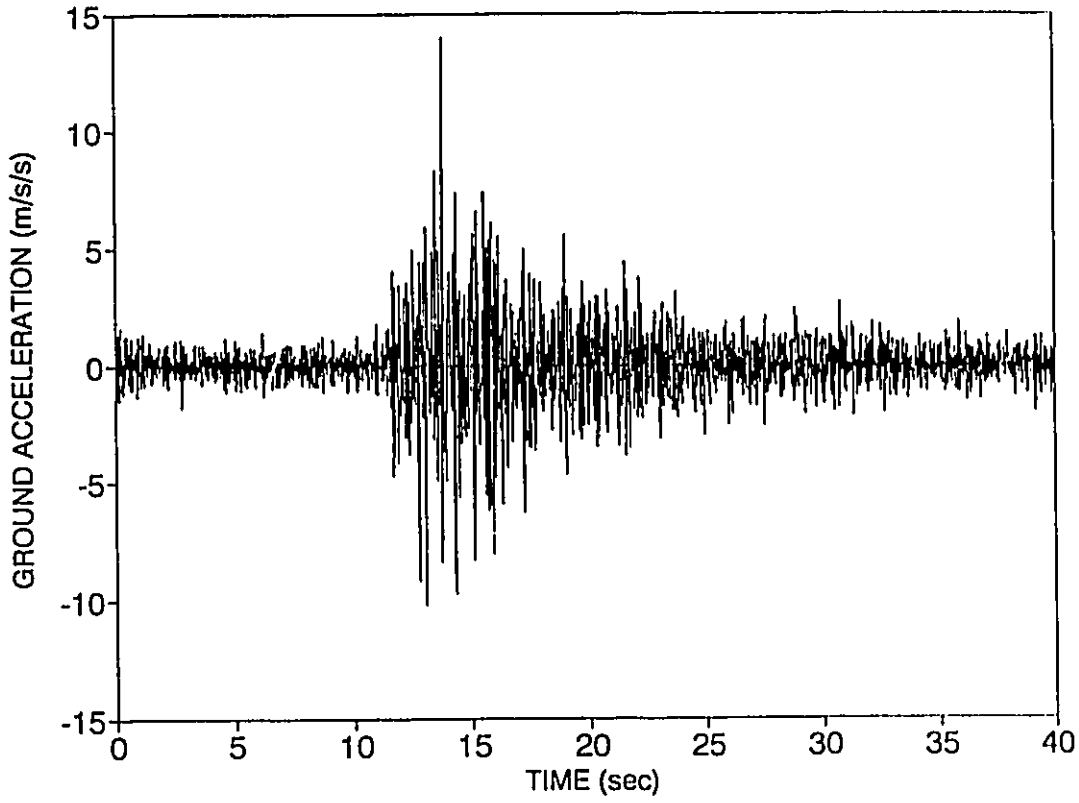

Figure 5.6 - Acceleration time history of the Saguenay earthquake event

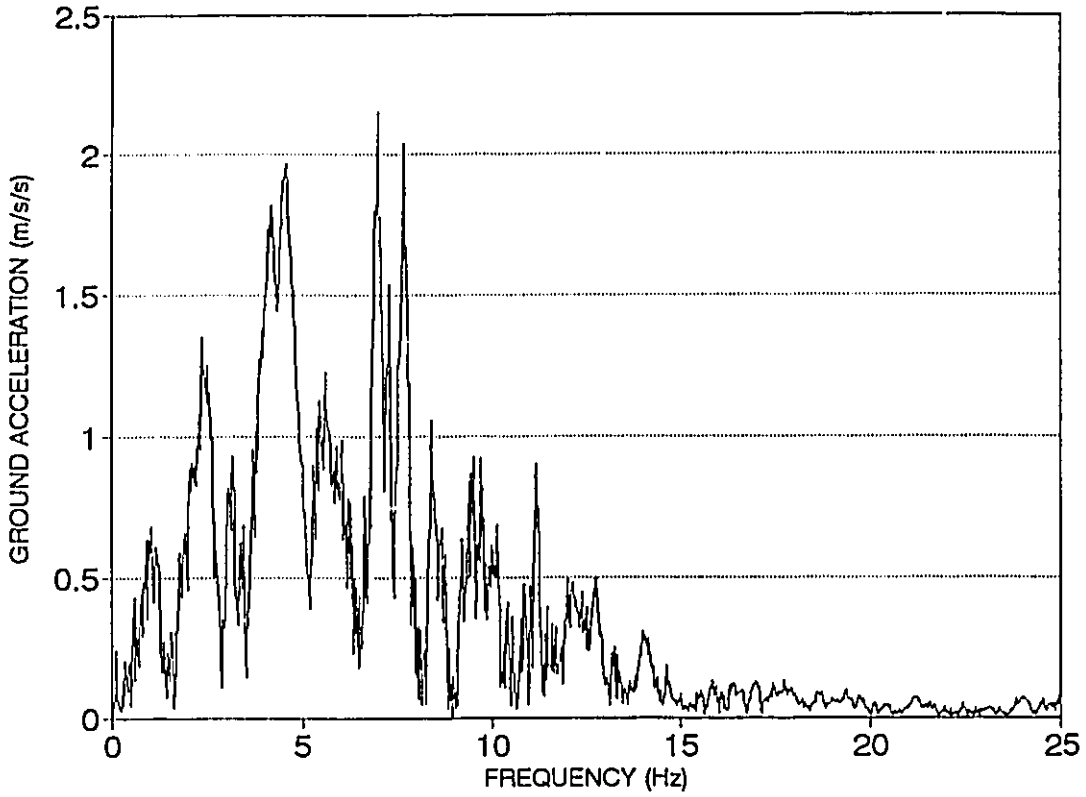

Figure 5.7 - Fourier representation of the San Francisco (March 22, 1957) earthquake event

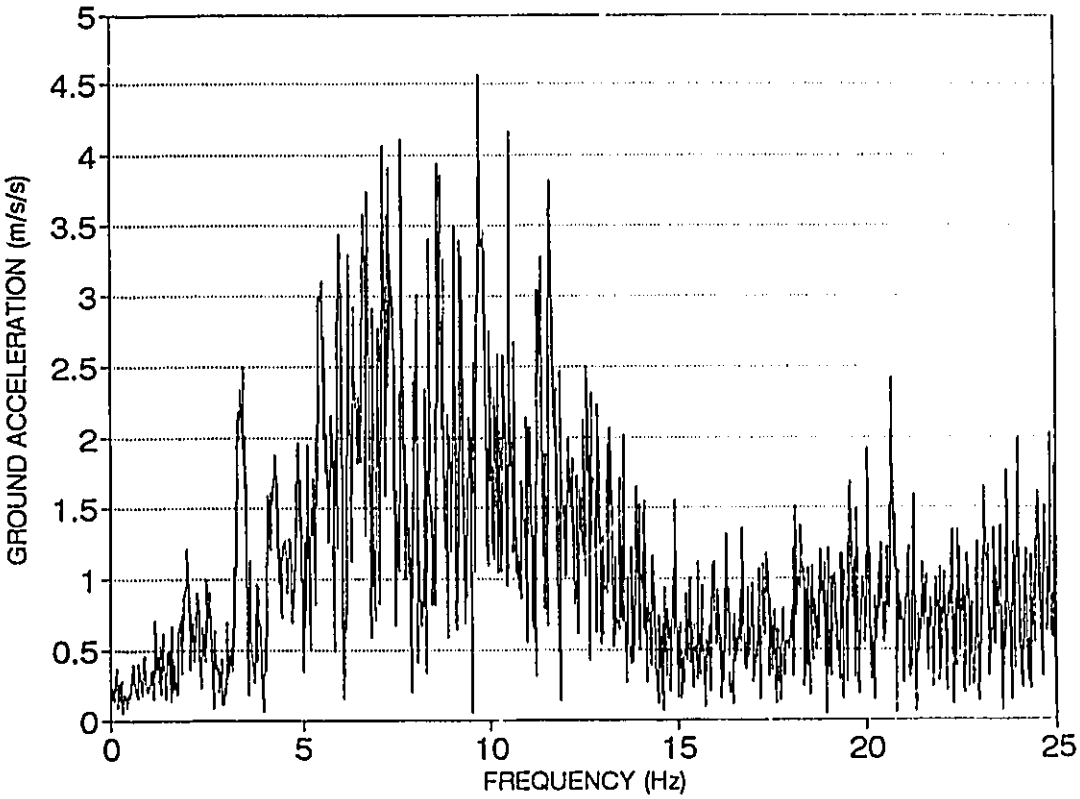

Figure 5.8 - Fourier representation of the Saguenay (November 25, 1988) earthquake event

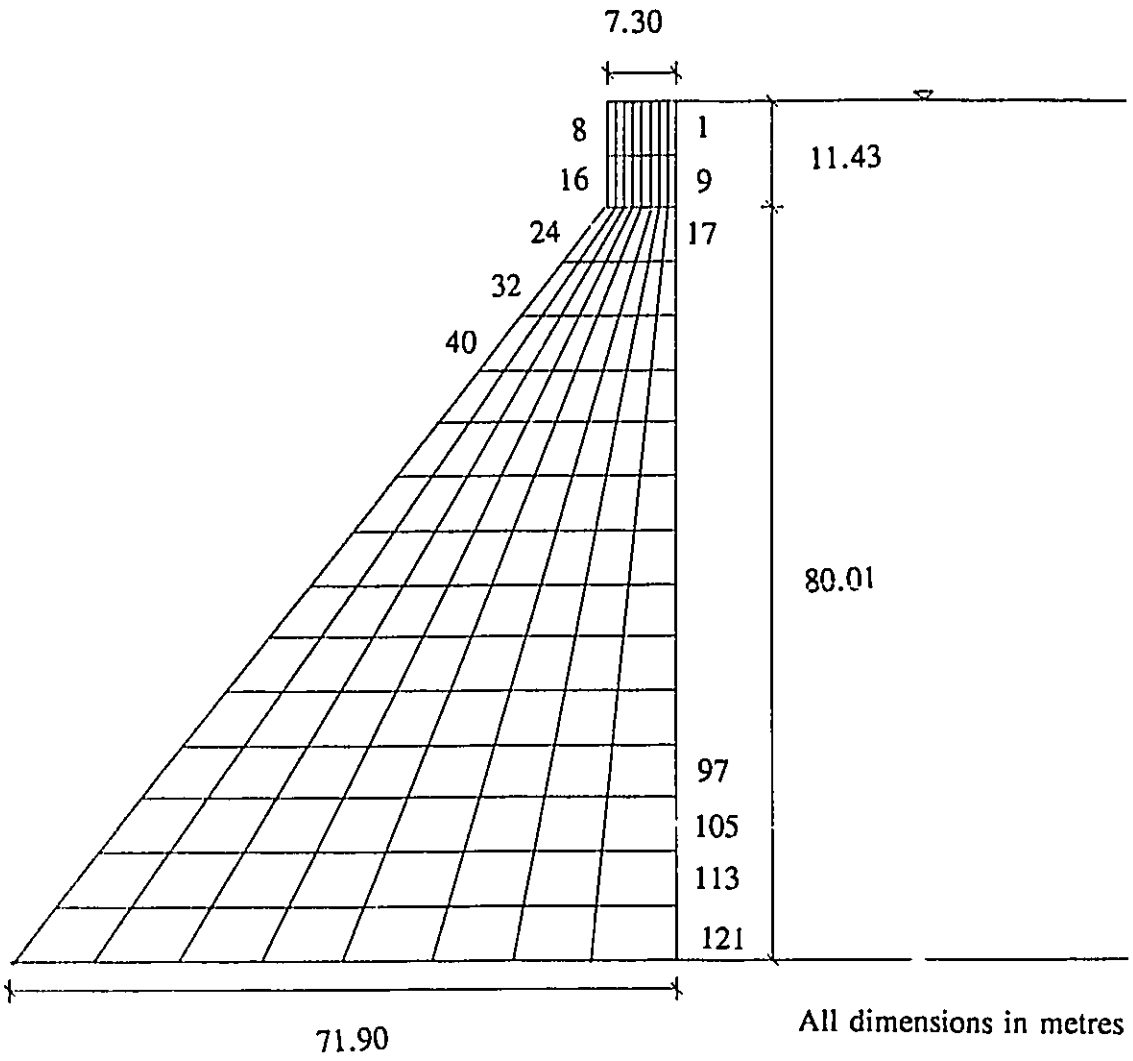

Figure 5.9 - Finite element discretization of the dam monolith

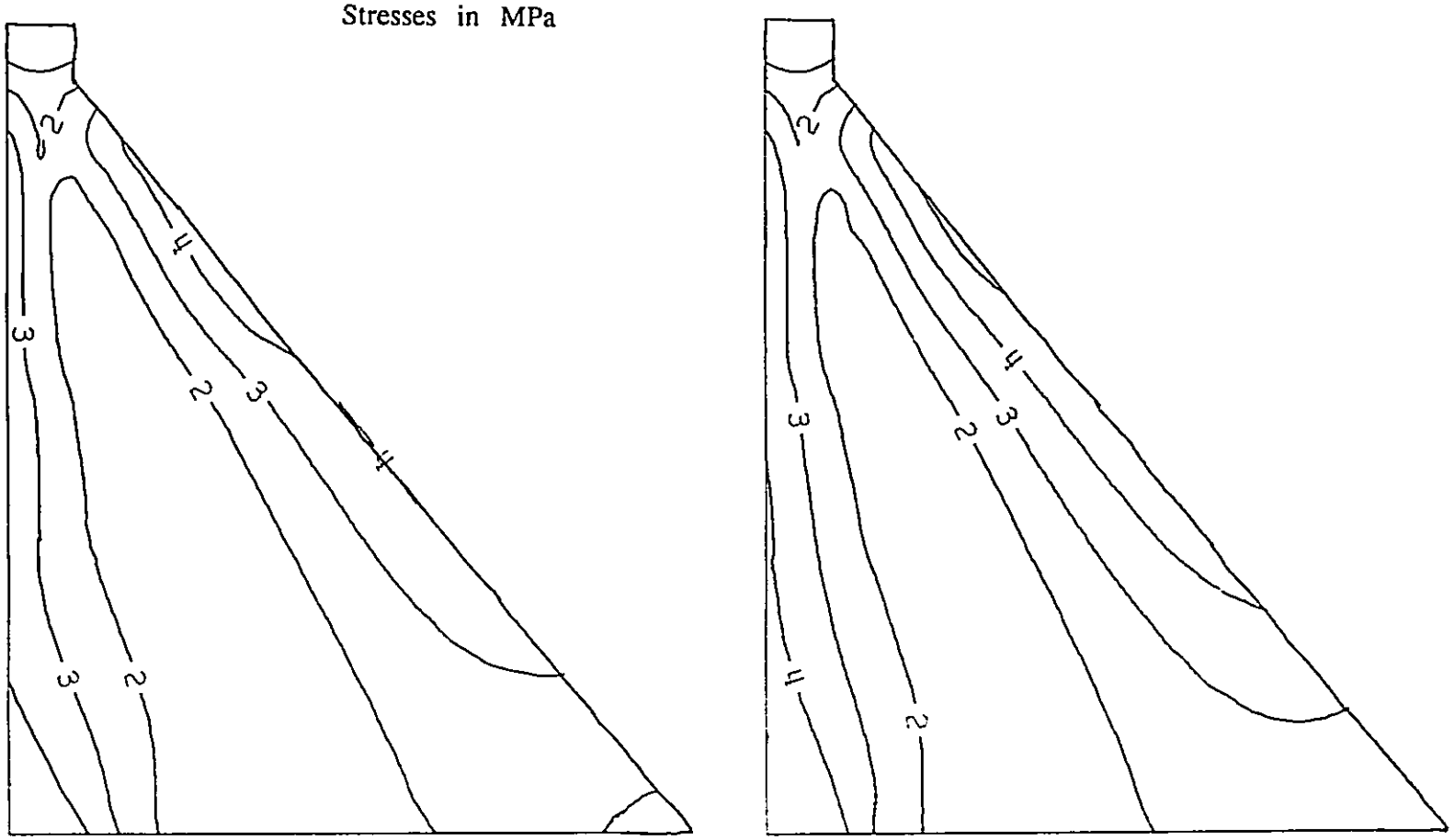

L/H = ∞ L/H = 5.0

Figure 5.10 - Dynamic tensile stress profile for L/H = ∞ and L/H = 5.0 when only dam monolith excited by the Imperial Valley acceleration record

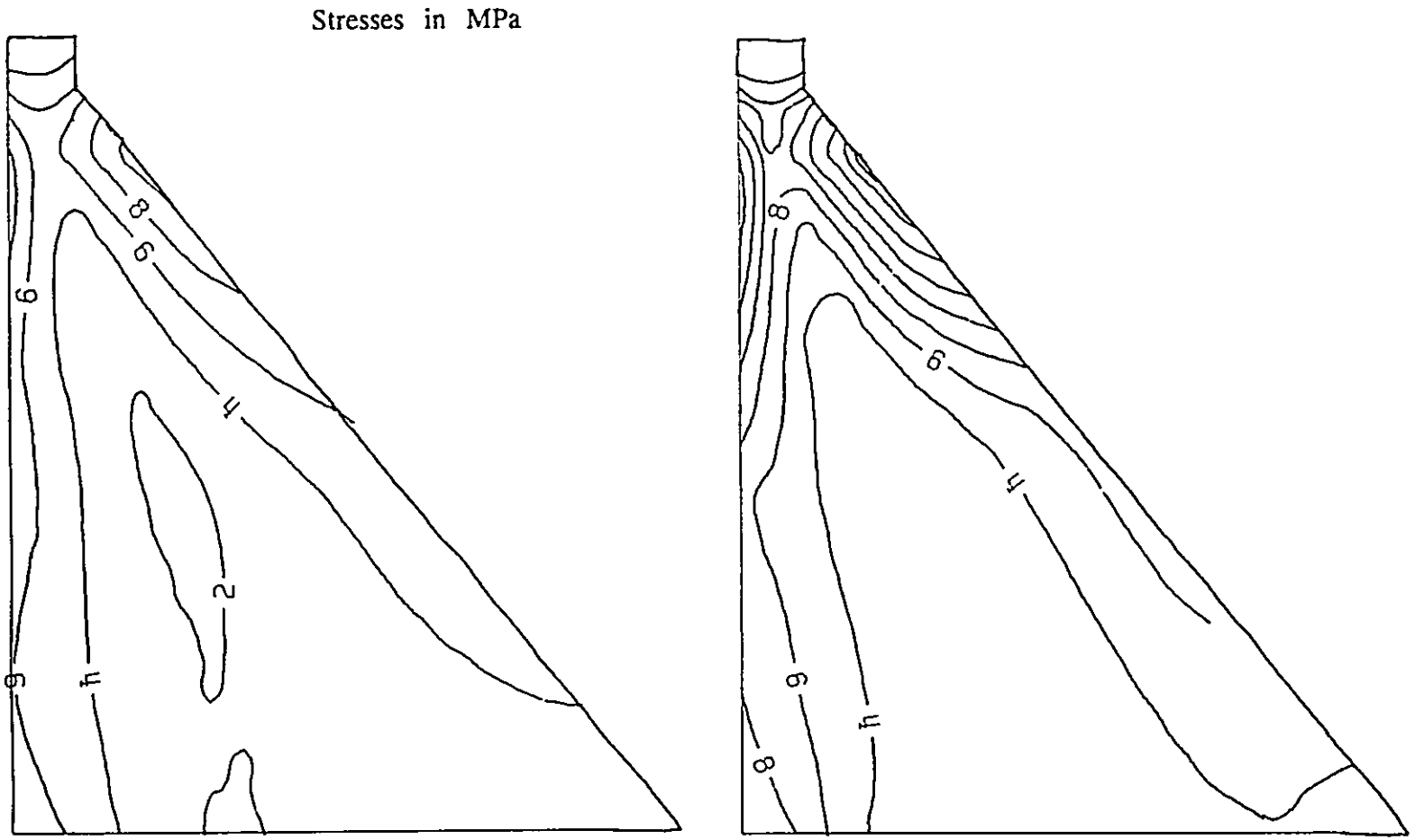

L/H = ∞ L/H = 1.0

Figure 5.11 - Dynamic tensile stress profile for L/H = ∞ and L/H = 1.0 when only dam monolith excited by the Saguenay acceleration record

Stresses in MPa

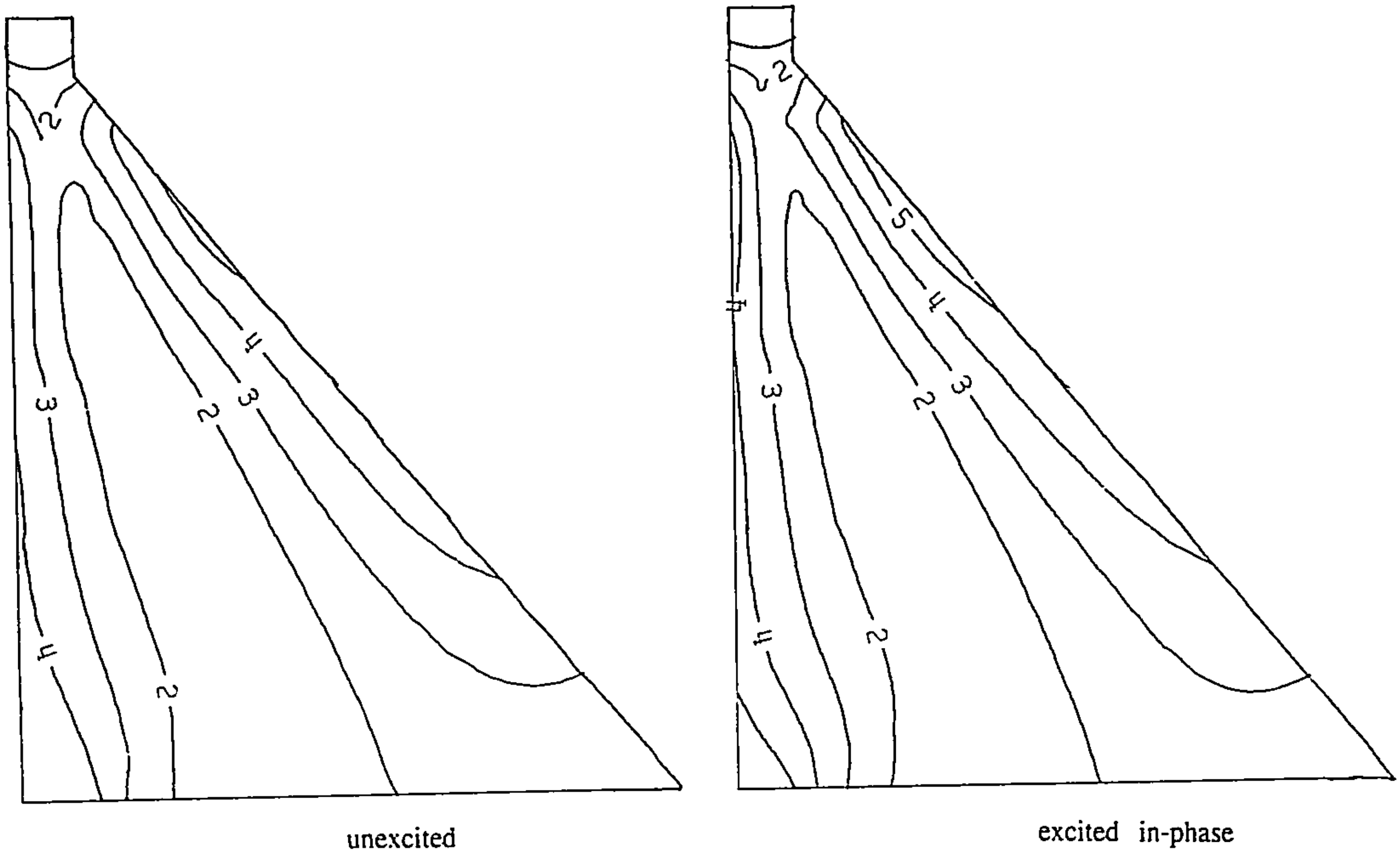

Figure 5.12 - Dynamic tensile stress profile for L/H = 5.0 when far boundary is both unexcited and excited in-phase with the monolith by the Imperial Valley acceleration record

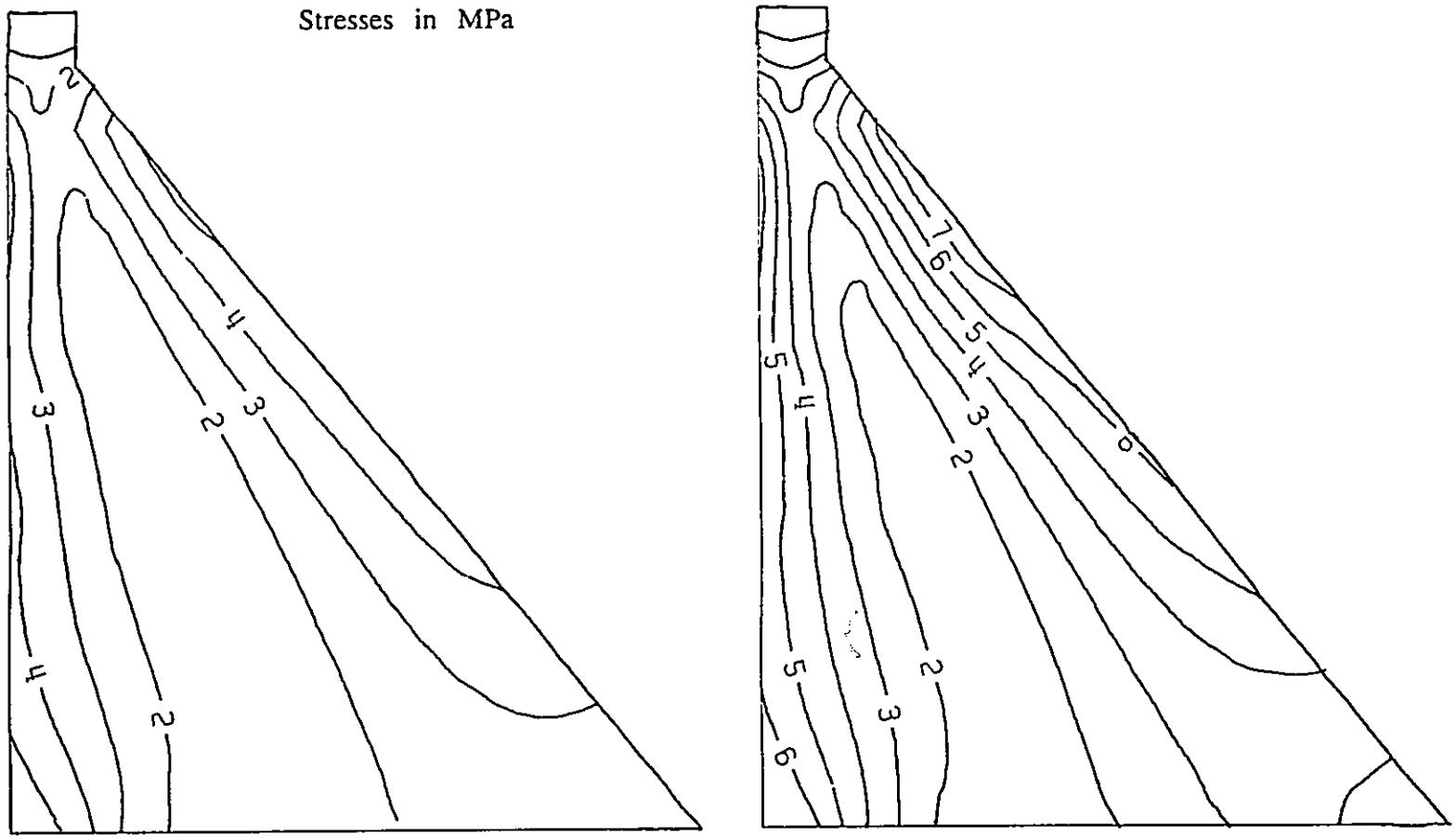

Figure 5.13 - Dynamic tensile stress profile for L/H = 1.0 when far boundary is both unexcited and excited out-of-phase with the monolith by the Imperial Valley acceleration record

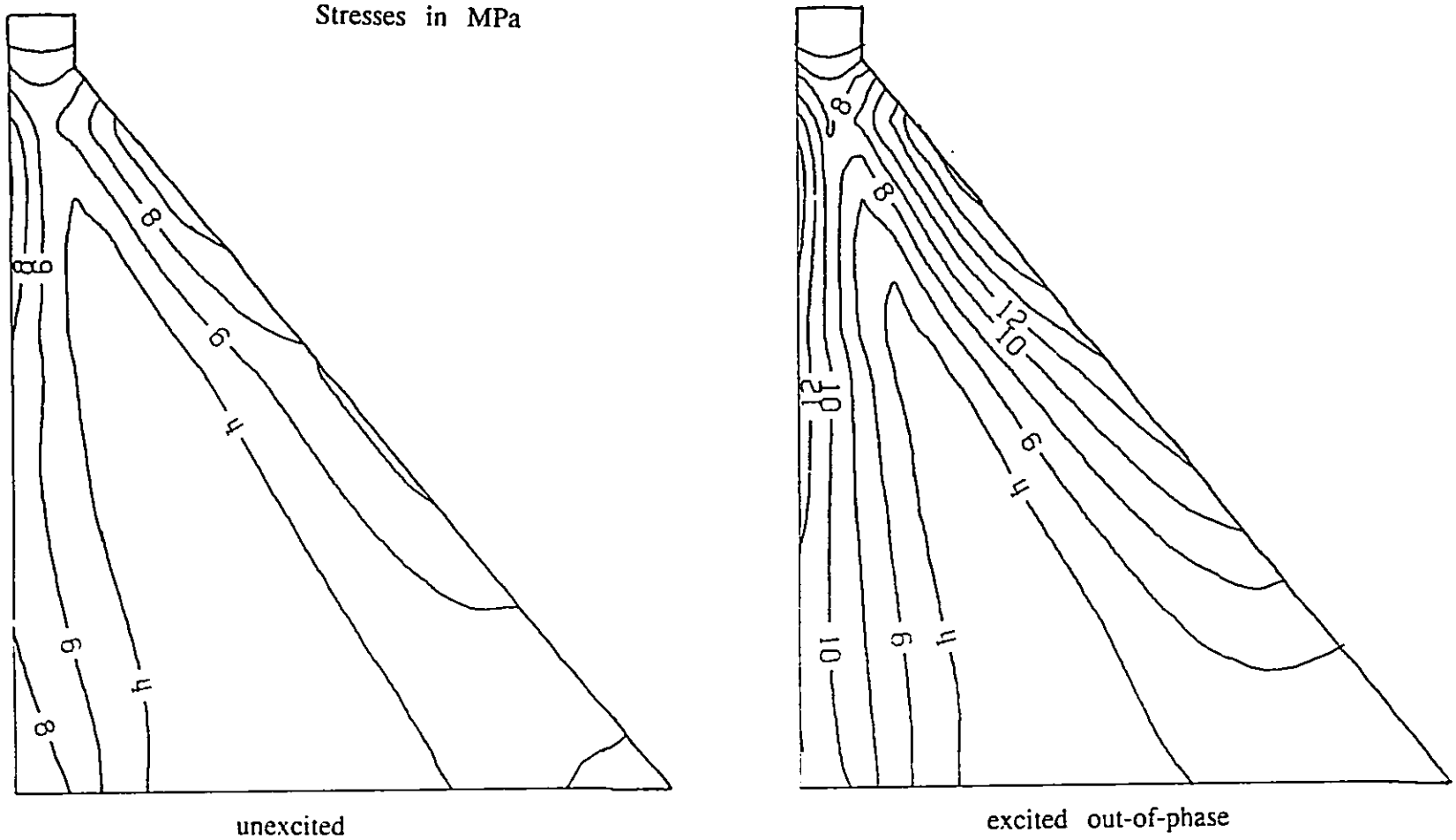

Figure 5.14 - Dynamic tensile stress profile for L/H = 1.0 when far boundary is both unexcited and excited out-of-phase by the San Francisco acceleration record

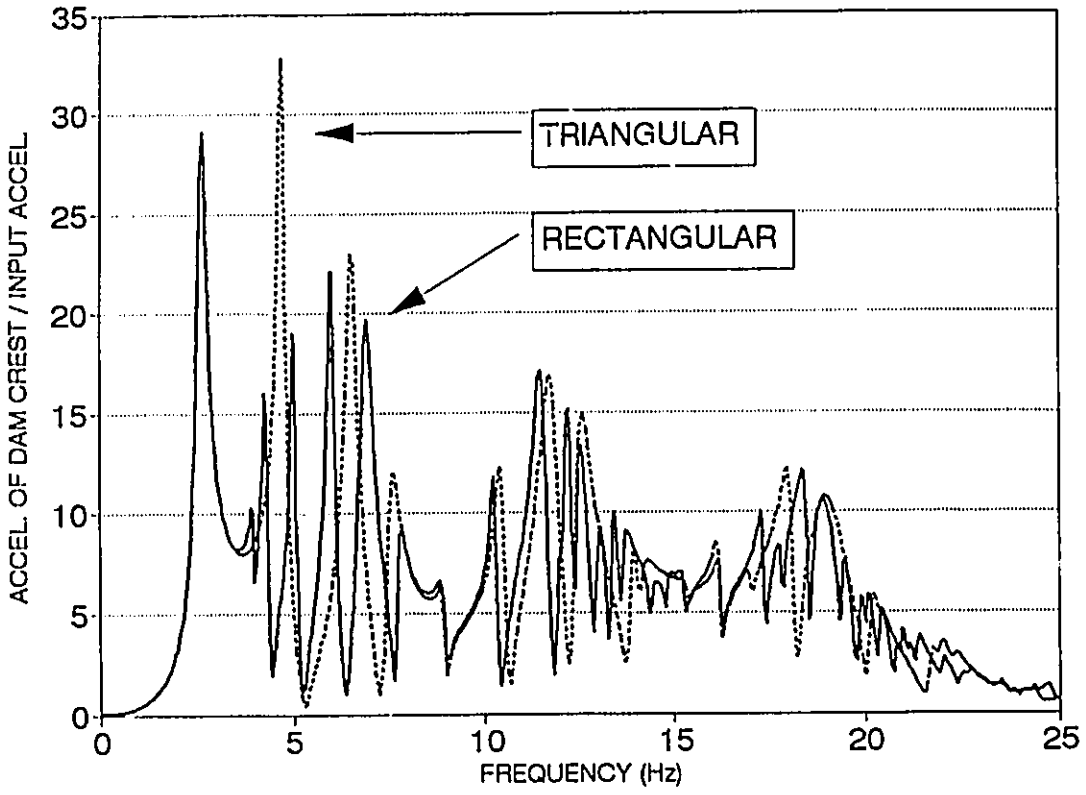

Figure 5.15 - Fourier representation of monolith's response (L/H = 5.0) for both a rectangular and triangular reservoir geometry when ground motion only excites monolith

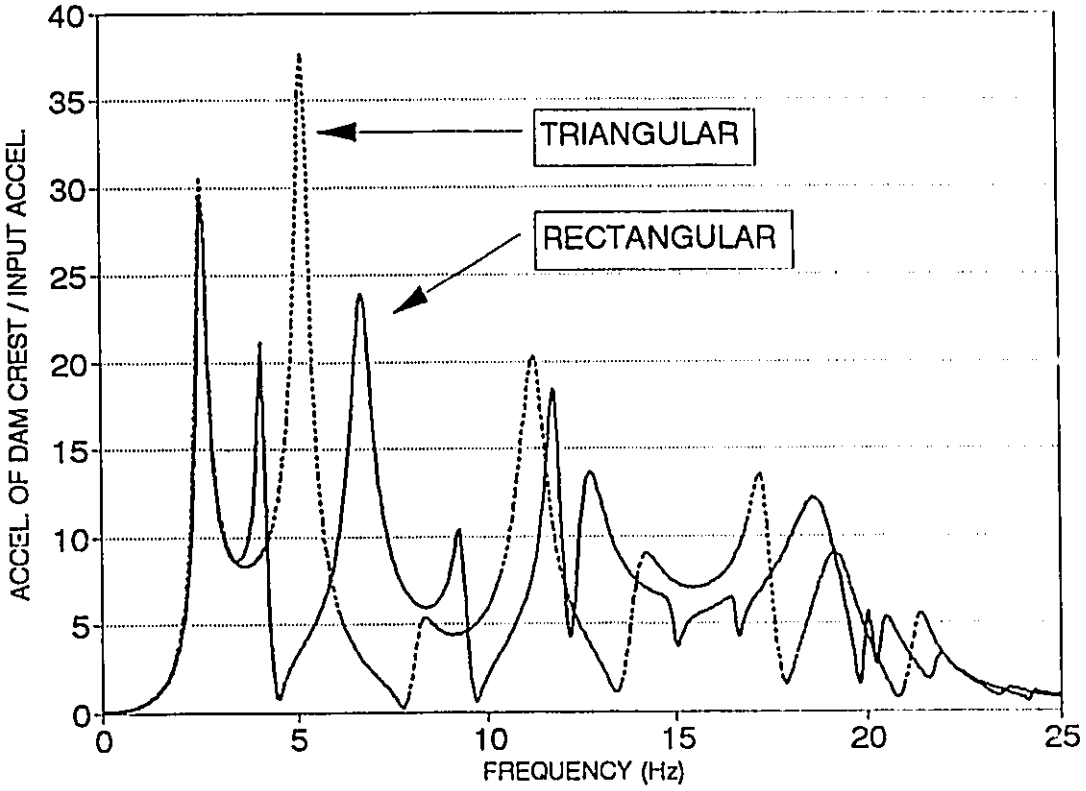

Figure 5.16 - Fourier representation of monolith's response (L/H = 1.0) for both a rectangular and triangular reservoir geometry when ground motion only excites monolith

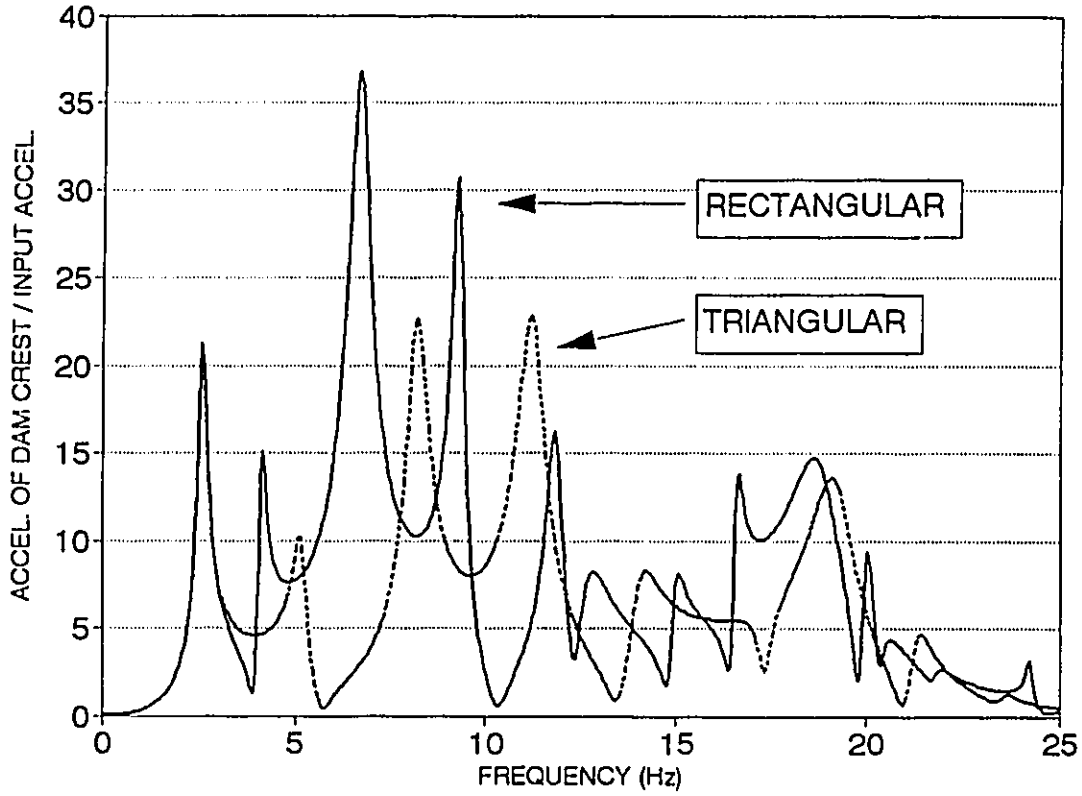

Figure 5.17 - Fourier representation of monolith's response (L/H = 1.0) for both a rectangular and triangular reservoir geometry when ground motion excites monolith and far boundary in-phase

CHAPTER 6

CONCLUSIONS

6.1 CONCLUSIONS

In this thesis, the effects of a finite length upstream reservoir on the response of a concrete gravity dam monolith to earthquake ground motion were investigated. Three components comprised the analytical study that was conducted. First, a closed form solution of the reservoir substructure of the dam-reservoir-foundation system was developed. A study was conducted that determined the effect of the ratio of the reservoir length to the dam height (L/H), the effect of the wave reflection coefficient, and the effect of the monolith's elastic modulus. Second, a detailed analytical procedure was developed for the dynamic analysis of the dam-finite reservoir-foundation system. A two-dimensional boundary condition for the reservoir-foundation interface was also developed. The numerical study that was conducted determined the effect of the L/H ratio, the model for the reservoir-foundation interface, and the cross sectional geometry of the upstream reservoir on the response of the monolith when the ground motion is assumed to excite both the far end boundary of the finite length reservoir and the dam monolith. Lastly, a stress analysis was conducted which determined the effect of the overall system when a

finite length reservoir was assumed. This study has shown the importance of the specific characteristics of a finite length reservoir on the response of a concrete gravity dam monolith. The major conclusions of this research investigation are summarized below:

1. Supplementary response peaks are created in the Fourier representation of the monolith's response when the effect of a finite length upstream reservoir is considered. These supplementary response peaks are generated through the coupled horizontal and vertical resonance of the upstream reservoir. Large monolith response and higher levels of stress are created at the frequencies of excitation at which this coupled resonance occurs.

2. For small values of the L/H ratio ($L/H \leq 5$), the supplementary response peaks can have significant magnitude particularly near the frequencies of the monolith's modes of vibration. These supplementary response peaks occur at frequencies which correspond to the predominant frequency content of both intermediate and high a/v ratio earthquake ground motion records. The number and magnitude of the supplementary response peaks are dependent upon the L/H ratio of the upstream reservoir.

3. Finite length reservoir effects must be considered in the dynamic and stress analyses of dam structures subjected to earthquake ground motion characterized as having an intermediate a/v ratio when the upstream reservoir has a L/H ratio of 2.5 or less. These effects are important for reservoirs that have a L/H ratio of 5.0 or less when the earthquake ground motion is characterized as having a high a/v ratio.

4. The value of the wave reflection coefficient significantly affects the magnitudes of the supplementary response peaks when the one-dimensional boundary condition is used in the analysis. As the coefficient decreases from 1.0 (indicating increasing damping at the reservoir-foundation interface), the response of the monolith eventually approaches that of the infinite reservoir case. The supplementary response peaks that are generated solely through the resonance of the reservoir substructure are most significantly affected.

5. The interaction between the soil columns, or shear effects, is a source of damping at the boundary of the reservoir and foundation. The damping provided by the proposed two-dimensional boundary condition was greater than that provided by the one-

dimensional boundary condition for the same value of the wave reflection coefficient. Neglecting the interaction between soil columns therefore ignores a significant source of energy dissipation in the reservoir substructure.

6. The value of the modulus of elasticity of the concrete used in the monolith substructure has a significant influence on the supplementary response peaks. Increasing the modulus of elasticity increases the frequencies at which the monolith's modes of vibration occur. The magnitude and frequency of the supplementary response peaks are subsequently altered. The dam monolith consequently will behave differently when subjected to earthquake ground motion as the modulus of elasticity is varied.

7. The proposed simplified analysis procedure can be used for the initial dynamic analysis of the dam-reservoir-foundation system in the preliminary design stage. It provides an accurate estimate of the monolith's response when the ground motion is assumed only to affect the dam monolith. A more detailed dynamic analysis is required for the later design stages to consider the combined effects of reservoir characteristics such as the reservoir geometry, the phase of ground

motion, the L/H ratio of the reservoir, and the specific frequency content of the earthquake ground motion.

8. The phase of the ground motion that excites the far end boundary of the finite length upstream reservoir significantly alters the magnitudes of the supplementary response peaks relative to the case where only the monolith is excited. The change in magnitude that occurs is directly dependent on the assumed phase of the ground motion which excites the far end boundary. Ground motion at the far boundary of the reservoir that is out-of-phase with that at the monolith is the worst case of ground motion excitation.

9. Short length upstream reservoirs ($L/H \leq 2.5$) are the most susceptible to earthquake ground motion when both the monolith and the far boundary of the reservoir are excited. Large monolith response and high levels of dynamic tensile stress occur for these cases.

10. The geometry of the finite length upstream reservoir significantly affects the response of the monolith. The upstream reservoir will resonate at different frequencies for different reservoir geometries. The monolith may respond quite differently to the

earthquake ground motion depending on the geometry that is assumed for the upstream reservoir.

11. The frequency content of the earthquake ground motion, the L/H ratio of the reservoir, the phase of the ground motion at the far end boundary of the reservoir, and the specific geometry of the reservoir all must be considered together in order to obtain a reasonable estimate of the monolith's response. If one of these reservoir characteristics is omitted or determined incorrectly, the reliability of the dynamic and stress analyses will be in doubt.

6.2 RECOMMENDATIONS

A list of recommendations for future research is presented below. These recommendations have arisen during the course of this research and from the conclusions drawn from it.

1. The effect of the vertical component of the earthquake ground motion on the response of a concrete gravity dam monolith when a finite length upstream reservoir is assumed, should be investigated. Several studies have indicated that this ground motion component has a significant effect on the monolith's response when the

upstream reservoir is assumed to be infinite in length. Its effect should also be significant for a finite length upstream reservoir.

2. The effect of assuming that the height of the water in the reservoir is less than the height of the dam monolith should be evaluated. The reservoir height is never equal to that of the dam monolith's height in existing structures. The behaviour of the monolith to different heights of reservoir should be investigated.

3. A more detailed investigation of the reservoir should be undertaken to determine the effect of viscosity, convection, and other sources of energy dissipation in the upstream reservoir. Very little attention, if any, has been given to these topics to establish their relative importance in the response of the dam monolith.

4. A time domain model of the dam-finite reservoir-foundation system should be developed. The frequency domain model used in this study has many limitations including long solution times and difficulty in adding new components to the model. Using the time domain will allow the model for the system to be expanded and new solution techniques implemented to decrease the solution time required.

5. The effect of the amplification of the pressure waves as they propagate into a region of decreasing water depth should be investigated. A large hydrodynamic force may be created as these pressure waves travel up the reservoir. Some of the energy may be transmitted back towards the monolith and impose a large force onto the dam face. This should be examined in conjunction with the effect of the vertical component of the ground motion.

6. The reservoir's foundation should be modelled as a two-dimensional elastic body. The models for the monolith's foundation and the reservoir's foundation should also be combined into one single model. The dam and reservoir foundation is an extremely important part of the overall system and must be treated as rigorously as possible. The effect of sediments on the reservoir bottom must be considered as well in this new model. The foundation that forms the far end boundary of the reservoir should also be modelled as accurately as possible. This study assumed that it vibrated in its rigid body mode. The flexibility of this boundary on the response of the monolith should also be examined.

7. The response of arch dams assuming a finite reservoir length should be investigated. These structures may be very susceptible to finite reservoir effects as they are usually quite flexible. These types of structures are also more likely to impound a finite length reservoir, especially those structures sited in mountainous areas.

8. A scale model test of the dam-finite reservoir system should be undertaken to verify the analytical model. The scale model itself should be numerically analyzed using the procedure presented in this thesis. Such experimental and numerical investigation would verify the reliability of the analytical procedure that is currently being used in the dynamic analysis of dam-reservoir-foundation systems.

REFERENCES

Antes, H., and O. Von Estorff. 1987. Analysis of Absorption Effects on the Dynamic Response of Dam Reservoir Systems by Boundary Element Methods. Earthquake Engineering and Structural Dynamics, Vol. 15, No. 8, pp. 1023-1036.

Aviles, J., and F. J. Sanchez-Sesma. 1989. Water Pressures on Rigid Gravity Dams with Finite Reservoir During Earthquakes. Earthquake Engineering and Structural Dynamics, Vol. 18, No. 4, pp. 527-537.

Bougacha, S., and J. L. Tassoulas. 1991a. Seismic Analysis of Gravity Dams. I: Modelling of Sediments. Journal of Engineering Mechanics, ASCE, Vol. 117, No. 8, pp. 1826-1837.

Bougacha, S., and J. L. Tassoulas. 1991b. Seismic Response of Gravity Dams. II: Effects of Sediments. Journal of Engineering Mechanics, ASCE, Vol. 117, No. 8, pp. 1839- 1850.

Chakrabarti, P., and A. K. Chopra. 1973a. Hydrodynamic Pressures and Response of Gravity Dams to Vertical Earthquake Component. Earthquake Engineering and Structural Dynamics, Vol. 1, No. 4, pp. 325-335.

Chakrabarti, P., and A. K. Chopra. 1973b. Earthquake Analysis of Gravity Dams Including Hydrodynamic Interaction. Earthquake Engineering and Structural Dynamics, Vol.2, No. 2, pp. 143-160.

Cheng, A. H.-D. 1986. Effect of Sediment on Earthquake-Induced Reservoir Hydrodynamic Response. Journal of Engineering Mechanics, ASCE, Vol. 112, No. 7, pp. 654-665.

Chopra, A. K. 1967. Hydrodynamic Pressures on Dams during Earthquakes. Journal of the Engineering Mechanics Division, ASCE, Vol. 93, No. EM 6, pp. 205-223.

Chopra, A. K. 1968. Earthquake Behaviour of Reservoir-Dam Systems. Journal of the Engineering Mechanics Division, ASCE, Vol. 94, No. EM 6, pp. 1475-1500.

Chopra, A. K. 1987. Earthquake Analysis, Design, and Safety Evaluation of Concrete Dams. Proceedings of the Fifth Canadian Conference on Earthquake Engineering, Ottawa, Ontario, July, pp. 39-62.

Chopra, A. K., and P. Chakrabarti. 1972. The Earthquake Experience at Koyna Dam and Stresses in Concrete Gravity Dams. Earthquake Engineering and Structural Dynamics, Vol. 1, No. 2, pp. 151-164.

Chopra, A. K., P. Chakrabarti, and S. Gupta. 1980. Earthquake Response of Concrete Gravity Dams including Hydrodynamic and Foundation Interaction Effects. Earthquake Engineering Research Center, University of California, Berkeley, UCB/EERC-80/01.

Clough, R. W., and J. Penzien. 1975. Dynamics of Structures. McGraw-Hill Book Company, New York.

Clough, R. W., K.-T. Chang, H.-Q. Chen, R. M. Steven, G.-L. Wang, and Y. Ghanaat. 1984a. Dynamic Response Behavior of Xiang Hong Dian Dam. Earthquake Engineering Research Center, University of California, Berkeley, UCB/EERC-84/02.

Clough, R. W., K.-T. Chang, H.-Q. Chen, R. M. Steven, Y. Ghanaat, and J.-H. Qi. 1984b. Dynamic Response Behavior of Quan Shui Dam. Earthquake Engineering Research Center, University of California, Berkeley, UCB/EERC-84/20.

Clough, R. W., R. M. Stephen, and J. S.-H. Kuo. 1982. Dynamic Response Analysis of Techi Dam. Earthquake Engineering Research Center, University of California, Berkeley, UCB/EERC-82/11.

Clough, R. W., Y. Ghanaat, and X.-F. Qiu. 1987. Dynamic Reservoir Interaction with Monticello Dam. Earthquake Engineering Research Center, University of California, Berkeley, UCB/EERC-87/21.

Crouch, S. L. and A. M. Starfield. 1983. Boundary Element Methods in Solid Mechanics. George Allen and Unwin, London.

CSA. 1984. Design of Concrete Structures for Buildings. CAN3-A23.3-M84. Canadian Standards Association, Rexdale, Ontario, Canada.

Dasgupta, G., and A. K. Chopra. 1977. Dynamic Stiffness Matrices for Homogeneous Viscoelastic Halfplanes. Earthquake Engineering Research Center, University of California, UCB/EERC-77/26.

Donlon, W. P.,and J. F. Hall. 1991. Shaking Table Study of Concrete Gravity Dam Monolith. Earthquake Engineering and Structural Dynamics, Vol. 20, No. 8, pp. 769-786.

Duron, Z. H. 1987. Experimental and Finite Element Studies of a Large Arch Dam. Earthquake Engineering Research Laboratory, California Institute of Technology, Pasadena, EERL 87-02.

El-Aidi, B., and J. F. Hall. 1989a. Non-Linear Earthquake Response of Concrete Gravity Dams Part 1: Modelling. Earthquake Engineering and Structural Dynamics, Vol. 18, No. 6, pp. 837-851.

El-Aidi, B., and J. F. Hall. 1989b. Non-Linear Earthquake Response of Concrete Gravity Dams Part 2: Behaviour. Earthquake Engineering and Structural Dynamics, Vol. 18, No. 6, pp. 853-865.

Fenves, G., and A. K. Chopra. 1984a. EAGD-84. A Computer Program for Earthquake Analysis of Concrete Gravity Dams. Earthquake Engineering Research Center, University of California, Berkeley, UCB/EERC-84/11.

Fenves, G., and A. K. Chopra. 1984b. Earthquake Analysis and Response of Concrete Gravity Dams. Earthquake Engineering Research Center, University of California, Berkeley, UCB/EERC-84/10.

Fenves, G., and A. K. Chopra. 1985a. Simplified Earthquake Analysis of Concrete Gravity Dams: Separate Hydrodynamic and Foundation Interaction Effects. Journal of Engineering Mechanics, ASCE, Vol. 111, No. 6, pp. 715-735.

Fenves, G., and A. K. Chopra. 1985b. Simplified Earthquake Analysis of Concrete Gravity Dams: Combined Hydrodynamic and Foundation Interaction Effects. Journal of Engineering Mechanics, ASCE, Vol. 111, No. 6, pp. 736-756.

Hall, J. F. 1988. The Dynamic and Earthquake Behavior of Concrete Dams: Review of Experimental Behavior and Observational Evidence. Foundation Engineering and Soil Dynamics, Vol. 7, No. 2, pp. 58-121.

Hall, J. F., and A. K. Chopra. 1980. Dynamic Response of Embankment Concrete-Gravity and Arch Dams including Hydrodynamic Interaction. Earthquake Engineering Research Center, University of California, Berkeley, UCB/EERC-80/39.

Jablonski, A. M., and J. L. Humar. 1990. Three-Dimensional Boundary Element Reservoir Model for Seismic Analysis of Arch and Gravity Dams. Earthquake Engineering and Structural Dynamics, Vol. 19, No. 3, pp. 359-376.

Lamb H. 1945. Hydrodynamics. Sixth edition, Dover Publications, New York.

Leger, P., and M. Katsouli. 1989. Seismic Stability of Concrete Gravity Dams. Earthquake Engineering and Structural Dynamics, Vol. 18, No. 6, pp. 889-902.

Liu, P. L.-F. 1986. Hydrodynamic Pressures on Rigid Dams During Earthquakes. Journal of Fluid Mechanics, Vol 165, pp. 131-145.

Lofti, V., J. M. Roesset, and J. L. Tassoulas. 1987. A Technique for the Analysis of the Response of Dams to Earthquakes. Earthquake Engineering and Structural Dynamics, Vol. 15, No. 4, pp. 463-490.

Mandzhavidze, N. F., and G. P. Mamradze. 1966. The High Dams of the World. Systemic Tables of Data and Bibliography on Dams over 75m High. Israel Program for Scientific Translations, Jerusalem.

Medina, F., J. Dominguez, and J. L. Tassoulas. 1990. Response of Dams to Earthquakes Including Effects of Sediments. Journal of Structural Engineering, ASCE, Vol. 116, No. 11, pp. 3108-3121.

National Academy Press. 1990. Earthquake Engineering for Concrete Dams: Design, Performance, and Research Needs. Panel on Earthquake Engineering for Concrete Gravity Dams, Committee on Earthquake Engineering, Division of Natural Hazard Mitigation, Commission on Engineering and Technical Systems, National Research Council, Ottawa, Ontario.

Naumoski, N., W. K. Tso, and A. C. Heidebrecht. 1984. A Selection of Representative Strong Motion Earthquake Records Having Different A/V ratios. McMaster University Earthquake Engineering Research Group, McMaster University, Hamilton, Ontario, Canada, EERG Report 88-01.

Outland, C. F. 1977. Man-Made Disaster, The Story of St. Francis Dam. California: The Arthur H. Clark Company.

Pal, N. 1976. Seismic Cracking of Concrete Gravity Dams. Journal of the Structural Division, ASCE, Vol. 102, No. ST9, pp. 1827-1844.

Saini, S. S., P. Bettess, and O. C. Zienkiewicz. 1978. Coupled Hydrodynamic Response of Concrete Gravity Dams using Finite and Infinite Elements. Earthquake Engineering and Structural Dynamics, Vol. 6, No. 4, pp. 363-374.

Secretaria de Recursos Hidraulicos. 1976. Behavior of Dams built in Mexico. Contribution to the XII International Congress on Large Dams, Mexico.

Wang, J. 1990. Influence of Epicentral Distance and Soil Conditions on Ground Motion Characteristics and Structural Response to the Saguenay Earthquake, 1988. Master of Engineering Thesis, McMaster University, Hamilton, Ontario, Canada.

Wepf, D. H., J. P. Wolf, and H. Bachmann. 1988. Hydrodynamic-Stiffness Matrix based on Boundary Elements for Time-Domain Dam-Reservoir-Soil Analysis. Earthquake Engineering and Structural Dynamics, Vol. 16, No. 3, pp. 417-432.

Werner, P. W., and K. J. Sundquist. 1949. On Hydrodynamic Earthquake Effects. EOS Transactions of the American Geophysical Union, No. 30, pp. 636-657.

Westergaard, H. M. 1933. Water Pressures on Dams During Earthquakes. Transactions of the American Society of Civil Engineers, Vol. 98, pp. 418-433.